COVALENT SELF-ASSEMBLY OF AN ENERGY CASCADE IN ONE STEP

A THESIS SUBMITTED TO

THE GRADUATE SCHOOL OF ENGINEERING AND SCIENCE

OF BILKENT UNIVERSITY

IN PARTIAL FULFILLMENT OF THE REQUIREMENTS FOR

THE DEGREE OF

MASTER OF SCIENCE

IN

CHEMISTRY

By

CEREN ÇAMUR

August, 2015

COVALENT SELF-ASSEMBLY OF AN ENERGY CASCADE IN ONE STEP

By Ceren Çamur

August, 2015

We certify that we have read this thesis and that in our opinion it is fully adequate, in scope and in quality, as a thesis for the degree of Master of Science.

_____

Prof. Dr. Engin Umut AKKAYA (Advisor)

_____

Assoc. Prof. Dr. Dönüş TUNCEL

_____

Assist. Prof. Dr. Fazlı SÖZMEN

Approved for the Graduate School of Engineering and Science:

_____

Prof. Dr. Levent ONURAL

Director of the Graduate School

ABSTRACT

COVALENT SELF-ASSEMBLY OF AN ENERGY CASCADE IN ONE STEP

CEREN ÇAMUR

M.S. in Chemistry

Supervisor: Prof. Dr. Engin Umut AKKAYA

August 2015

Light harvesting mechanisms include absorption of energy by donor and transfer of the absorbed energy to acceptor. The aim of this process is the channeling of the light at certain wavelength. In this study, energy transfer process was sustained by BODIPY based Förster type light harvesting cascade. The donor and acceptor units of the cascade were synthesized to be combined by self-assembly. Passerini reaction was used in the assembly of the three units. Designed molecule consists of three moieties: BODIPY, monostyryl- BODIPY and distyryl-BODIPY. The expected process of energy transfer starts with the absorption of light at around 502 nm and ends with the emission at around 674 nm. The spectral overlap between donors and acceptors were shown. Under the light of the results, the designed molecule is promising to work as an effective energy transfer cascade.

Keywords: Boradiazaindacene, Förster type energy transfer, energy transfer cascade, styryl BODIPY, Passerini reaction

ÖZET

TEK ADIMDA KOVALENT BAĞLARLA KENDİLİĞİNDEN BİR ARAYA GELEN ENERJİ TRANSFERİ SİSTEMİ

CEREN ÇAMUR

Kimya Bölümü Yüksek Lisans Tezi

Tez Yöneticisi: Prof. Dr. Engin Umut AKKAYA

Ağustos 2015

Işık hasatlama sistemleri, verici birim tarafından absorblanan enerjinin alıcı birime aktarılmasını içerir. Bu tarz sistemler belirli bir dalga boyundaki enerjinin alıcı birimlere doğru yönlendirilmesini amaçlar. Bu çalışmada, BODİPY tabanlı Förster tipi enerji transfer mekanizması ile çalışan enerji transfer sistemi tasarlanmıştır. Sistem içindeki verici ve alıcı birimler sentezlenmiştir ve birimler kendiliğinden bir araya gelerek, enerji transfer sistemini oluşturması planlanmıştır. Birimlerin kendiliğinden bir araya gelmesini sağlamak için Passerini reaksiyonu kullanılacaktır. Tasarlanan molekül üç farklı birime sahiptir ve bu birimler BODİPY, monositril BODİPY ve disitril BODİPY den oluşmaktadır. Enerji transfer süreci, enerjinin verici birim tarafından yaklaşık 502 nm de absorblanmasından ve enerji transferleri sonucunda 674 nm deki emisyonun gözlenmesinden oluşur. Alınan fotometrik sonuçlar, tasarlanan enerji transfer sisteminin planlandığı gibi çalışacağını göstermektedir.

Anahtar Kelimeler: Boradiazaindasen, Förster tipi enerji transferi, enerji transferi sistemleri, sitril BODİPY, Passerini reaksiyonu

Dedicated to my family…

ACKNOWLEDGEMENT

First of all I would like to thank my supervisor Prof. Dr. Engin Umut AKKAYA for his patience, support and guidance. We all gain valuable and outstanding point of view to the science in his laboratory. I feel lucky to be able to have a chance to work with him and benefit from his experiences and knowledge. On the other hand, he is very good person and helpful. I will never forget him and his contributions to my life.

Secondly, I would like to thank MSc thesis committee members Assoc. Prof. Dr. Dönüş TUNCEL and Asst. Prof. Dr. Fazlı SÖZMEN for their patience and valuable advices.

Additionally, I owe a special thanks to Dr. Tuğba ÖZDEMİR KÜTÜK and Dr. Safacan KÖLEMEN for sharing experiences and valuable knowledge with me. They were always guiding, realist, helpful and supportive.

I would like to thank to our group members, Dr. Özlem SEVEN, Dr. Murat IŞIK, Dr. Ruslan GULIYEV, Dr. Dilek TAŞGIN, Cpt. Bilal KILIÇ, Bilal UYAR, Yiğit ALTAY, Tuba YAŞAR, Ahmet ATILGAN, Tuğçe DURGUT, Nisa YEŞİLGÜL, Hale ATILGAN, José Luis BILA, Melek BAYDAR BAYTAK, Darika OKEEV, Tuğçe KARATAŞ, Cansu KAYA, Veli POLAT and rest of the SCL (Supramolecular Chemistry Laboratory) for creating wonderful environment to work in. They are like family to me right now and their friendship is very valuable.

Other than laboratory, I want to thank my best friends Pınar AYDOĞAN, Saadet KAYMAZ and Ece KIZILKAYA. We grew up and spent our most enjoyable and crazy years together. Their support and existence is very important for me.

I want to express my gratitude to my father Kemal Sami ÇAMUR, to my mother Esma Işık Nil ÇAMUR and my brother Mert ÇAMUR. They were always encouraging. I could not be here if the support they were providing me was not exist. They are always understanding and loving through my entire life so I would like to thank each of them.

Finally, I would like to thank my fiancée Civan AVCI. He was always encouraging, loving, helpful and understanding. Without his patience and support, writing this thesis would not be possible. Thank you for all of it. It is wonderful to have you in my life.

LIST OF ABBREVIATIONS

BODIPY	: 4,4-difluoro-4-bora-3a,4a-diaza-s-indacene
DCM	: Dichloromethane
EtOAc	: Ethyl acetate
THF	: Tetrahydrofuran
AcOH	: Acetic acid
TFA	: Trifluoroacetic acid
HOMO	: Highest occupied molecular orbital
LUMO	: Lowest occupied molecular orbital
TLC	: Thin layer chromatography
FRET	: Förster resonance energy transfer
NMR	: Nuclear magnetic resonance
MS	: Mass spectrometry
RT	: Room temperature

TABLE OF CONTENTS

LIST OF FIGURES

LIST OF TABLES

1. INTRODUCTION

1.1. Supramolecular Chemistry

As a distinct area, supramolecular chemistry has been growing since the late 1960s as an interdisciplinary field that includes chemistry, biochemistry, medicinal chemistry, and physics and so on.[1,2,3,4] Defining the supramolecular chemistry is confusing task because it has many application areas in many fields. According to a book named *Core Concepts in Supramolecular Chemistry and Nanochemistry* supramolecular chemistry defined as "The study of systems involving aggregates of molecules or ions held together by non-covalent interactions, such as electrostatic interactions, hydrogen bonding, dispersion interactions and solvophobic effects." It is a general definition that can include most of the concepts in supramolecular chemistry.

The concepts creating the base of the field are Paul Ehrlich's receptor idea, Alfred Werner's coordination chemistry, and Emil Fischer's lock-and-key model. Those are crucial improvements in supramolecular chemistry.[5] As a modern theme, Jean–Marie Lehn introduced the molecular self-assembly and intermolecular bond.[6] Under the light of these information, supramolecular chemistry can be examined in two subtitles. First is host-guest chemistry which includes supramolecules composed of a host and a guest that has reversible non covalent interaction between them (Figure 1).[1] Second is self-assembly of molecules that involves spontaneous array of two or more components to form larger noncovalently bound network.[7]

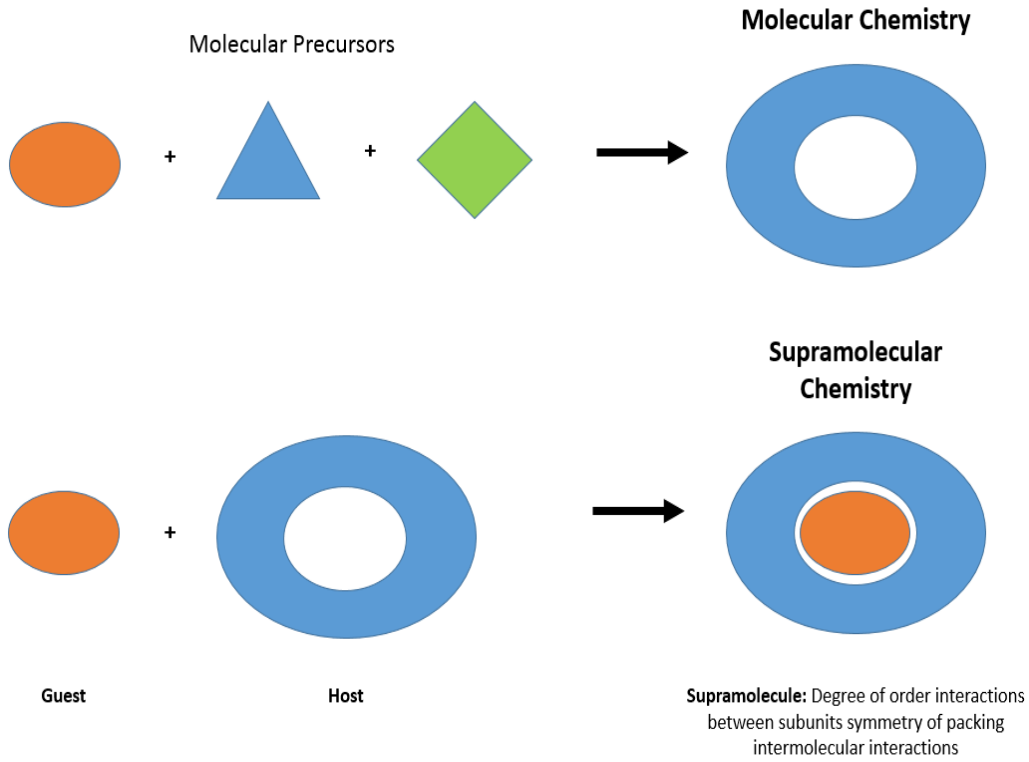

Figure 1: Differences of molecular and supramolecular chemistry.

As mentioned before, supramolecular chemistry is broad field and has many applications such as medicine,[8,9,10] catalysis,[11,12,13] green chemistry,[14,15,16] molecular devices,[17,18,19] sensors[20,21,22] and etc. Most of these work by self-assembled structures. Enzyme systems,[23,24] DNA,[25,26,27] energy transfer mechanisms in the plants[28,29,30] etc. are examples for mimicked systems in nature.

In addition to that supramolecular chemistry has important role to understand working mechanism of therapeutic agents or drug delivery mechanisms.[31,32,33] Therefore, supramolecular chemistry is wide area that is rapidly improving and it has crucial effects to human life in direct way.

1.2. Fluorescence

Luminescence is general concept that involves fluorescence. The definition of luminescence is emission of radiation from electronically or vibrationally excited state compound. Once a compound absorb a photon, molecule become excited and the way of turning in ground state can be in two ways basically. First is intramolecular processes which includes radiative and non-radiative transitions. Second one is intermolecular processes involves vibrational relaxation, energy transfer and electron transfer.[34]

Fluorescence is a radiative transition and the process occurs with the relaxation of molecule from excited state to ground state. In order to understand excitation and relaxation process properly, Jablonski diagram should be examined first (Figure 2). [35]

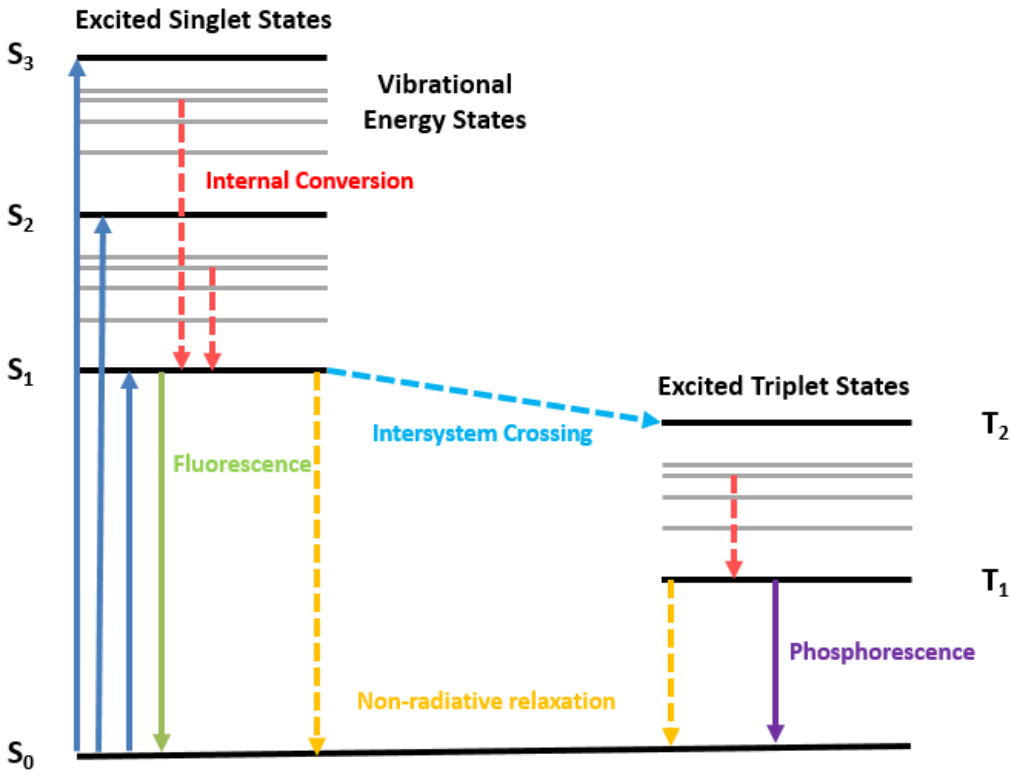

Figure 2: The Jablonski Diagram

Absorption energy of a molecule results excitation of one electron from S_0 state to excited singlet states (S_1, S_2,…). Relaxation of the molecule includes turning back to the lowest vibrational level (S_1) and after that to the ground state (S_0). While electron relaxes to the S_0, there are many ways to free absorbed energy. Only heat release can be observed as non-radiative relaxation. As radiative relaxation, emission of light can be occur and that process called fluorescence. These processes are allowed since the spin multiplicities are same so the lifetime of fluorescence is very short (picoseconds to microseconds). On the other hand, there is a chance to cross from singlet state to triplet state (from S_1 to T_1) called intersystem crossing. This is forbidden transition but it is observable when molecule has heavy atoms like bromide or iodide because larger orbitals provide large spin orbit coupling and make the transition possible. After crossing to T_1, there could be radiative and non-radiative relaxation. Radiative one is called phosphorescence. It has longer lifetime comparing with fluorescence (miliseconds to seconds).[36]

In addition to these, it is clear that energy of absorption is higher that energy of emission due to the loss of energy in vibrational levels. As a consequence of that, absorption occurs at lower wavelength and this phenomena called Stock's shift.(Figure 3) Stock's shift can be affected by solvent, transfer of energy and complex formation.[37]

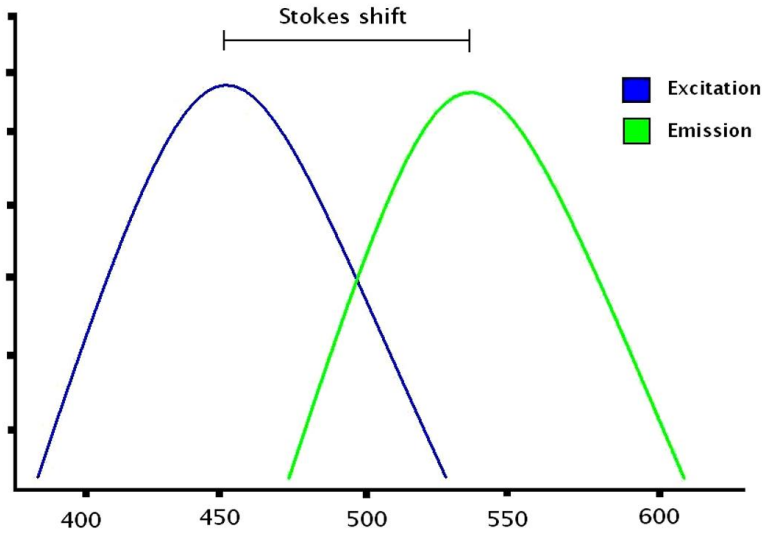

Figure 3 Representation of Stock's Shift

Fluorescent molecules are very popular in the field of supramolecular chemistry since they can be functionalized as sensors,[38,39,40] light harvesters,[41,42,43] photosensitizers,[44,45,46] etc. Some of fluorescent molecules are shown in Figure 4.

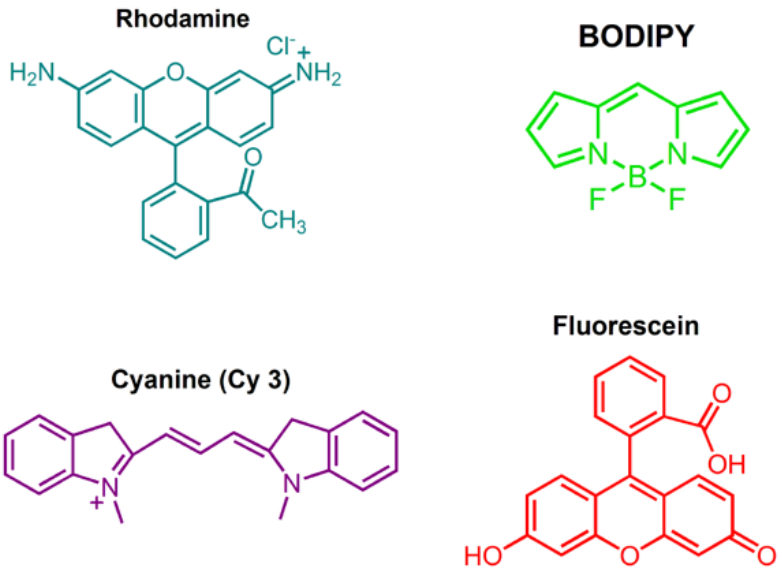

Figure 4: Examples of fluorescent molecules in literature.

1.3. BODIPY Dyes and It's Applications

As mentioned before fluorescent molecules are very popular in literature especially as fluorescent probes. Boradiazaindacene (BODIPY) dyes which were synthesized first by Kreuzer and Treibs are one of the popular fluorophores investigated around the world (Figure 5).[47]

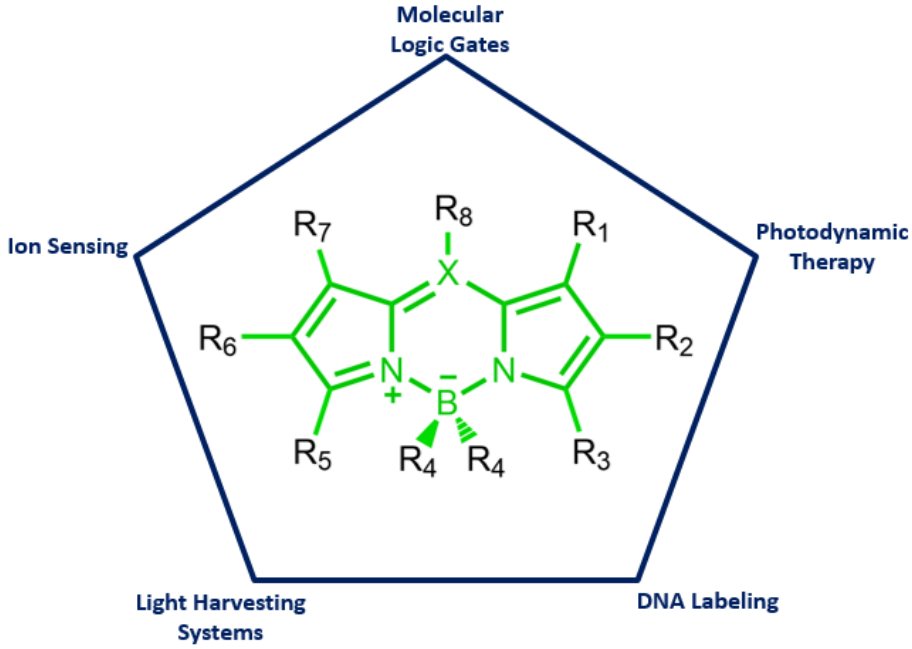

Figure 5: BODIPY core and its potential applications.

BODIPY dyes are preferred fluorescent molecules to work with due to their high molar extinction coefficients and high quantum yields. They have intense absorption bands and good solubility in organic solvents. [48] In addition to that, they are easy to synthesize and functionalize. Knoevenagel condensation reaction is used to modificate BODIPY dyes on 1-3 and 5-7 positions to produce mono-, di-, tri- and tetra-styryl types of them with the help of acidic character of methyl groups.[49] By using this modification technique, it is possible to tune emission and absorption wavelengths in visible spectrum without decrease in the intensity of the bands as shown in Figure 6.[50] 2-6 positions in BODIPY core have high electron density so

they are favorable positions for electrophilic attack to perform halogenation,[51] sulfonation[52] and nitration[53] reactions. Halogenation (especially for heavy atoms like I and Br atoms) on these positions is used to obtain effective intersystem crossing due to heavy atom effect although it results quenching of fluorescence.[54] On the other hand, they has high photochemical and thermal stability. [55] Because of these reasons, BODIPY chemistry takes attentions in order to be used for variety of purposes.

As indicated in Figure 5, BODIPY dyes has broad application area. The first application of BODIPY was labeling of DNA and proteins in biological researches.[56,57,58] After then, it is used in logic gates,[59,60,61] ion sensors,[62,63,64] light harvesting systems,[65,66,67] photodynamic therapy[68,69,70]and etc.

Fluorescent molecules have been modified as sensor to heavy and transition metal ions to be used in environmental and biological applications. Fluorophores that have emission beyond 650 nm are preferred in biological media due to scatter of light at longer wavelengths.[71] As mentioned in Figure 6, BODIPY emission wavelength can be tuned by functionalization of the molecule. [50]

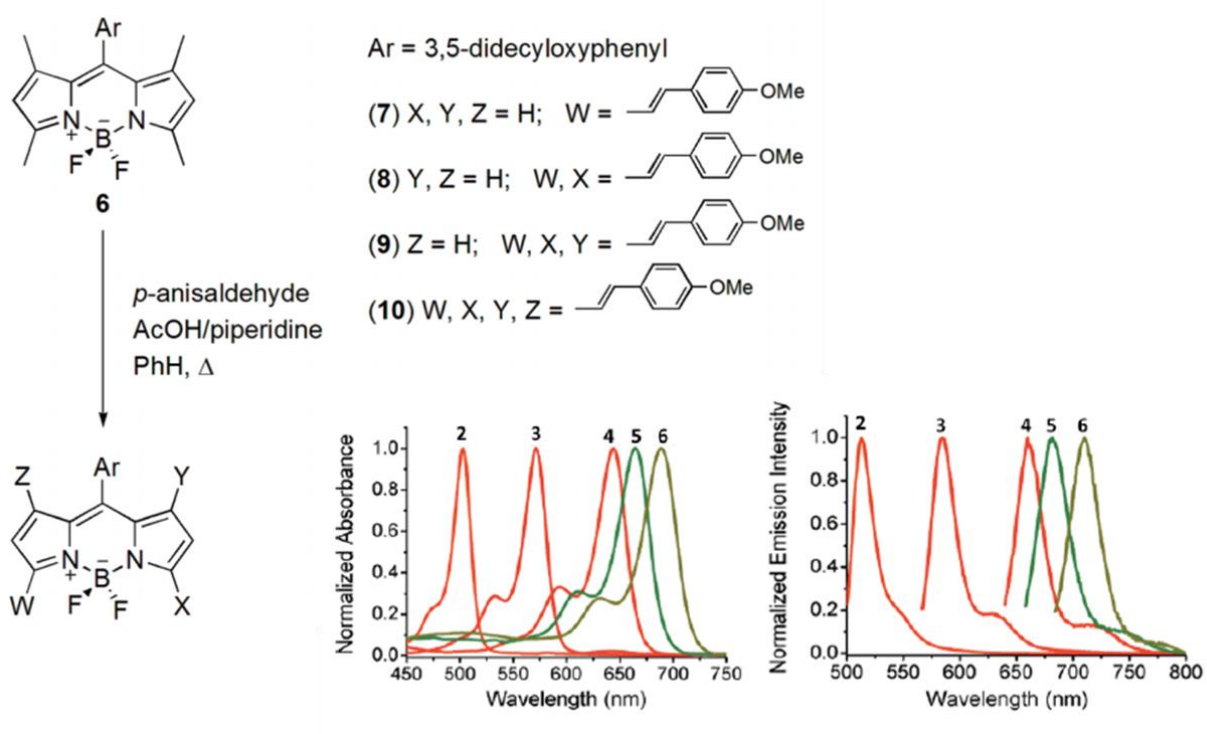

Figure 6: Absorption and emission spectra of functionalized BODIPYs on the positions 3,5 and 1,7 positions by Knoevenagel condensation reaction. Copyright © 2009, American Chemical Society. Reprinted with permission from ref (50)[50].

In addition to that, there are two more important concept for ion sensors. They are sensitivity and selectivity. These requirements can be sustained through crown ether, terpyridyl etc. moieties bound to BODIPY core. Therefore, functionalized BODIPY dyes have been successful ion sensors and some literature examples are shown in Figure 7.[72,73]

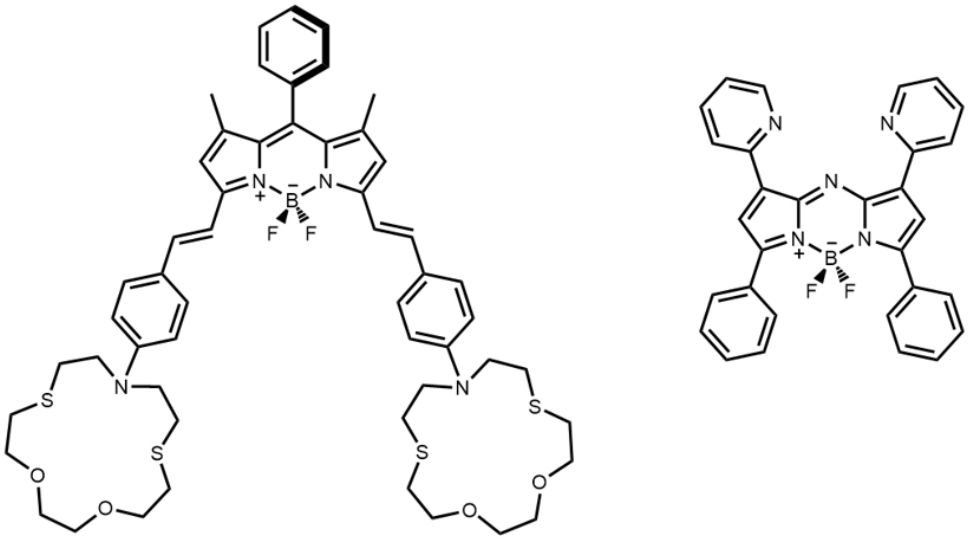

Figure 7: Some literature examples of BODIPY dye based ion sensors.

Molecular logic gates is a different application of BODIPY dyes. The aim is creating small chemical system capable of data processing. These systems include structures that has switch mechanism between states of the molecule used as logic gate. Switching mechanism can depend on many variables such as pH, temperature, light and so on. Fluorescent molecules are appropriate to create these kind of systems and BODIPY dye is one of those molecules in the literature. Some examples of molecules are shown in Figure 8.[74,75]

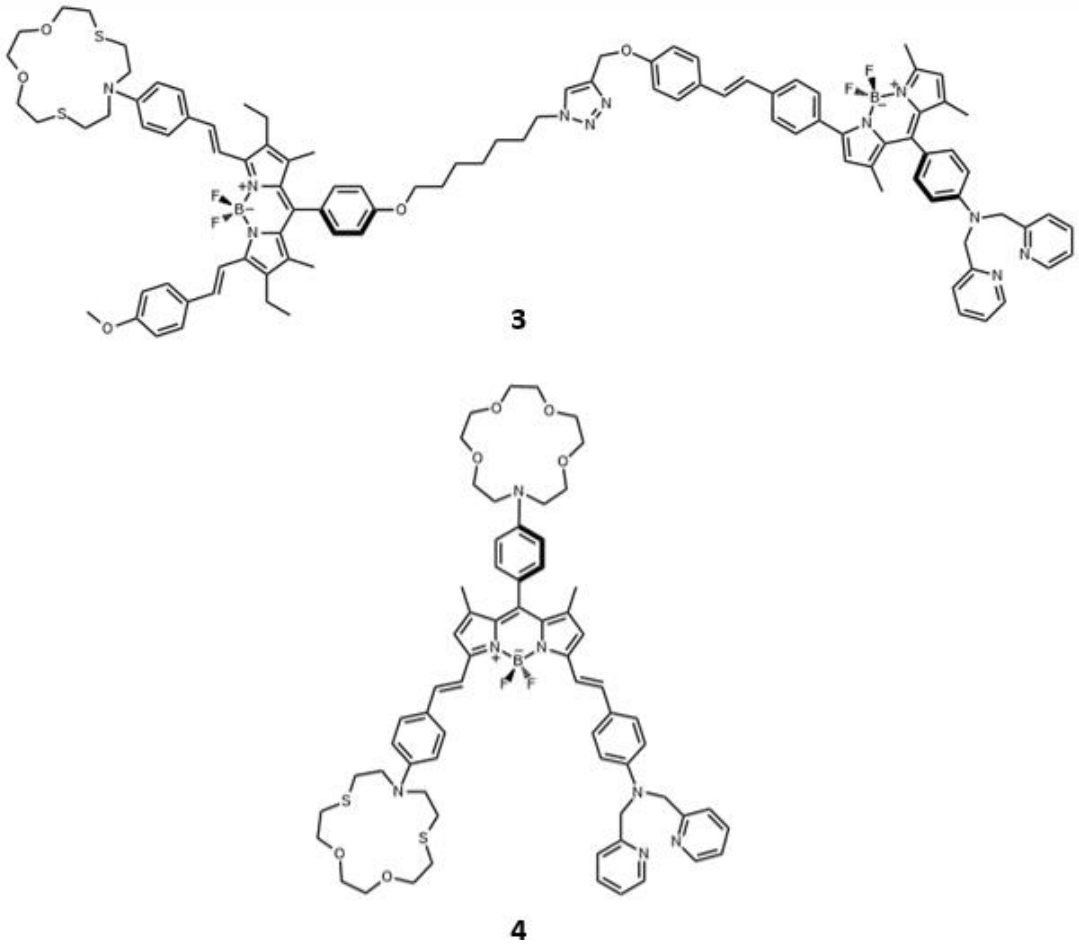

Figure 8: Some literature examples of BODIPY dye based molecular logic gates.

1.4. Light Harvesting and Energy Transfer

Light harvesting is one of the key process in nature for continuation of life. In photosynthesis, needed energy is collecting by light harvesting system and transmitted to the reaction center. These systems includes light harvesting chromophore molecules which absorb energy and channeling process of absorbed energy to where reaction goes on. These type of systems are called light harvesting antenna systems.[76] Different representations of these systems can be used to visualize the harvesting process as shown in Figure 9.

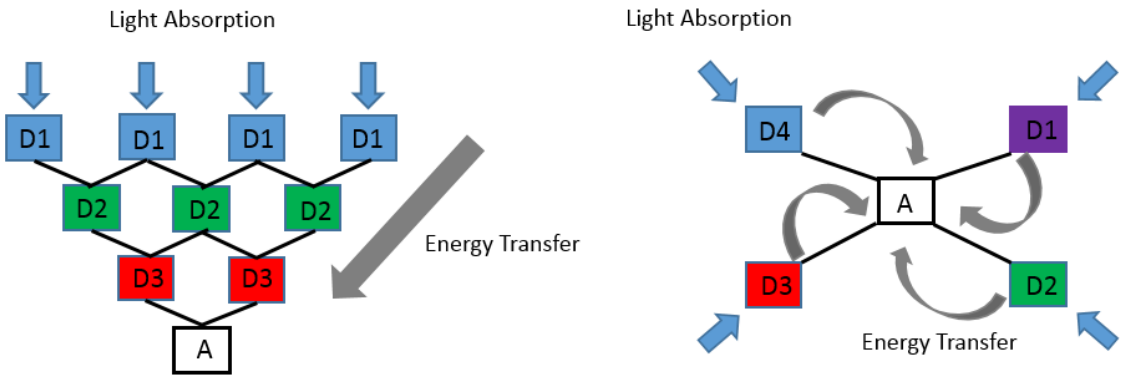

Figure 9: Different representations of light harvesting process.

It is possible to create such light harvesting system units by using energy transfer cascades with the help of supramolecular chemistry.[77] The cascades are composed of donor units which absorbs light at short wavelengths and acceptor units which has emission at longer wavelengths. In order to obtain these process, there are some important parameters. Those are time, space and energy.[78] Energy transfer occurs in two ways in cascade systems either through space (Förster type energy transfer mechanism) or through bond (Dexter type energy transfer mechanism).

1.4.1. Dexter Type Energy Transfer Mechanism

Energy transfer cascades must contain at least two chromophores (donor and acceptor). Energy transfer occurs through bond between the chromophores in this type of mechanism so conjugation between donor and acceptor is needed. The key parameter for the energy transfer is orbital overlap. Because of that, there must be short distance between moieties (less than 10 Aº). Chromophore units should be linked to each other and the way of the linkage is crucial point in the efficiency of energy transfer (Figure 10).[79,80,81]

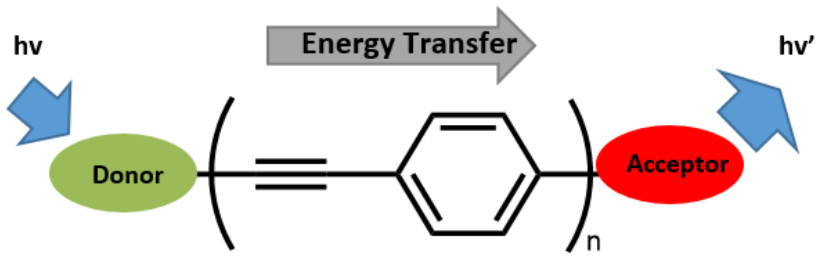

Figure 10: Schematic representation of through bond energy transfer.

During the energy transfer, electron exchange between donor and acceptor observed. Exchange occurs from excited state electrons of donor to the excited state levels of acceptor and from ground state electron of acceptor to ground state energy levels of donor as shown in Figure 11.[82]

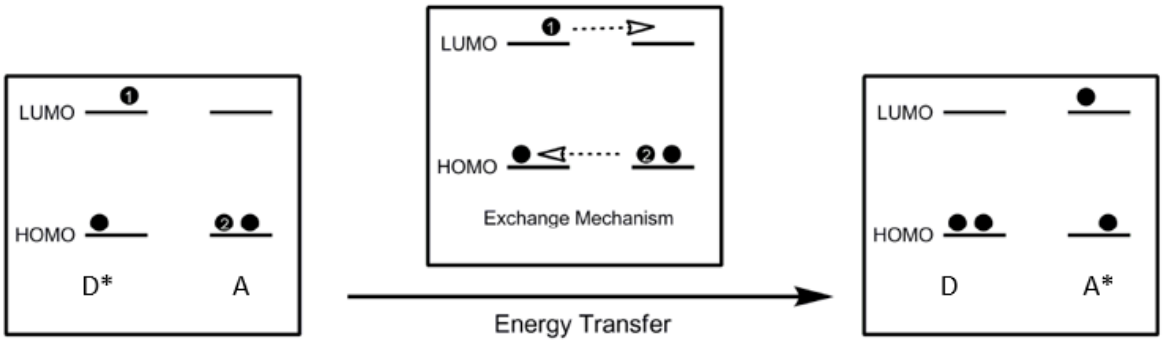

Figure 11: Representation of electron exchange mechanism in Dexter type.

In literature, there are many small systems works with Dexter type energy transfer are synthesized that are used in light harvesting or biological applications. For instance, Compound 5 is one of them and it has two moieties donor (green) and acceptor (red) (Figure 12).

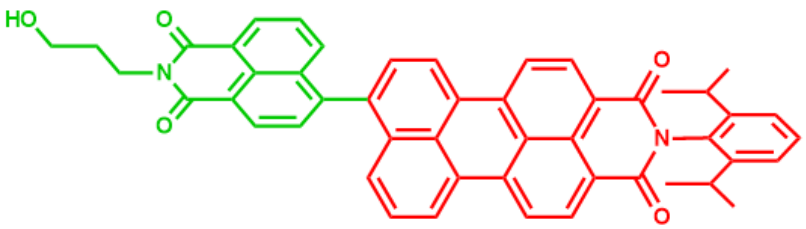

5

Figure 12: Literature example of molecules working with Dexter type energy transfer.

Distance between donor (naphthalenimide) and acceptor (perylenimide) is approximately 1.49 Aº and orbital overlap is shown by DFT calculations. Donor absorbs light at 345 nm and with the Dexter type energy transfer the acceptor give emission at 520-585 nm (Figure 13). Since it has quick response and high quantum yield, it is applicable in biological applications as Rijo et al reported. [83]

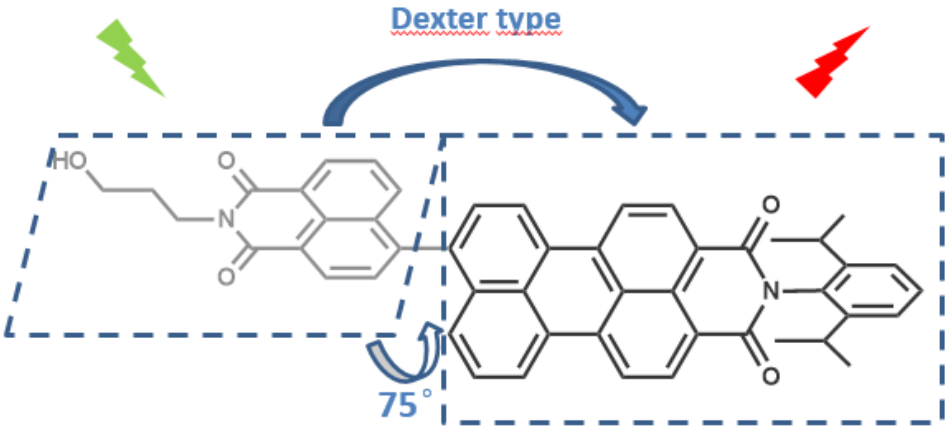

Figure 13: Working mechanism of Compound 5.

Another example can be Compound 6 as shown in Figure 14. The molecule has macrocycle part as donor (green) and BODIPY core as acceptor (red). Donor absorbs at 287 nm and emission observed at 510 nm according to Yousaf et al. The orbital overlap between donor and acceptor is shown by using TDDFT calculations. They reported the molecule as an efficient light harvester due to its visible spectrum abortion values. [84]

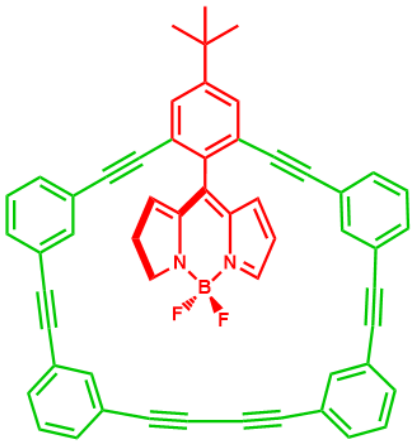

6

Figure 14: Literature example of Dexter type energy transfer units.

1.4.2. Förster Type Energy Transfer Mechanism (FRET)

In contrast to Dexter type energy transfer, the key parameters for the transfer are distance between chromophores and the spectral overlap. These moieties can be located away from each other (distance between units 10-100 Aº) and it is not necessary link between the moieties. Then, energy transfer occurs through space depending on the spectral overlap in the emission of donor and absorption of acceptor (Figure 15).[85,81]

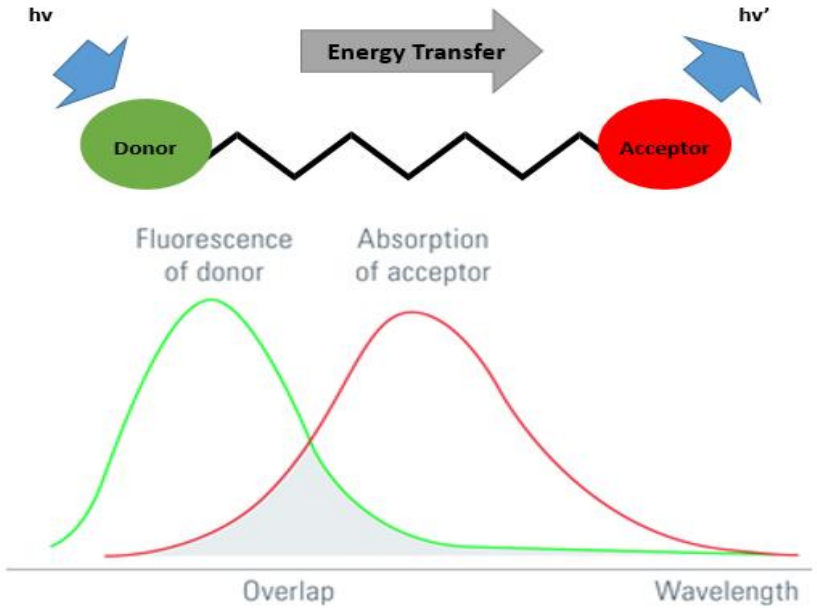

Figure 15: Schematic representation of through space energy transfer.

In order to understand process more detailed, HOMO and LUMO of the chromophores should be examined as shown in Figure 16. Once donor electrons are in excited state, the relaxation of the donor electrons occurs and the relaxation energy absorbed by acceptor due to the spectral overlap. This process called columbic mechanism. There is no electron exchange like in the Dexter type. Then, acceptor moiety becomes excited with the help of relaxation energy of donor and energy transfer through space is processed by the at least two chromophores.

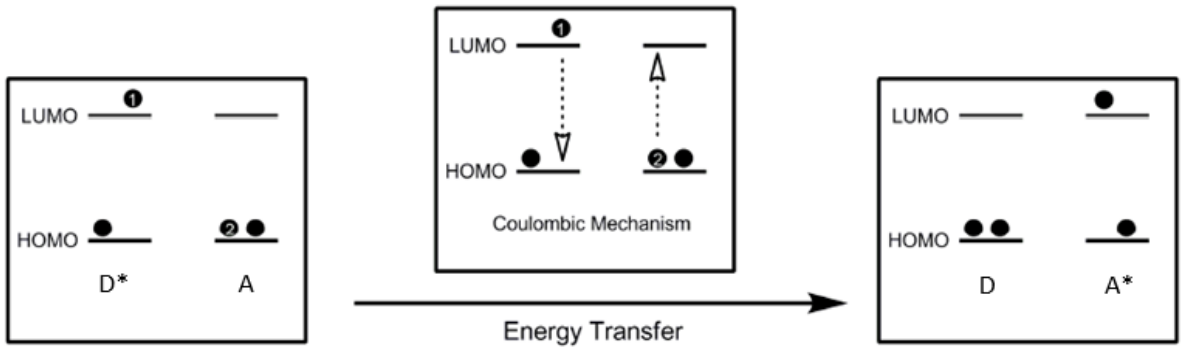

Figure 16: Representation of Columbic Mechanism in FRET.

It is possible to calculate efficiency of FRET energy transfer in two ways: time-resolved and steady state. In time resolved technique, emission lifetime of donor in the presence and in the absence of acceptor is needed. The equation is given below:

$$\mathbf{E = 1 - \tau_{DA} / \tau_{D}}$$

where τ_{DA} and τ_{D} indicates the excited state life time of donor with and without the acceptor and E indicates the energy transfer efficiency.[86,87]

This technique gives more accurate results than steady state technique since inner filter effect and integration error are eliminated. In other words, there is no dependence of emission lifetime of donor on the concentration in this technique.

In steady state technique, the quantum yield decrease of donor unit is the key parameter. The equation for the efficiency is given below:

$$\mathbf{E = 1 - \Phi_{DA} / \Phi_{D}}$$

where Φ_{DA} and Φ_{D} indicate quantum yield of donor with and without acceptor and E is the energy transfer efficiency. On the other hand, there is one more equation, which includes excitation spectra or enhancement in fluorescence emission of the acceptor, used in steady state technique. [88,89]

$$E = A_A(\lambda_D) / A_D(\lambda_D) * [\, I_{AD}(\lambda_A^{em}) / I_A(\lambda_A^{em}) - 1 \,]$$

where I_{AD} and I_A indicates the integrated emission area of acceptor with and without donor at λ_A^{em}. A_A and A_D indicates absorbance values of acceptor and donor at maximum absorbance wavelength of donor.

There are some error sources in this method as mentioned before. Concentration of the samples should be very dilute and it is very crucial since high concentrations can cause self-quenching of fluorescence. This situation called inner filter effect. Therefore, this technique is highly depended to the concentrations.[90]

There are many examples of molecules working with FRET mechanism. For instance, Compound 7 was designed as dendritic chemosensor to Hg^{+2} by Cheng et al. Perylene bisimide (PDI) part of the molecule is acceptor and BODIPY molecules act as donor. (Figure 17)[91]

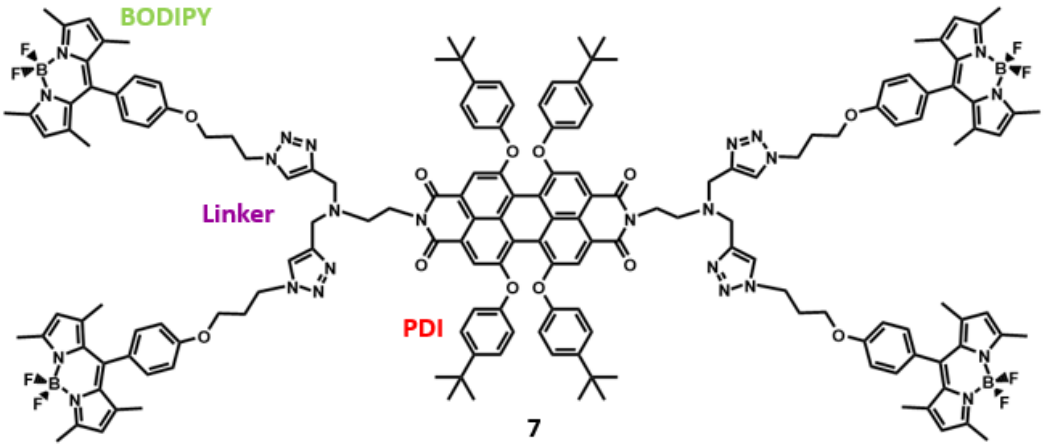

Figure 17: Literature example of molecular sensor works with FRET mechanism.

They observe emission at 600 nm when BODIPY is exposed to 500 nm light. After Hg^{+2} cation binding to the molecule, the emission at 600 nm becomes higher in intensity compare to molecule in absence of mercury cation as shown in Figure 18. They claimed that photo-induced electron transfer (PET) between linker and PDI quenched the observed emission but intensity increase is reported after PET is blocked by the binding of mercury cation to nitrogen atoms in the linker part of the molecule. Additionally, they calculated the FRET efficiency in the

presence of mercury cation as %98. As a result, they reported the new molecule as FRET based chemosensor working with emission intensity change with FRET high efficiency.

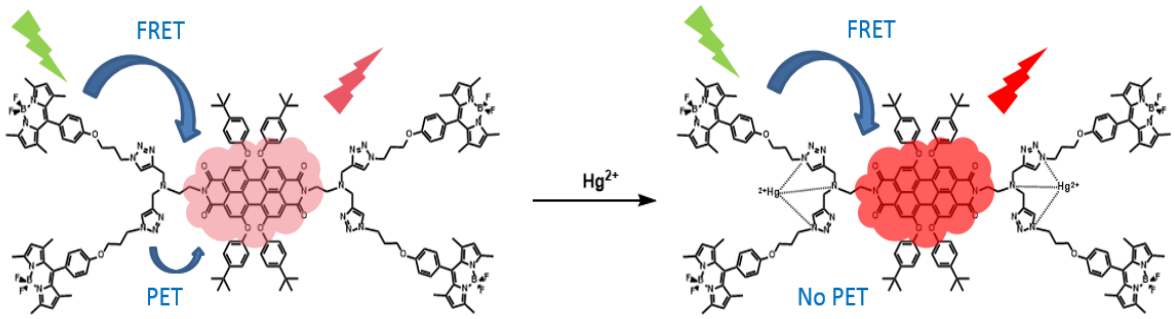

Figure 18: Working mechanism of Compound 7.

Another example for molecules working with FRET mechanism is Compound 8 shown in Figure 17. Compound 8 is synthesized with the aim of achieving pH switching of the triplet excited state formation by Xu et al as shown in Figure 19.[92]

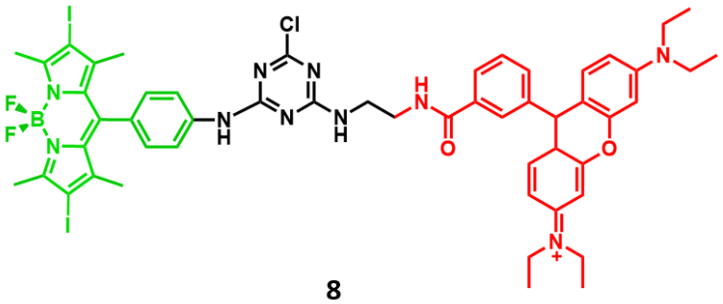

Figure 19: Literature example of molecular sensor works with FRET mechanism.

In this molecule rhodamine unit is acceptor (red) and iodo-BODIPY unit is donor (green) in the acidic environment. Since acceptor is in the open form in acidic environment, spectral overlap occurs and FRET is observed between two moieties and the FRET efficiency is

calculated as 84%. In basic environment, conformational change in acceptor is observed. In other words, the rhodemine part goes to the closed form so emission wavelength of acceptor shifts to lower values and spectral overlap cannot occur. Once iodo-BODIPY is excited, inter system crossing is carried out due to heavy atom effect caused by iodine atoms in the 6 and 2 positions on the BODIPY core. Then, iodo-BODIPY produces singlet oxygen at the end of the relaxation process (Figure 20). As a result, they claimed that FRET is a distraction for inter system crossing for donor part of the molecule and triplet excited state formation is controllable by pH with this molecule and they reported a new molecule generates triplet excited state by pH switching of the environment.

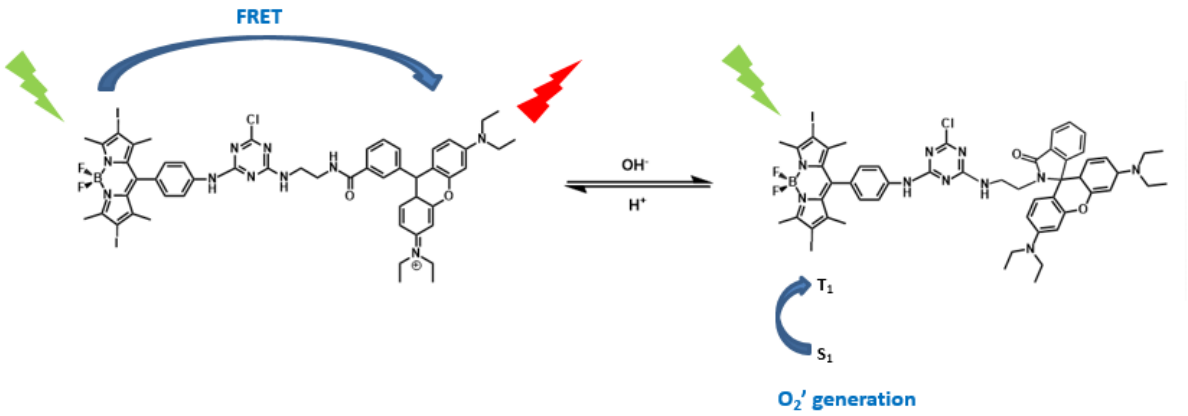

Figure 20: Working mechanism of Compound 8.

1.5. Passerini Reaction

Passerini reaction is a multicomponent reaction that include three compounds union in one step. These three compounds are a carboxylic acid, a carbonyl compound such as a ketone or aldehyde, and an isocyanide.[93] These three compounds produces an α-acyloxy carboxamide.[94] The mechanism includes addition of isocyanide to aldehyde and acyl rearrangement (Figure 21).[95,96]

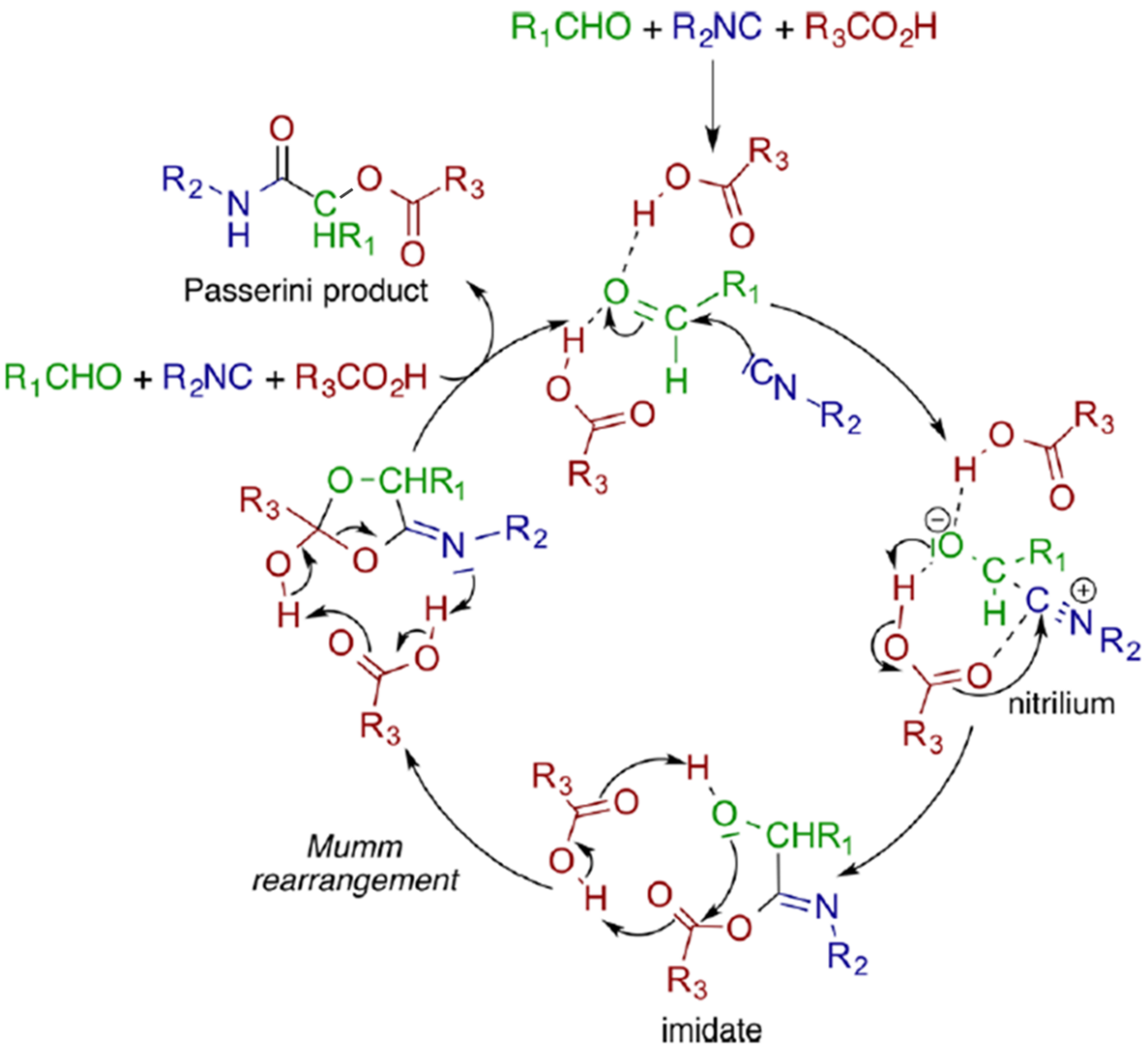

Figure 21: Mechanism of Passerini reaction. Copyright © 2009, American Chemical Society. Reprinted with permission from ref (97)[97]

As shown in the mechanism aldehyde and carboxylic acid units produces an intermediate structure indicated at first place. Then, isocyanide addition to the carbonyl carbon of aldehyde occurs and nitrilium intermediate were produced. Nitrilium intermediate is important and kind of yield determining step. The reason of use of aprotic solvents in Paserrini reaction is nitrilium intermediate is stable in aprotic solvents. Protic solvents cause H-bonding with the intermediate so life time of it become shorter. Then, nucleophilic attack of oxygen to hydrogen of carboxylic acid results imidate intermediate. Mumm rearrangement occurs and finally with the acyl rearrangement, desired product is produced. [97,98]

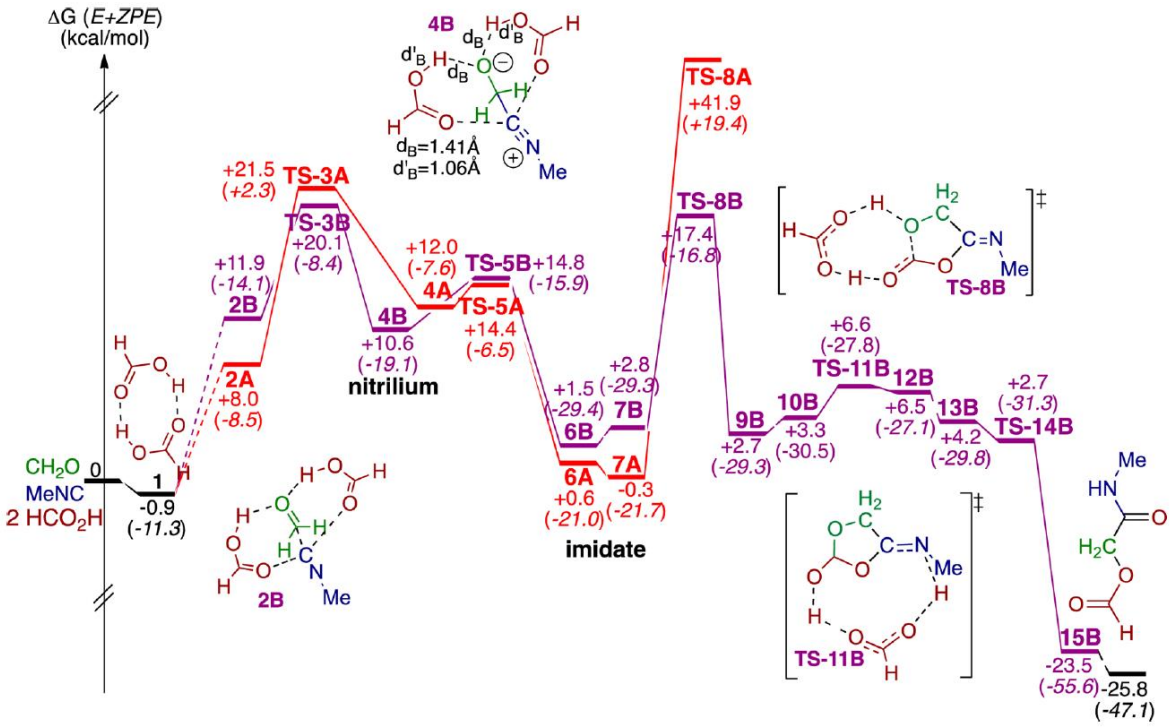

Figure 22: Gibbs free energy profile for the Passerini Reaction in DCM. . Copyright © 2009, American Chemical Society. Reprinted with permission from ref (97)[97]

The reaction mechanism obtained by DFT calculations and Figure 22 shows Gibbs free energies of the reaction intermediates.

The reaction has been used since 1921 and is widely applied in natural product synthesis, drug discovery and delivery and biological probe synthesis. (Figure 22). Vazquez-Romeo et al. used the multicomponent reactions to synthesize BODIPY based probes for imaging of phagocytic macrophages. Probes are shown as Compound 17, 18, 19, 20 and 21. [99]

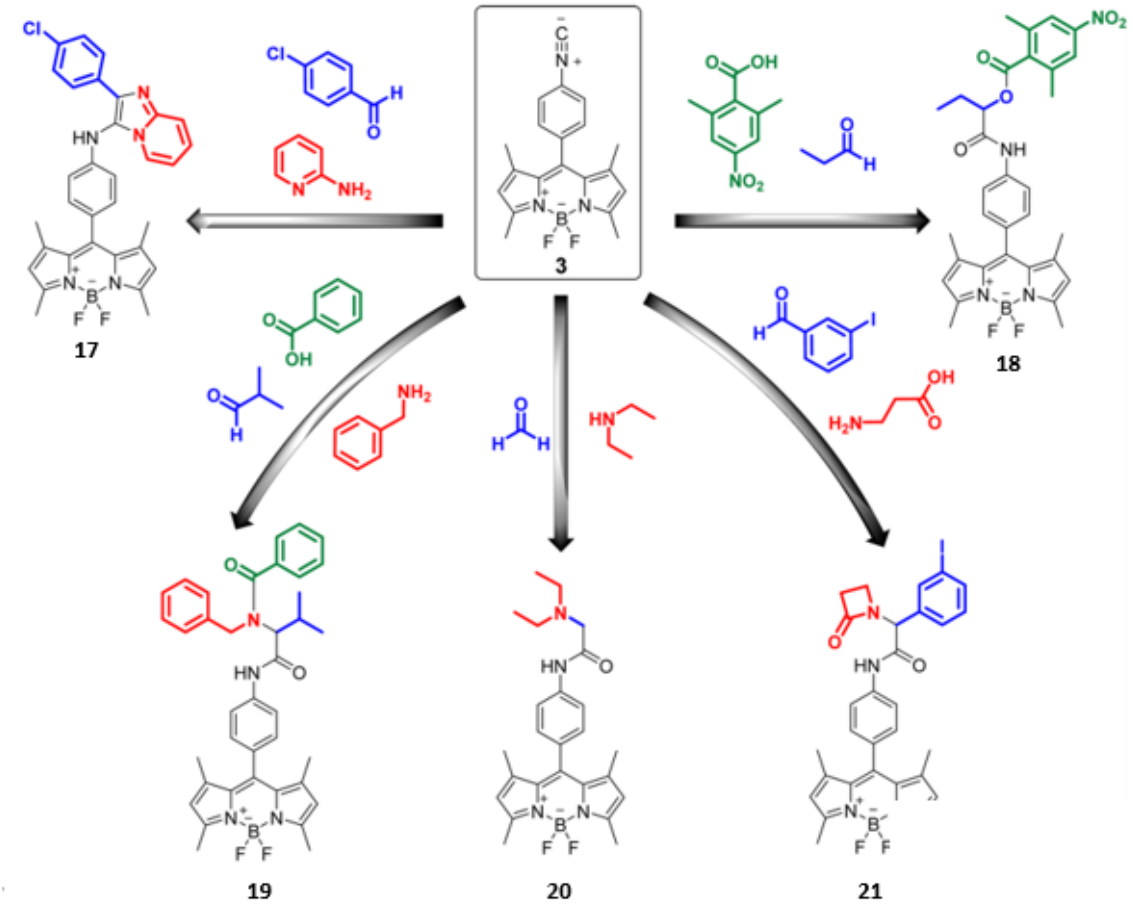

Figure 23: Literature example of synthesized molecules by multicomponent reactions. Copyright © 2009, American Chemical Society. Reprinted with permission from ref (99).[99]

They used multicomponent reaction as a tool to synthesize variable cell permeable fluorescent compounds as shown in Figure 22. They preferred Ugi and Passerini reactions to use in the synthesis pathway of probes.

In addition to that, Lin et al. used Passerini reaction to synthesize micelles for anti-cancer drug delivery as shown as Compound 22 in Figure 23. They synthesized amphiphilic polymers by using Passerini reaction and produce micelles for drug delivery by using the polymers. It is known that glutathione concentration is higher in cancer cells than heathy cells so they chose to include disulfide structure in the micelle polymer since disulfide bonds are sensitive to glutathione. During micelle production, drug was trapped inside of the micelle. Once micelles in the cancer cells, glutathione breaks disulfide bonds and micelle loses its integrity so drug is released as shown in Figure 23.[100]

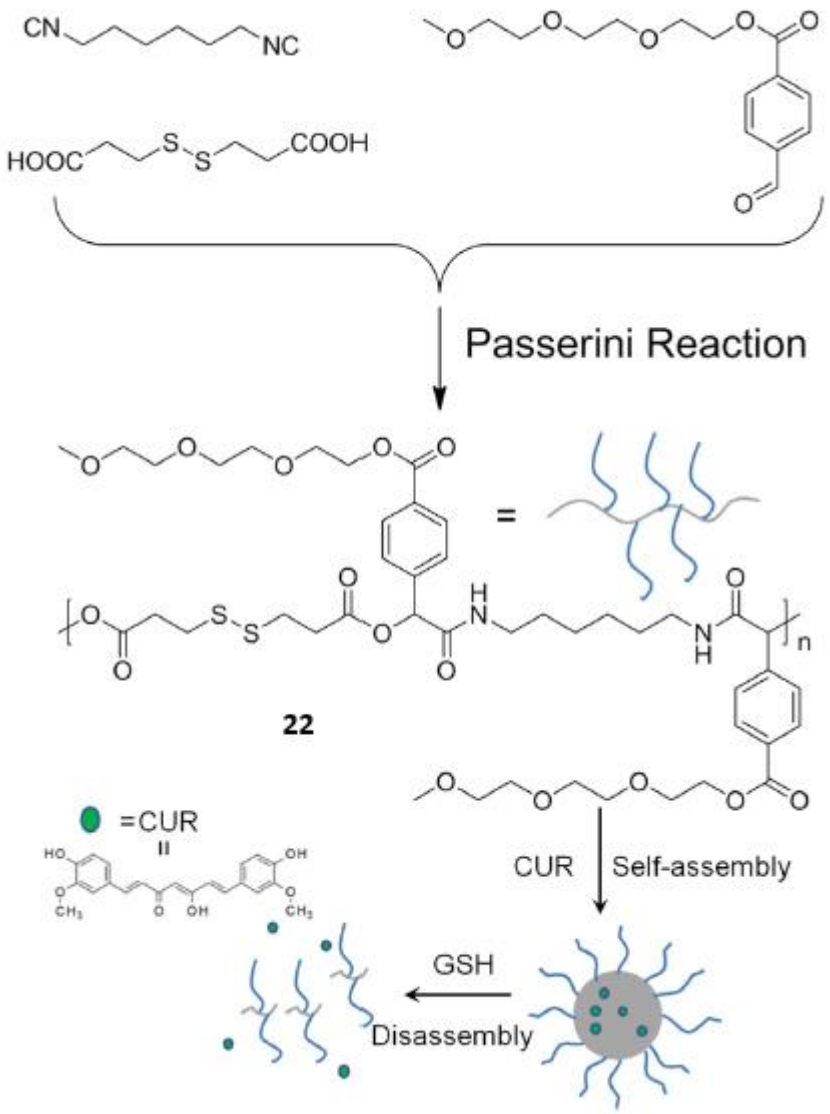

Figure 24: Literature example of synthesized molecules by Passerini reaction. Copyright © 2014 Elsevier B.V. Reprinted with permission from ref (100).[100]

2. EXPERIMENTAL PROCEDURE

2.1. General

All chemicals and solvents used in the project were purchased from Sigma-Aldrich. To purify products, column chromatography on silica gel was performed and as silica Merck Silica gel 60 (particle size: 0.040-0.063 mm, 230-400 mesh ASTM) is used. In order to monitor reactions, thin layer chromatography (Merck TLC Silica gel 60 F254) was used.

^{1}H NMR and ^{13}C NMR spectra were received by using Bruker DPX-400 working at for 100 MHz for ^{13}C NMR and 400 MHz for ^{1}H NMR. The measurements were obtained in $CDCl_3$ and deuterated DMSO with tetramethylsilane as internal standard. Coupling constants (J values) are reported in Hz and chemical shifts are written in parts per million (ppm). Splitting patterns are indicated as s (singlet), d (doublet), t (triplet), q (quartet), m (multiplet), and p (pentet).

Varian Cary-100 spectrophotometer is used to obtain absorption spectra. Fluorescence measurements were taken on a Varian Eclipse spectrofluorometer. All spectroscopy experiments were obtained by using spectrophotometric grade solvents. Mass spectroscopy measurements were performed by using MSBQTOF at Bilkent University, UNAM, Mass Spectrometry Facility.

2.2. Synthesis Pathway

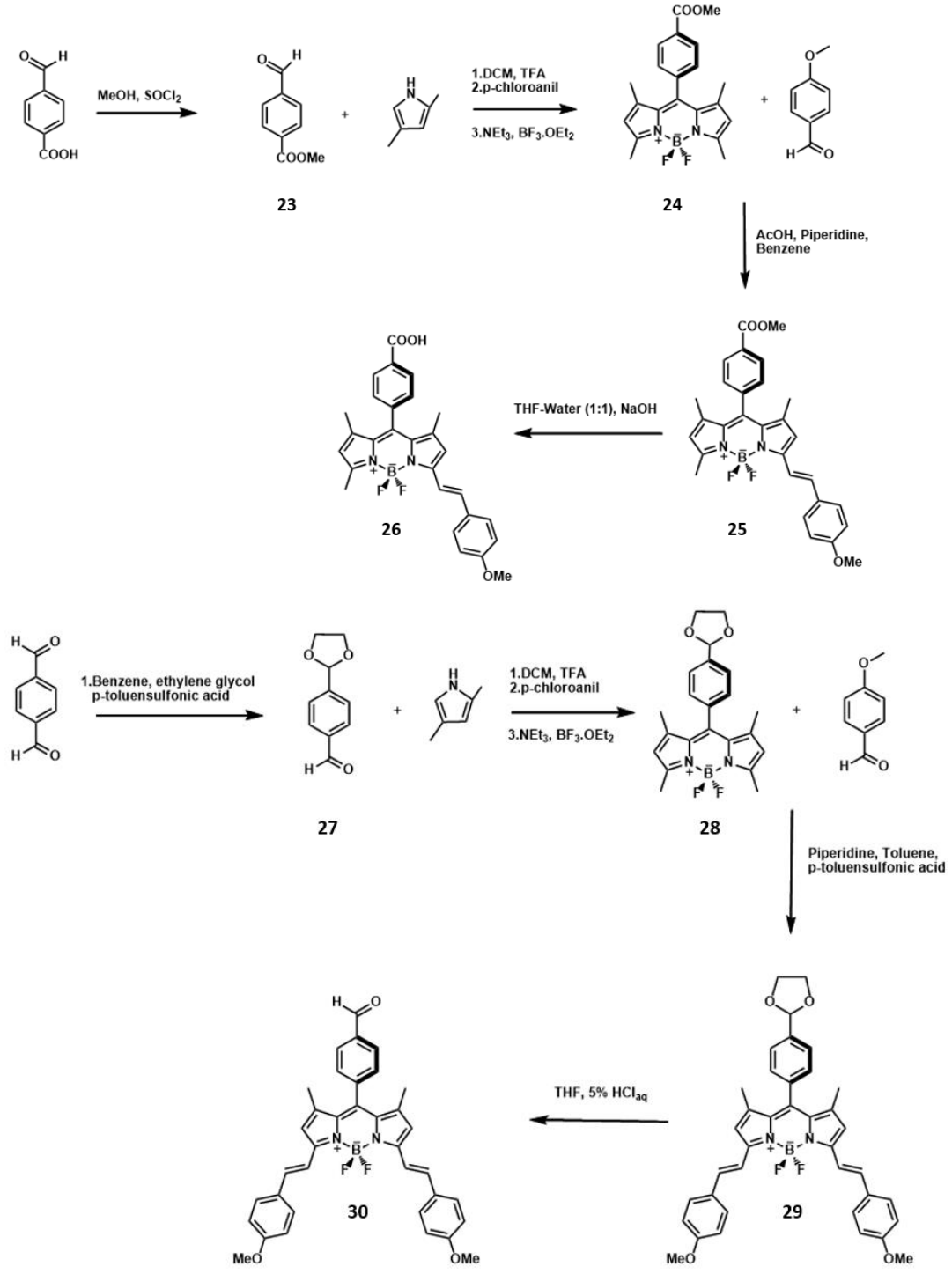

Figure 25: Synthesis pathway for Compound 26 and 30.

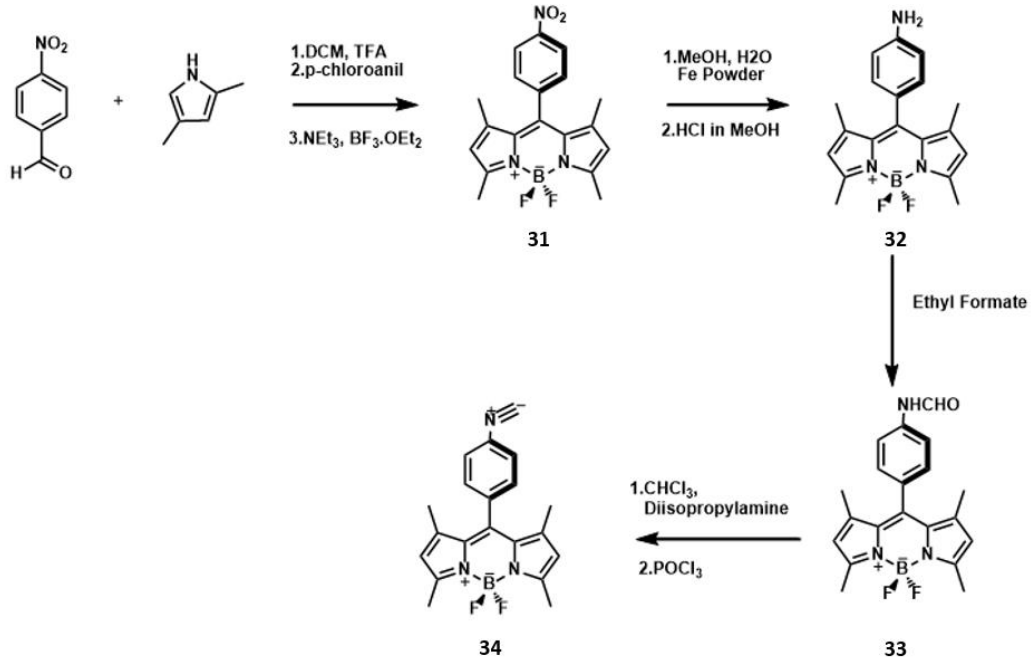

Figure 26: Synthesis pathway for Compound 34.

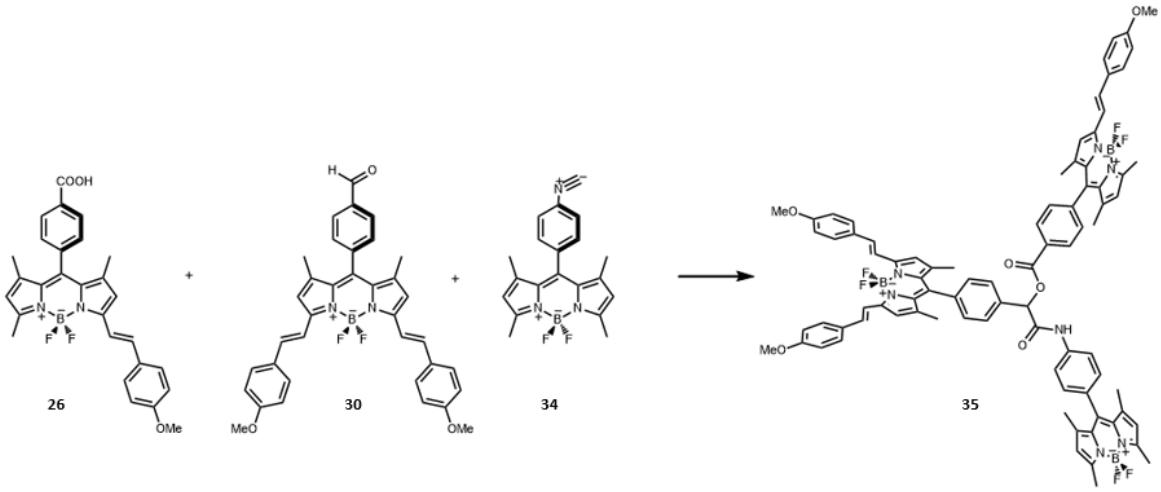

Figure 27: Synthesis pathway for the Compound 35.

2.3. Synthesis

2.3.1. Synthesis of Compound 23

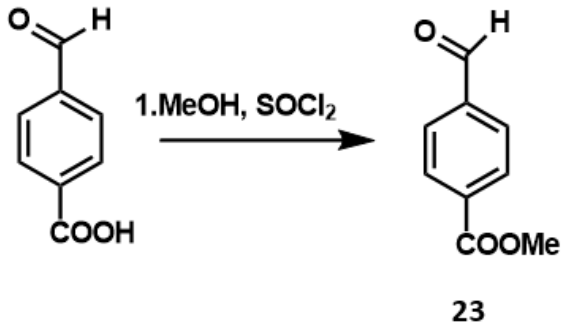

Figure 28: Synthesis of Compound 23.

4- carboxybenzaldehyde (13mmol, 2g) was dissolved in 275 ml methanol and the solution cooled to the 0 C˚. Then, dropwise addition of thionylchloride (15 ml) was performed. Reaction followed by TLC monitoring and after all starting material is finished, methanol was vaporized with the addition of DCM (100 ml x 3). Then, organic layer concentrated in vacuo. (Yield: 90%, 1.92 g)

^{1}H NMR (400 MHz, $CDCl_3$): δ 9.87 (s, 1H), 7.91 (d, J = 7.0 Hz, 2H), 7.71 (d, J = 7.2 Hz, 2H), 3.72 (s, 3H).

^{13}C NMR (100 MHz, $CDCl_3$): δ 191.3, 165.6, 139.0, 129.9, 129.2, 52.2.

2.3.2. Synthesis of Compound 24

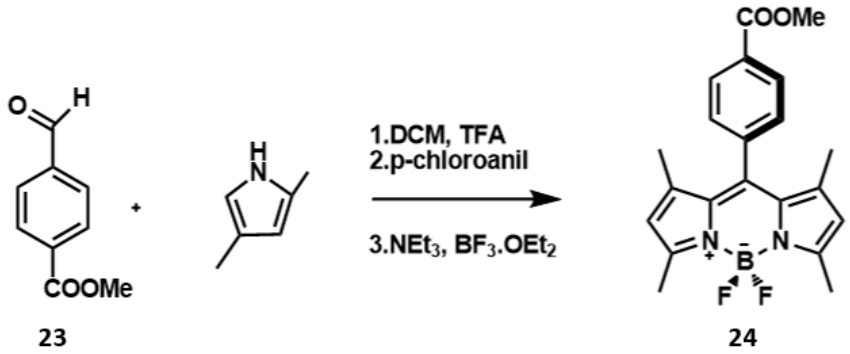

Figure 29: Synthesis of Compound 24.

By using argon degassed DCM, a solution of 400mL DCM, 2,4-dimethyl pyrrole (9,81 mmol, 2.2 mL) and compound 23 (4.905 mmol, 0.805 g) was prepared. Then, 1 drop of TFA was added to the solution. The reaction mixture was stirred under inert atmosphere for 1 day at room temperature. p-chloroanil (4.905 mmol, 1.207 g) was added to the mixture and stirred for 40 min. Then, Et_3N (8 mL) and $BF_3.OEt_2$ (8 mL) was added with 40 min waiting time and reaction mixture was stirred for 90 min. Extraction is done by using brine (3x100mL). As a drying agent sodium sulfate is used. The organic layer was concentrated in vacuo and residue was purified by column chromatography (DCM). (Yield 30%, 562 mg)

^{1}H NMR (400 MHz, $CDCl_3$): δ 8.20 (d, J = 4.7 Hz, 2H), 7.43 (d, J = 4.7 Hz, 2H), 6.01 (s, 2H), 3.99 (s, 3H), 2.58 (s, 6H), 1.38 (s, 6H).

^{13}C NMR (100 MHz, $CDCl_3$): δ 166.4, 156.0, 142.9, 140.2, 139.9, 130.9, 130.8, 130.3, 128.4, 121.5, 52.4, 14.6, 14.5.

ESI-HRMS ($M-H^+$) calculated 382.1773, found 382.1786, Δ= -3.26ppm

2.3.3. Synthesis of Compound 25

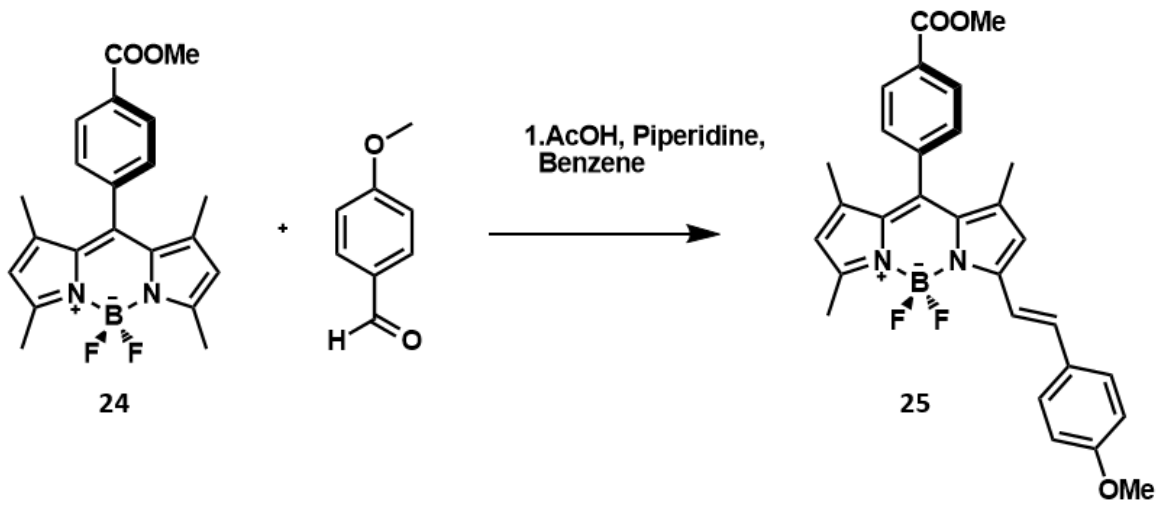

Figure 30: Synthesis of Compound 25.

Compound 24 (100 mg, 0.25 mmol), 200 µl acetic acid and 200 µl piperidine were added to the 20 mL benzene containing round bottomed flask. Reaction mixture was heated under reflux by using Dean Stark trap. The production of the Compound 25 is monitored by TLC. Then, the solution was cooled to the room temperature and solvent was evaporated. Extraction is done by using water (3x 25 mL) and DCM (20 mL). As a drying agent sodium sulfate is used. The organic layer was concentrated in vacuo and residue was purified by column chromatography (DCM : Hexane) (1:1). (Yield: 10%, 12.5 mg)

^{1}H NMR (400 MHz, $CDCl_3$): δ 8.21 (d, J = 8.0 Hz, 2H), 7.57 (d, J = 8.9 Hz, 2H), 7.46 (d, J = 7.9 Hz, 2H), 7.24 (d, J = 15.9 Hz, 1H), 6.93 (d, J = 8.4 Hz, 2H), 6.62 (s, 1H), 6.03 (s, 2H), 4.00 (s, 3H), 3.87 (s, 3H), 2.62 (s, 3H), 1.43 (s, 3H), 1.39 (s, 3H).

^{13}C NMR (100 MHz, $CDCl_3$): δ 166.5, 160.6, 155.1, 153.9, 142.3, 141.9, 140.1, 138.4, 138.1, 136.6, 130.8, 130.3, 129.6, 129.5, 129.4, 129.4, 129.3, 129.1, 128.7, 121.3, 117.8, 116.9, 114.4, 114.3, 55.4, 52.4, 15.8, 15.0, 14.8, 14.7, 14.5.

ESI-HRMS ($M-H^+$) calculated 500.2191, found 500.2200, Δ= -1.78 ppm

2.3.4. Synthesis of Compound 26

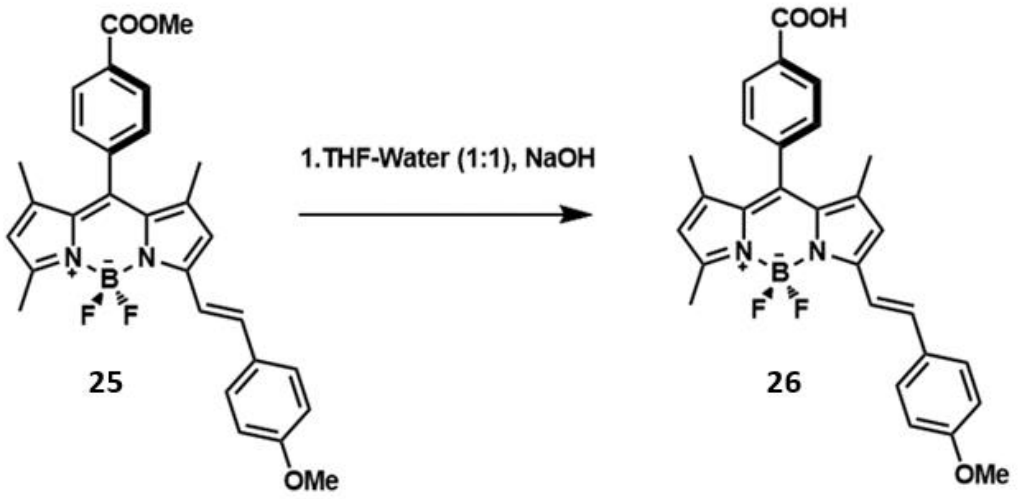

Figure 31: Synthesis of Compound 26.

Compound 25 (0.046 g, 0.091 mmol) was dissolved in 10 ml THF-water (1:1) solution and sodium hydroxide (0.011 g, 0.3 mmol) is dissolved in little amount of water and added to the solution. The reaction heated to 50 C˚. Production of compound 26 was monitored by TLC. After reaction is finished, 10% HCl_{aq} solution was added to reaction mixture until its pH is 3-4. Then, extraction was performed by using water (3x 25 mL) and DCM (20 mL). As a drying agent sodium sulfate is used. The organic layer was concentrated in vacuo and residue was purified by column chromatography (DCM : MeOH) (95:5). (Yield: 90%, 39 mg).

^{1}H NMR (400 MHz, d-DMSO) δ 8.10 (d, J = 8.3 Hz, 2H), 7.62 – 7.48 (m, 6H), 7.37 (d, J = 15.7 Hz, 1H), 7.04 (d, J = 8.8 Hz, 2H), 6.94 (s, 1H), 6.21 (s, 1H), 3.82 (s, 3H), 2.68 (s, 3H), 1.40 (s, 3H), 1.35 (s, 3H).

ESI-HRMS ($M-H^+$) calculated 484.1889, found 484.1917, Δ= -5.57 ppm

2.3.5. Synthesis of Compound 27

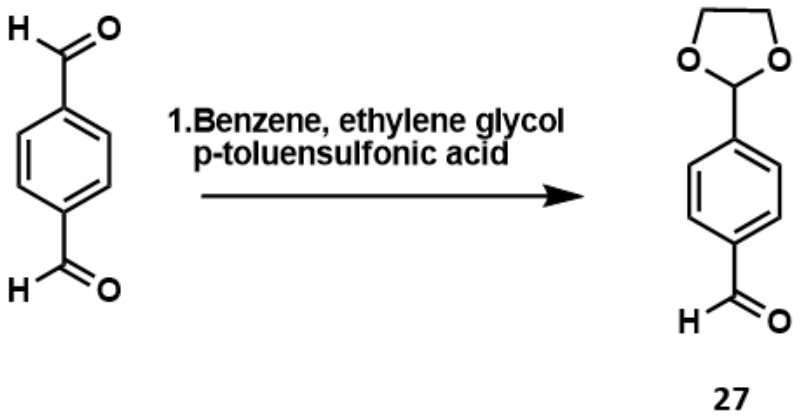

Figure 32: Synthesis of Compound 27.

Solution of terephthalaldehyde (1 g, 7.46 mmol) and ethylene glycol (277 ml, 4.97 mmol) is prepared and catalytic amount of p-toluensulfonic acid (0.50 g, 2.63 mmol) was added to the solution. Dean-stark apparatus was filled with benzene and the reaction mixture refluxed for 24h. After drying benzene, extraction was done by using DCM and water (15mL x 3). As a drying agent sodium sulfate is used. The organic layer was concentrated in vacuo residue was purified by column chromatography (MeOH : EtOAc) (5:95). (Yield: 30%, 398 mg).

^{1}H NMR (400 MHz, $CDCl_3$): δ 9.93 (s, 1H), 7.80 (d, J = 8.2 Hz, 2H), 7.55 (d, J = 8.2 Hz, 2H), 5.76 (s, 1H), 4.05 – 3.98 (m, 2H), 3.98 – 3.90 (m, 2H).

^{13}C NMR (100 MHz, $CDCl_3$): δ 191.8, 144.4, 136.8, 129.6, 127.0, 102.7, 65.3.

ESI-HRMS ($M\text{-}H^+$) calculated 178.0629, found 179.0718, Δ= -8.6 ppm

2.3.6. Synthesis of Compound 28

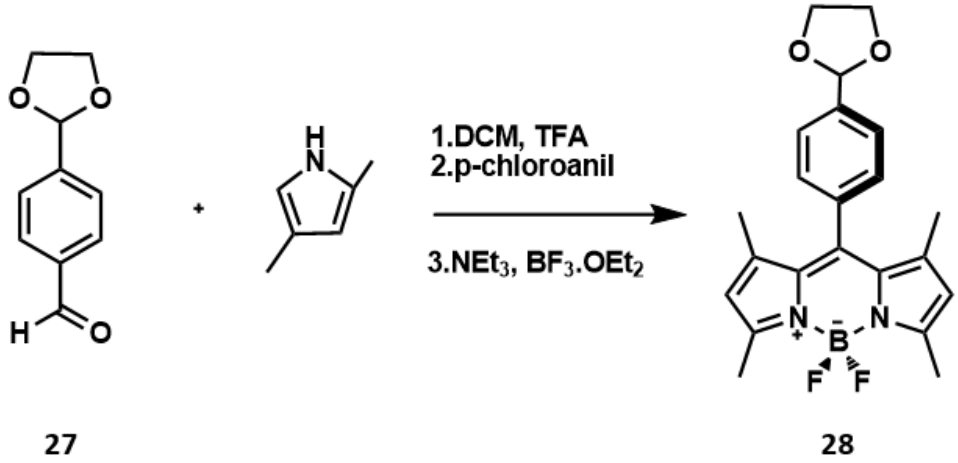

Figure 33: Synthesis of Compound 28.

By using argon degassed DCM, a solution of 400mL DCM, 2,4-dimethyl pyrrole (9,81 mmol, 2.2 mL) and compound 27 (4.905 mmol, 0.874 g) was prepared. Then, 1 drop of TFA was added to the solution. The reaction mixture was stirred under inert atmosphere for 1 day at room temperature. p-chloroanil (4.905 mmol, 1.207 g) was added to the mixture and stirred for 40 min. Then, Et_3N (8mL) and $BF_3.OEt_2$ (8mL) was added with 40 min waiting time and reaction mixture was stirred for 90 min. Extraction is done by using brine (3x100 mL). As a drying agent sodium sulfate is used. The organic layer was concentrated in vacuo and residue was purified by column chromatography (DCM). (Yield: 20%, 388 mg)

^{1}H NMR (400 MHz, $CDCl_3$): δ 7.64 (d, J = 8.0 Hz, 2H), 7.34 (d, J = 8.2 Hz, 2H), 6.00 (s, 2H), 5.88 (s, 1H), 4.25 – 4.16 (m, 2H), 4.13 – 4.03 (m, 2H), 2.58 (s, 6H), 1.39 (s, 6H).

^{13}C NMR (100 MHz, $CDCl_3$): δ 155.6, 143.1, 141.2, 138.9, 135.9, 131.3, 128.0, 127.4, 121.3, 121.4, 103.3, 65.4, 14.5.

ESI-HRMS ($M\text{-}H^+$) calculated 395.1857, found 396.1950, Δ= -5.22 ppm

2.3.7. Synthesis of Compound 29

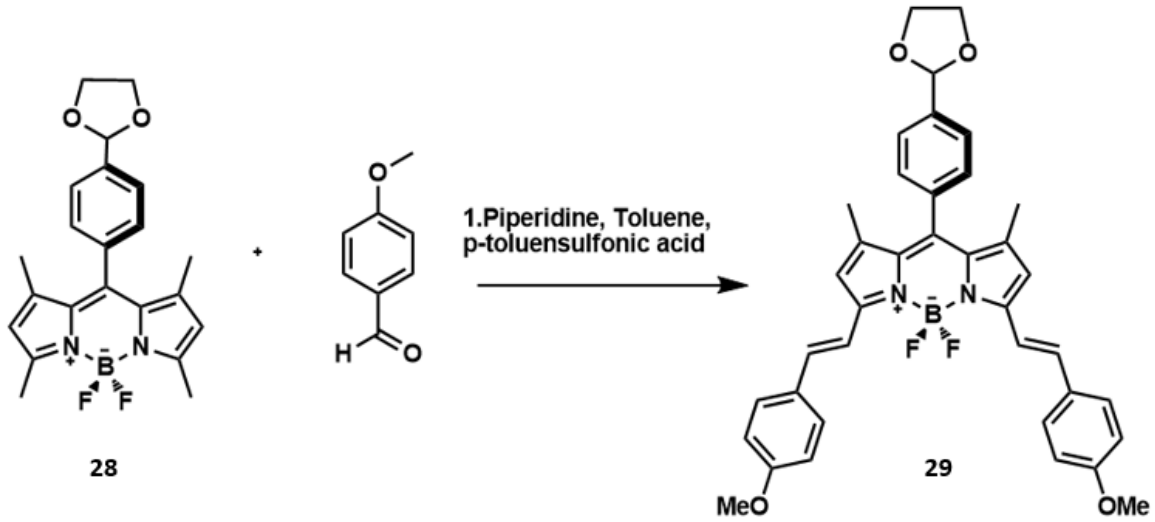

Figure 34: Synthesis of Compound 29.

Compound 28 (100 mg, 0.25 mmol), catalytic amount of p-toluenesulfonic acid and 158 µl piperidine were added to the 20 mL toluene containing round bottomed flask. Reaction mixture was heated under reflux by using Dean Stark trap. The production of the compound 29 is monitored by TLC. Then, the solution was cooled to the room temperature and solvent was evaporated. Extraction is done by using water (3x 25 mL) and DCM (20 mL). As a drying agent sodium sulfate is used. The organic layer was concentrated in vacuo and residue was purified by column chromatography (MeOH : DCM) (5:95). (Yield: 50%, 79 mg)

^{1}H NMR (400 MHz, $CDCl_3$): δ 7.65 (d, J = 8.1 Hz, 4H), 7.61 (d, J = 8.8 Hz, 4H), 7.39 (d, J = 8.0 Hz, 2H), 7. 4.24 – 4.20 (m, 2H), 4.14 – 4.10 (m, 2H), 4.25 – 4.08 (m, 2H), 3.88 (s, 6H), 1.46 (s, 6H).

^{13}C NMR (100 MHz, $CDCl_3$): δ 160.4, 152.8, 141.8, 138.8, 136.3, 135.8, 129.6, 129.1, 128.6, 128.3, 127.3, 117.6, 117.3, 114.3, 103.4, 103.4, 65.4, 55.38, 14.8.

ESI-HRMS ($M-H^+$) calculated 632.2767 found 632.2681, Δ= 13.61 ppm

2.3.8. Synthesis of Compound 30

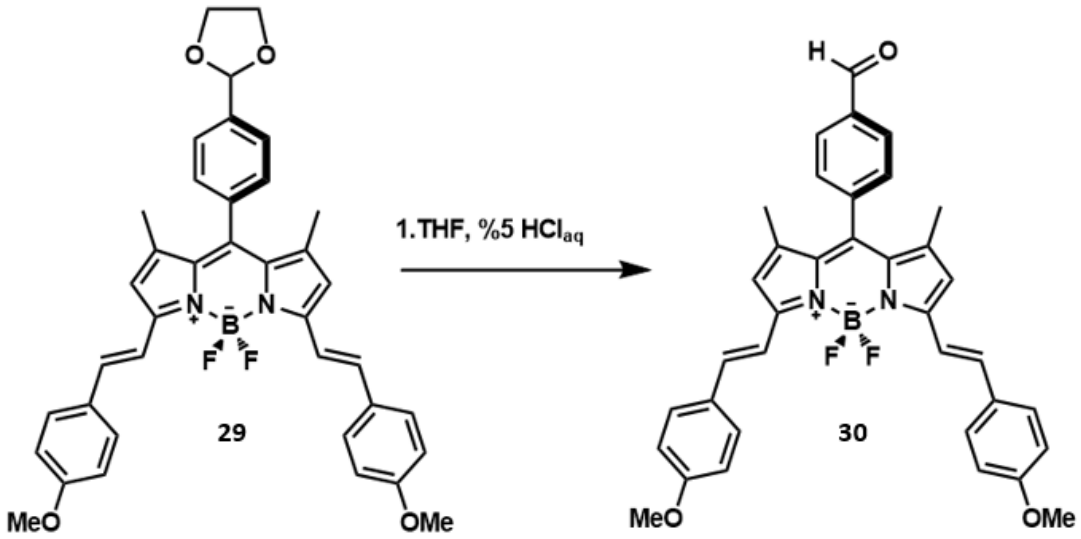

Figure 35: Synthesis of Compound 30.

To the solution of compound 7 (200 mg, 0.32 mmol) in THF, 15 mL %5 HCl_{aq} was added and the solution was stirred overnight. Then, 100 mL DCM was added and solution exracted with 1 M $NaHCO_3$ solution (3 x 100 mL). As a drying agent sodium sulfate is used. The organic layer was concentrated in vacuo and residue was purified by column chromatography (%5 MeOH : DCM). (Yield: 90%, 170 mg)

^{1}H NMR (400 MHz, $CDCl_3$): δ 10.15 (s, 1H), 8.06 (d, J = 7.9 Hz, 2H), 7.58-7.66 (m, 8H), 6.97 (d, J = 4.1 Hz, 4H), 6.65 (s, 2H), 6.02 (s, 2H), 3.89 (s, 6H), 1.44 (s, 6H).

^{13}C NMR (100 MHz, $CDCl_3$): δ 191.5, 160.6, 141.8, 141.2, 136.6, 136.3, 130.2, 129.8, 129.5, 129.5, 129.1, 125.5, 117.9, 117.1, 114.3, 114.0, 55.4, 14.8.

ESI-HRMS ($M-H^-$) calculated 586.23645, found 586.23916, Δ= -5.41ppm

2.3.9. Synthesis of Compound 31

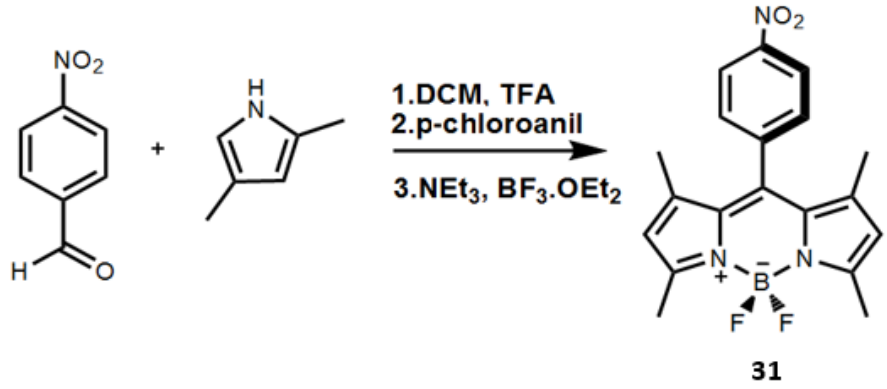

Figure 36: Synthesis of Compound 31.

By using argon degassed DCM, a solution of 400mL DCM, 2,4-dimethyl pyrrole (9,81 mmol, 2.20 mL) and 4-nitrobenzaldehyde (4.90 mmol, 0.74 g) was prepared. Then, 2 drops of TFA was added to the solution. The reaction mixture was stirred under inert atmosphere for 1 day at room temperature. p-chloroanil (4.905 mmol, 1.207 g) was added to the mixture and stirred for 40 min. Then, Et_3N (8 mL) and $BF_3.OEt_2$ (8 mL) was added with 40 min waiting time and reaction mixture was stirred for 90 min. Extraction is done by using brine (3 x 100 mL). As a drying agent sodium sulfate is used. The organic layer was concentrated in vacuo and residue was purified by column chromatography (DCM). (Yield: 30%, 542mg)

^{1}H NMR (400 MHz, $CDCl_3$): δ 8.41 (d, J = 8.8 Hz, 2H), 7.57 (d, J = 8.8 Hz, 2H), 6.04 (s, 2H), 2.59 (s, 6H), 1.39 (s, 6H).

^{13}C NMR (101 MHz, $CDCl_3$): δ 156.7, 148.4, 142.5, 142.0, 129.7, 129.6, 124.5, 124.3, 121.89, 14.7, 14.6.

ESI-HRMS ($M-H^-$) calculated 367.14237, found 567.14224, Δ= 0.35 ppm

2.3.10. Synthesis of Compound 32

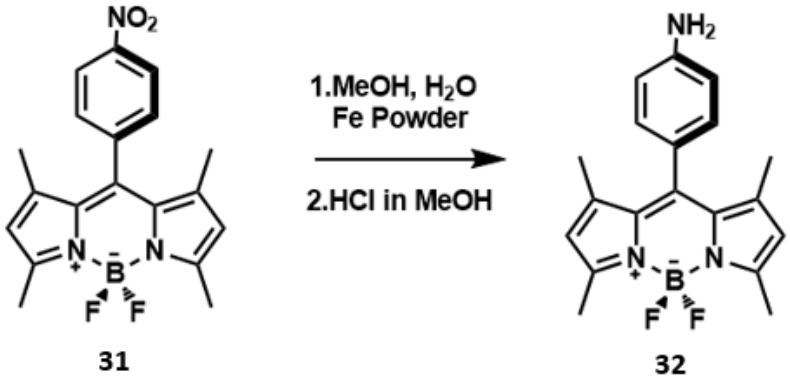

Figure 37: Synthesis of Compound 32.

To solution of compound 31 (240 mg, 0.66 mmol) and methanol (10 mL), H_2O (4 mL) and Fe powder (600 mg, 10.8 mmol) were added. After the solution mixture was heated to reflux, dropwise addition of HCl in methanol (4 mL, 0.5 mol/L) was performed and reaction mixture refluxed for 3h. After cooling the reaction to the RT, the mixture was filtrated and concentrated in vacuo and residue was purified by column chromatography (DCM). (Yield: 65%, 145mg)

^{1}H NMR (400 MHz, $CDCl_3$) δ 7.02 (d, J = 6.6 Hz, 2H), 6.79 (d, J = 6.6 Hz, 2H), 5.99 (s, 2H), 3.75 (s, 2H), 2.57 (s, 6H), 1.52 (s, 6H).

^{13}C NMR (101 MHz, $CDCl_3$) δ 155.0, 147.1, 143.7, 132.1, 129.0, 124.7, 121.0, 115.4, 14.6, 14.5.

ESI-HRMS ($M-H^+$) calculated 339.18274, found 339,18493 Δ= -6.36ppm

2.3.11. Synthesis of Compound 33

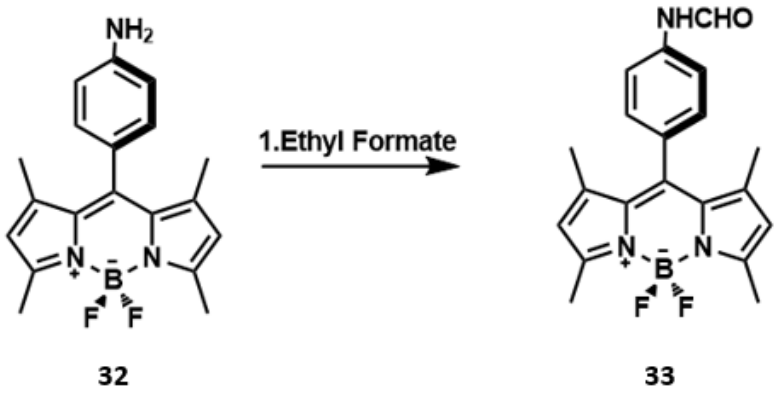

Figure 38: Synthesis of Compound 33.

Ethyl formate (5 mL, 0.06 mmol) was added to compound 32 (50 mg, 0.15 mmol) in a sealed tube. The solution heated to 60℃ for 4 days. Then, reaction mixture extracted by using DCM (5 mL) and NH_4Cl (5 mL x 3). As a drying agent sodium sulfate is used. The organic layer was concentrated in vacuo and residue was purified by column chromatography (DCM). (Yield: 70%, 38.55 mg)

^{1}H NMR (400 MHz, $CDCl_3$) δ 8.44 (s, 1H), 7.73 (d, J = 8.2 Hz, 1H), 7.31 – 7.24 (m, 4H), 6.00 (s, 2H), 2.57 (s, 6H), 1.44 (s, 6H).

^{13}C NMR (101 MHz, $CDCl_3$) δ 158.9, 155.6, 143.1, 137.7, 129.8, 128.9, 121.4, 121.3, 120.1, 118.8, 14.6, 14.6.

ESI-HRMS ($M-H^-$) calculated 365.1667, found 365.1654 Δ= -6.29ppm

2.3.12. Synthesis of Compound 34

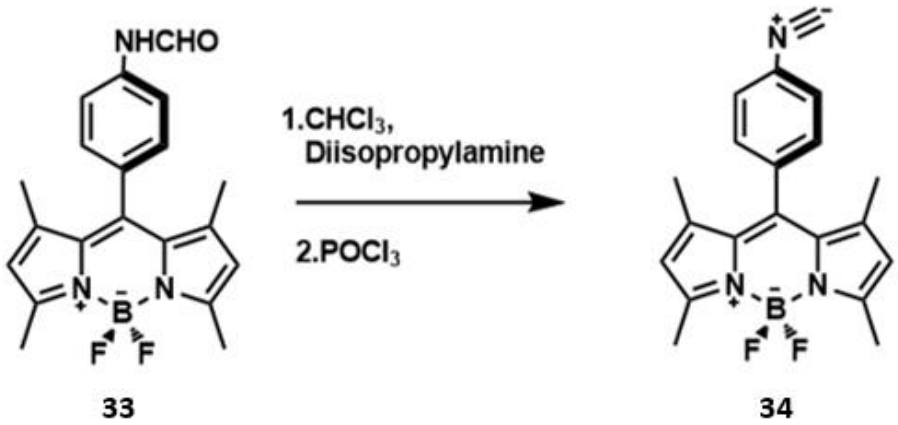

Figure 39: Synthesis of Compound 34.

To the solution of Compound 33 (0,380 mg, 1.05 mmol) in degassed $CHCl_3$ (11 mL), diisopropylamine (1 mL, 7.37 mmol) was added. The solution was cooled to 0℃ and dropwise addition of $POCl_3$ (240 µL, 2.60 mmol) was performed. Then, the reaction was stirred at 0℃ for 6 h. After that 10 mL of 2 M $NaHCO_3$ was added and extraction was made with DCM (3 mL x 3). As a drying agent sodium sulfate is used. The organic layer was concentrated in vacuo and residue was purified by column chromatography (MeOH : DCM) (5:95). (Yield: 98%, 360 mg).

^{1}H NMR (400 MHz, $CDCl_3$) δ 7.54 (t, J = 10.6 Hz, 2H), 7.39 (d, J = 8.1 Hz, 2H), 6.02 (s, 2H), 2.58 (s, 6H), 1.40 (s, 6H).

ESI-HRMS ($M-H^-$) calculated 347.1525, found 347.1556 Δ= -8.82ppm

2.3.13. Synthesis of Compound 35

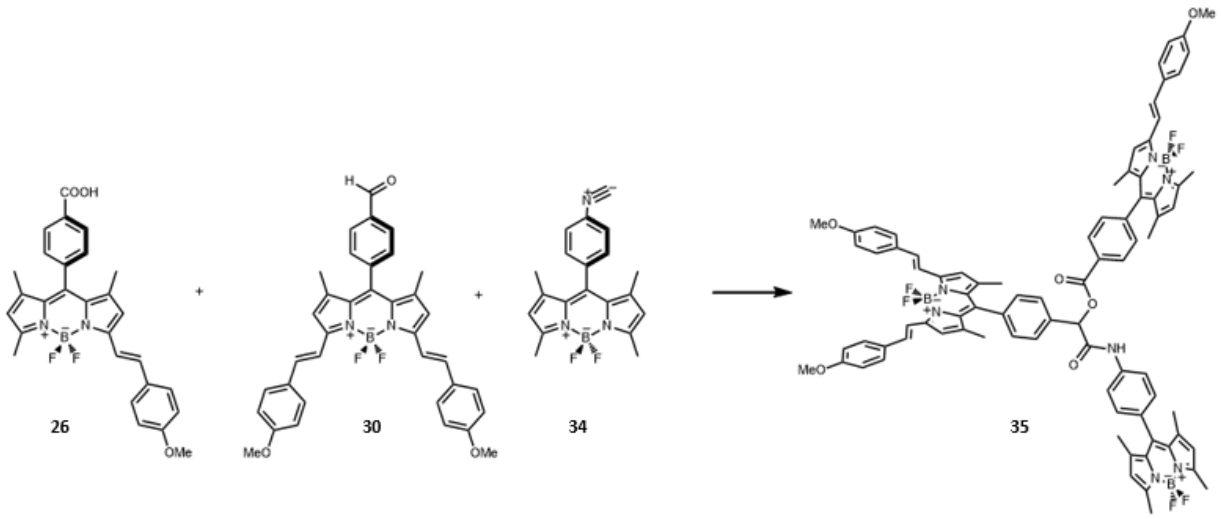

Figure 40: Synthesis of Compound 35.

Compound 26 (0.030 g, 0.061 mmol), compound 30 (0.036 g, 0.061 mmol) and compound 34 (0.021 mg, 0.061 mmol) dissolved in 1 ml THF. They stirred and refluxed for 2 days.

3. RESULTS & DISCUSSION

Scientists try to understand and create similar mechanisms found in nature in order to build the systems and apply into human life. These systems are mainly biological systems like photosynthesis, enzyme working systems, cell environment and so on. Photosynthesis is one of the key events to maintain continuity of life. Light harvesting is basic procedure of photosynthesis and the key process of green life. Therefore, it is one of that processes mimicked by scientists. Supramolecular chemistry is very convenient to be used in creating such systems. Therefore, there are many applications in literature used in solar cells mentioned in introduction part. Light harvesting mechanisms consists of many units that absorb energy at some wavelength of sun light and channel through one center at higher certain wavelength. One of the units that transfer energy to the reaction center is called energy transfer cascade and large energy transfer systems may composed of many different type of cascades. Consequently, light harvesting system in nature comprise of cascade units in order to collect energy at certain wavelength in reaction center.

In this study, an energy transfer cascade is designed to be used in light harvesting systems. This cascade works with Förster type (through space) energy transfer mechanism. It has three units and energy transfer will occur between them. The units are synthesized and they got together by self-assembly to form a cascade system with the help of Passerini reaction.

As shown in synthesis pathway (Figure 40), three different BODIPY molecules are synthesized with carboxylic acid, aldehyde and isocyanide units. The units are needed for Passerini reaction so in that way they can get together and form energy transfer cascade in one step as shown in Figure 41. Absorption and emission of BODIPY units tuned by Knoevenagel condensation reaction. There were some problems that we faced during synthesis.

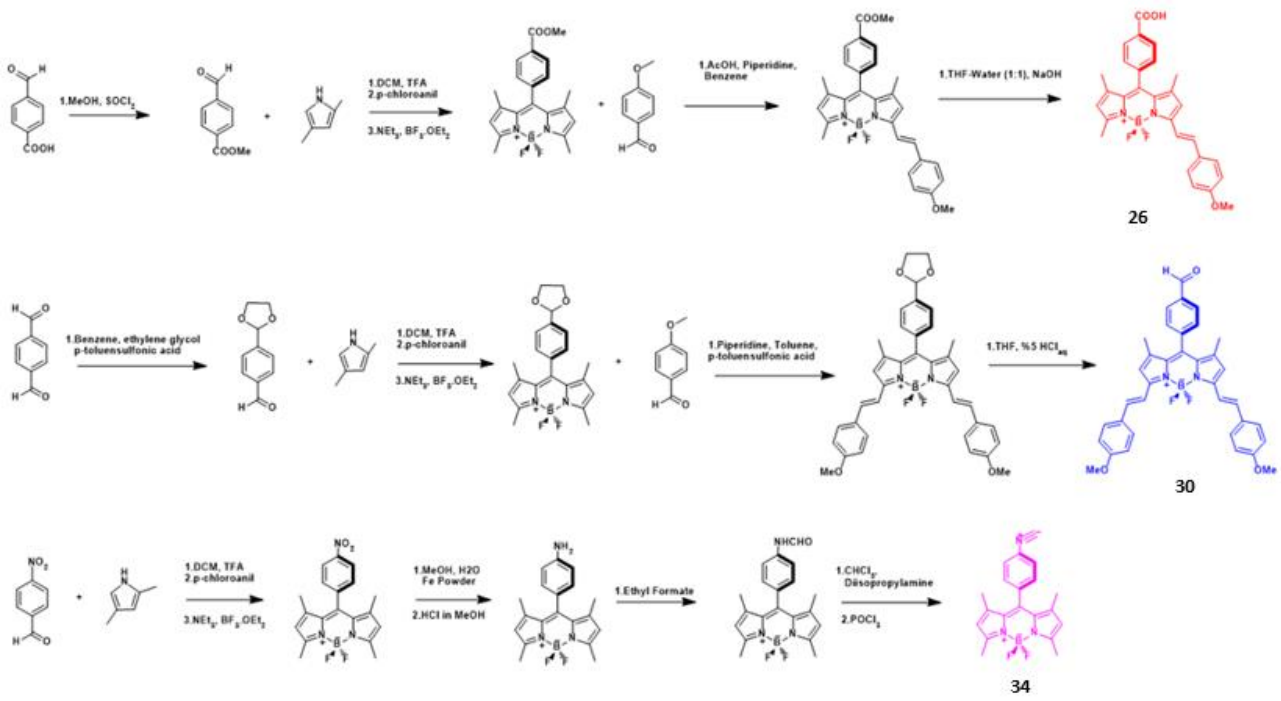

Figure 41: Synthesis pathway

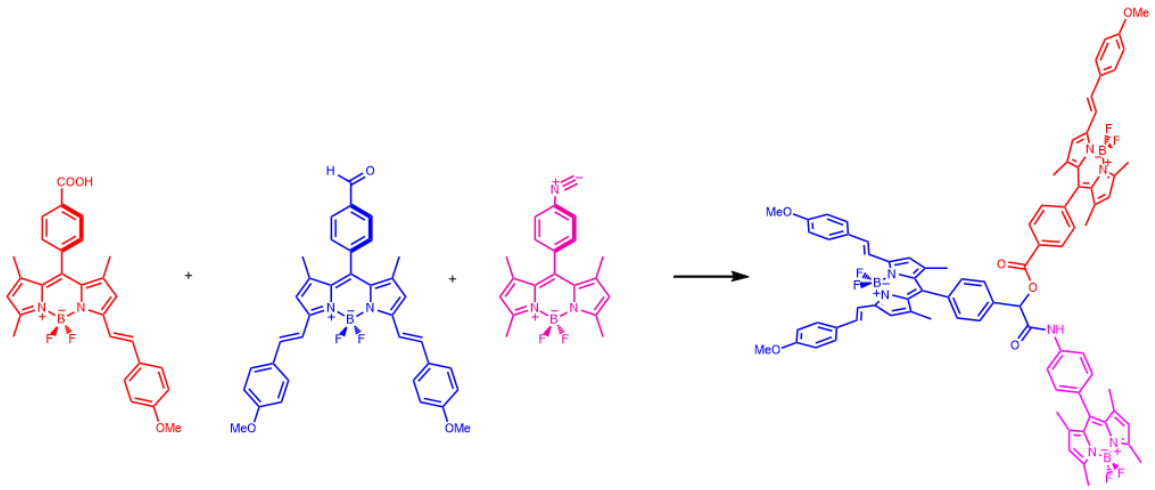

Figure 42: Passerini reaction

As a first step to obtain Compound 26, an ester (Compound 23) produced from the 4-carboxybenzaldehyde and three hydrogens in the methyl ester is shown in ^{1}H NMR data of Compound 23 at 3.72 ppm. Before doing that, we tried to continue with the BODIPY with carboxylic acid unit. However, the purification of the substance was very time and energy consuming and even the pure material obtained, it is impossible to have pure monostyryl-BODIPY after Knoevenagel condensation. That is why, we preferred to begin with Compound 23.

Compound 24 was synthesized by using Compound 23 and the ^{1}H NMR spectrum of Compound 24 contains basic BODIPY peaks as expected. Two doublets in aromatic region from phenylene at meso position, one singlet at around six from hydrogens on 2 and 6 positions and two singlet at around 2.5 and 1.3 ppm methyl hydrogens at 5,3 and 1,7 positions. The reason of down field shift of methyl hydrogens on 5, 3 positions is the electron withdrawing effect of nitrogen atom in BODIPY core.

Compound 25 was synthesized with Knoevenagel condensation reaction. The yield of Compound 25 is low since the Knoevenagel reaction tend to produce distyryl product. As a result, the reaction was had to be finished before starting material ends. If the ^{1}H NMR data of Compound 25 is analyzed, it is possible to see additional hydrogen peaks due to the asymmetry of the compound. There are two pyrrolic hydrogen peaks separately and three different peaks for methyl group hydrogens on 1,7 and 5 positions. Additional methoxy peak can be seen at around 3.9 ppm. In aromatic region phenylene peaks are observed and the styryl bond hydrogens observed at around 6.6 -7 ppm. For the final product (compound 26), it can be seen that the methyl ester peak is disappeared in ^{1}H NMR spectrum and compound 26 is obtained with high yield.

For compound 30, we started with terephthalic aldehyde and mono protection of aldehyde is obtained by using ethylene glycol. The protection can be seen in ^{1}H NMR data as two multiplets around 4 ppm.

BODIPY (Compound 28) is produced by using mono protected aldehyde. This step has lower yield than other BODIPY reactions since deprotection of aldehyde group occurs due to strong acid (TFA) used in BODIPY synthesis. Common BODIPY peaks and protection peaks are observed in ^{1}H NMR spectrum of Compound 28. In the Knoevenagel reaction, distyrl BODIPY produced in higher yield compared to Compound 26 but it is lower than literature values. This caused by the sensitivity of BODIPY with the protecting group. Then, deprotection occurs to

have Compound 30 by using acidic environment with high yield. After deprotection, aldehyde peak at around 10 ppm and hydrogens belong to protecting group is disappeared as shown in NMR data.

For compound 34, 4- nitrobenzaldehyde used as starting material and BODIPY (Compound 31) synthesized. In ^{1}H NMR common BODIPY peaks are observed clearly.

Then, reduction of nitro group was done by using Fe powder and acidic environment and amino group was obtained (Compound 32). The addition of broad peak to the ^{1}H spectrum of Compound 31 shows us the amine group bound to phenylene on meso position. BODIPY with amino group was produced with high yield. However, it is not stable and decomposes easily due to strong electron donating amine group bound to the BODIPY core.

Formylation of amino group was done with good yields by using ethyl formate. ^{1}H NMR spectrum of this compound includes formyl peak at around 8.5 ppm and a multiplet for phenylene hydrogens at around 7.3 ppm. Hydrogen on nitrogen atom observed at around 7.7 ppm.

Synthesis of compound 34 had very good yields and since the substance is very sensitive to acidic water, crude product was used to other step. Dry and inert reaction conditions are needed for good yields so degassed chloroform is used as solvent and molecular sieve was used to dry solvent. Column chromatography technique cannot be used because of humidity in silica gel. Acidic water reduces product immediately and produce starting material. Crude ^{1}H NMR is shown for Compound 34 and it is possible to see yield is almost 100% since common BODIPY peaks are observable and formyl peak is disappeared.

After the synthesis of three main component needed for Passerini reaction, self-assembly of three components at room temperature in dry THF was performed. In order to increase yield, the reaction heated to reflux. The reaction is very sensitive to moisture in the environment. One of the reasons of that, isocyanide is prone to be reduced in aqueous medium. The other reason is the intermediate products are not stable in protic solvents as mentioned in the introduction. In order to produce the product the intermediate should be stable. That is why, the reaction environment should be dry and inert. The reaction controlled by TLC and appearance of new spot was observed. The spot was very low in amount so Compound 35 could be analyzed by absorbance spectrometry.

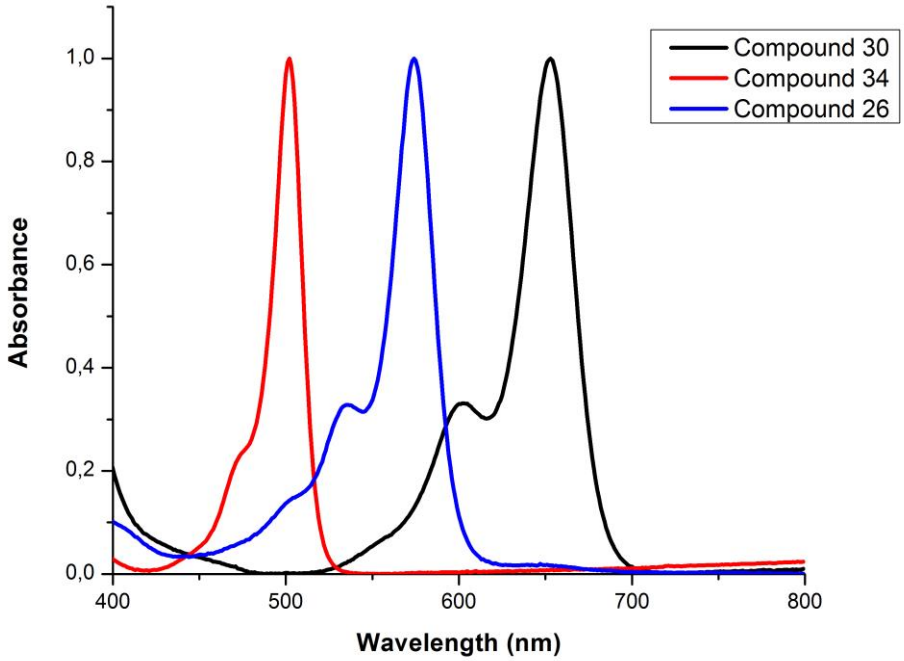

Figure 43: Normalized absorbance spectrum of Compounds 30, 34 and 26.

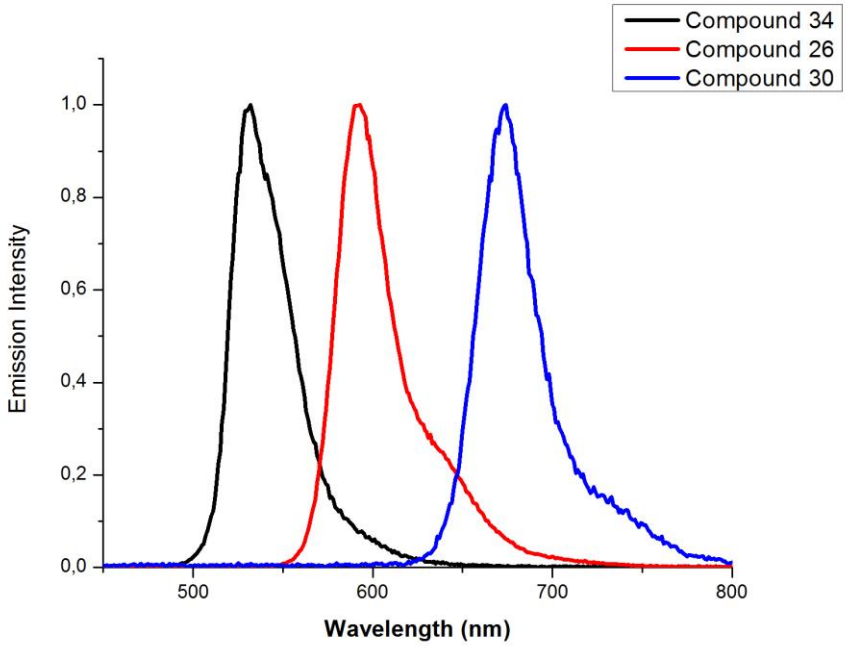

Figure 44: Normalized emission spectrum of Compounds 30, 34 and 26.

Three units are analyzed separately to see their photophysical properties and whether they are appropriate for Förster type energy transfer.

The units absorb light on different wavelengths. Compound 34 absorbs light at 502 nm, compound 26 at 574 nm and compound 30 at 653 nm as shown in Figure 42. As much as extension of conjugation increase in the molecule, absorption bands shifted towards to red wavelengths.

Emission peaks are shown in Figure 43. The excitations are done at the wavelength where absorbance is maximum for each unit. Same trend is observed in fluorescence emission peak shifts and Compound 34 emits light at 531 nm, compound 26 at 592 nm and compound 30 at 674 nm. Stocks shift is observable between absorption and emission spectrum.

As mentioned in introduction part, there should be spectral overlap between donors and acceptors for efficient energy transfer. The overlaps are shown in Figure 44 and Figure 45. The energy transfer occurs from short wavelength absorption unit to long wave length emission unit so the energy transfer mechanism starts with the absorption of Compound 34 at 502 nm. Then, it becomes excited and gives emission at 531 nm. Since emission peak is overlapping with absorption peak of compound 26, the emitted energy is absorbed by Compound 26 as shown in Figure 44.

The second transfer occurs between Compound 26 and Compound 30. After absorption of energy of compound 26, it produce excited state compound and emits light at around 592 nm. The emitted energy can be absorbed by Compound 30 since there is spectral overlap between emission peak of Compound 26 and absorption peak of Compound 30. Finally, there is emission at around 674 nm.

Therefore, the direction of energy transfer is from compound 34 to compound 26 and from compound 26 to compound 30. It starts when Compound 34 is excited after absorption at around 502 nm and ends with the emission at 674 nm as shown in Figure 45.

The overall process is shown in Figure 46.

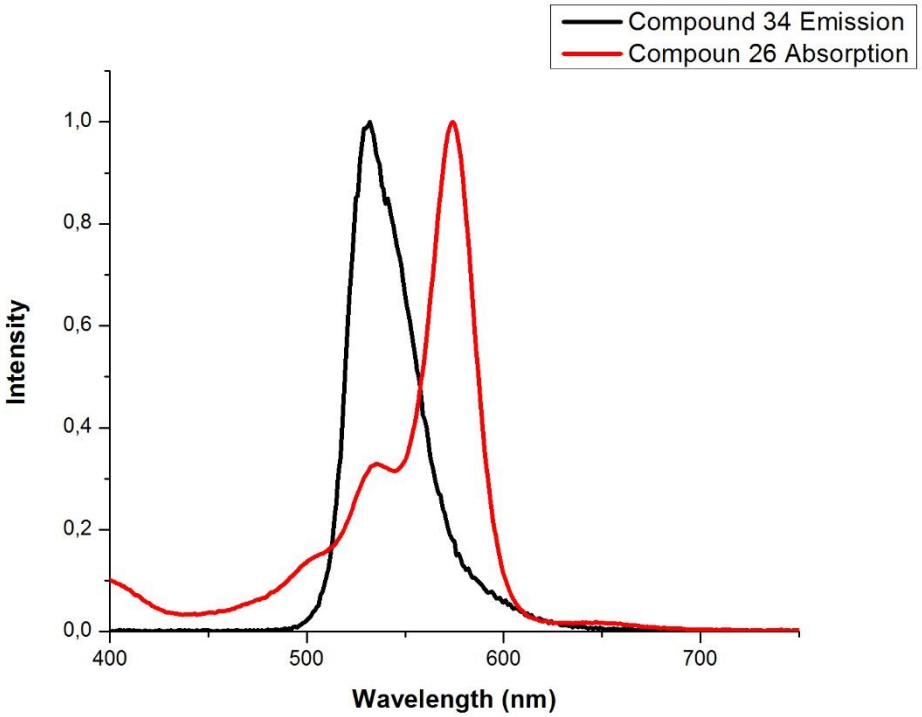

Figure 45: Spectral overlap between Compounds 26 and 34.

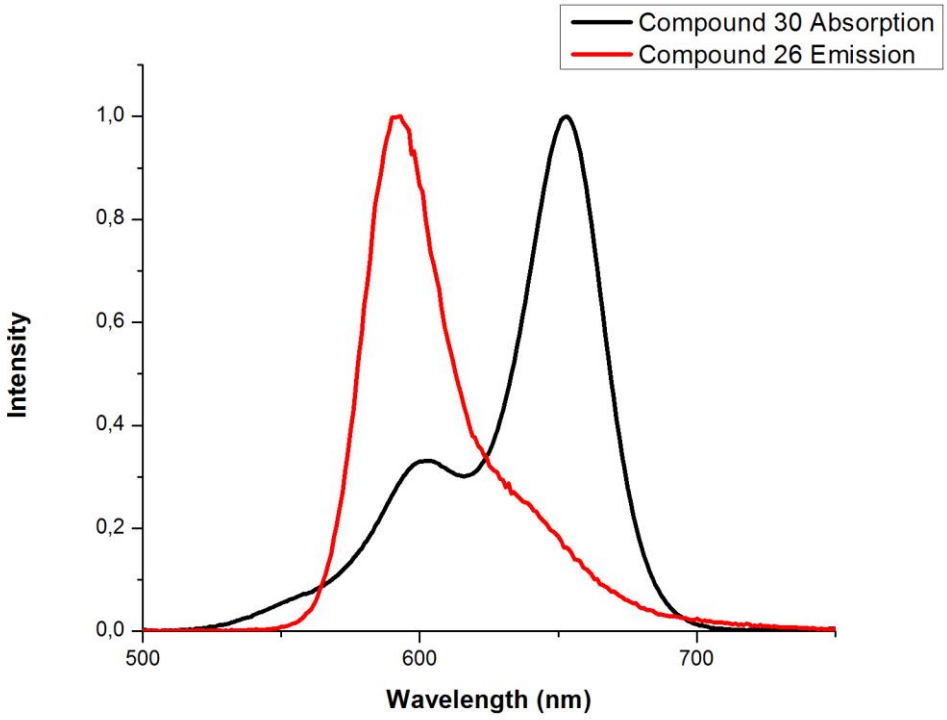

Figure 46: Spectral overlap between Compounds 30 and 26.

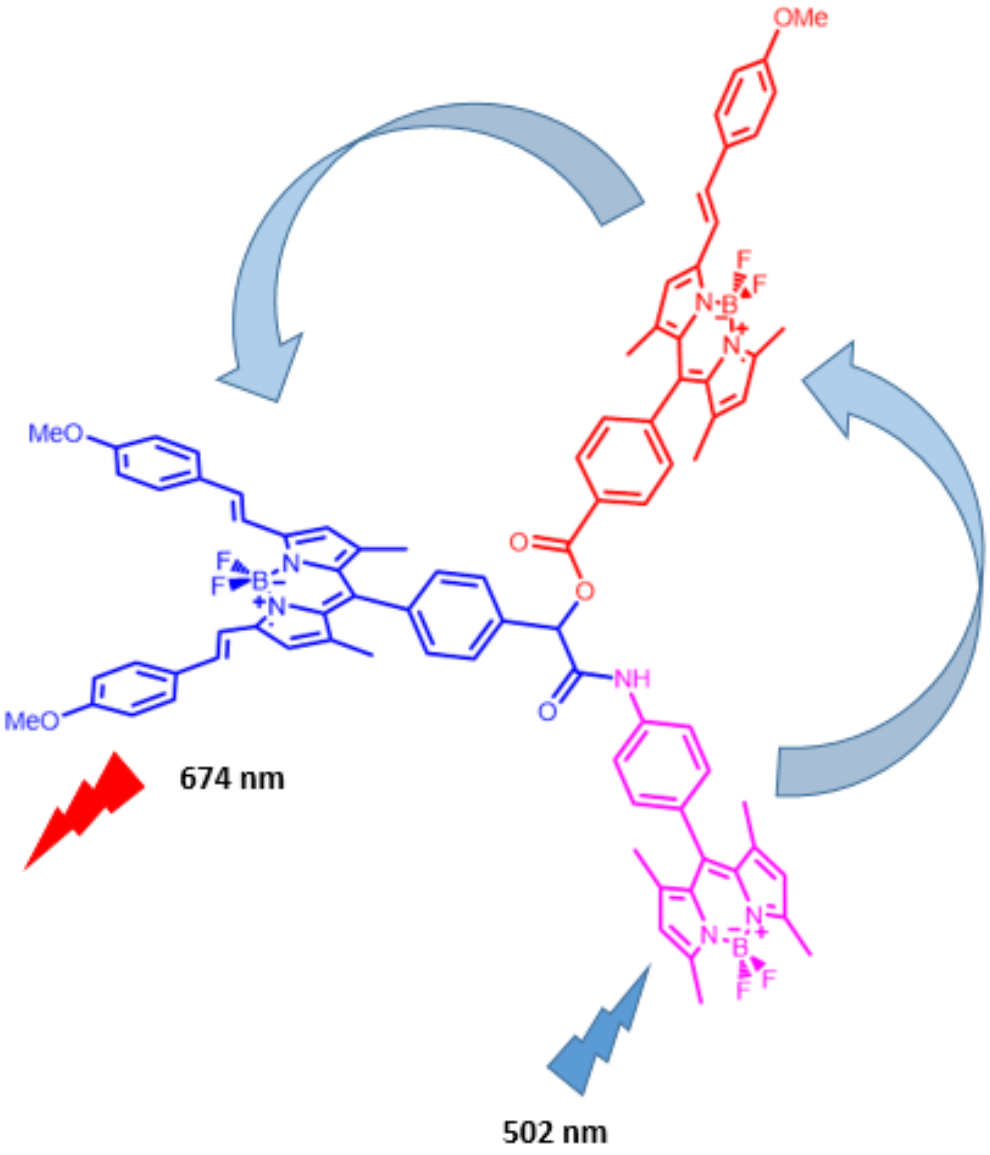

Figure 47: Energy transfer direction in Compound 35.

Table 1: Photophysical properties of Compounds 34,26 and 30.

Compound	**Φ** I_{exc} **(488 nm)**	**Φ** I_{exc} **(578 nm)**	**Φ** I_{exc} **(633 nm)**	**Extinction Coefficients**
34	0.30	-	-	84000
26	-	0.73	-	15000
30	-	-	0.26	40000

Further measurements and calculations were performed for three units of the energy transfer cascade as shown in Table 1. Quantum yield calculations were done for three units by using three different reference dyes which are rhodamine 6G (488 nm, ethanol), methylene blue (633 nm, ethanol) and cresyl violet (578 nm, ethanol).[101] All quantum yield calculations are done in DMSO as solvent of three units. Quantum yield calculations were done by using equation:

$$\Phi = (I/I_R)*(A_R/A)*(n^2/n_R^2)$$

Where I and I_R refer to area under emission curve of dye and reference dye respectively. A and A_R indicates absorbance values at wavelength at which dyes are excited and finally n is the refractive index of used solvents.

Additionally, excitation coefficients are calculated by using Beer's Law in chloroform. The concetrations were 7.47 x 10^{-6} M for compound 34, 5.87 x 10^{-5} M for compound 26 and 2.09 x 10^{-5} M for compound 30. Maximum values of absorbance measured as 0.626, 0.876 and 0.845 respectively. Based on these values extinction coefficients reported as shown in Table 1.

Compound 35 was synthesized as last step but the yield of the reaction was very low so the characterization of the compound has not been completed yet. However, there is an isolated distinct spot different than starting materials as shown in TLC in Figure 47. Its absorbance spectrum contains three peaks belongs three BODIPY units as expected shown in Figure 48.

Figure 48: TLC of starting compounds and product. The compounds are Compound 34, Compound 26, Compound 30 and the new spot (Compound 35) respectively.

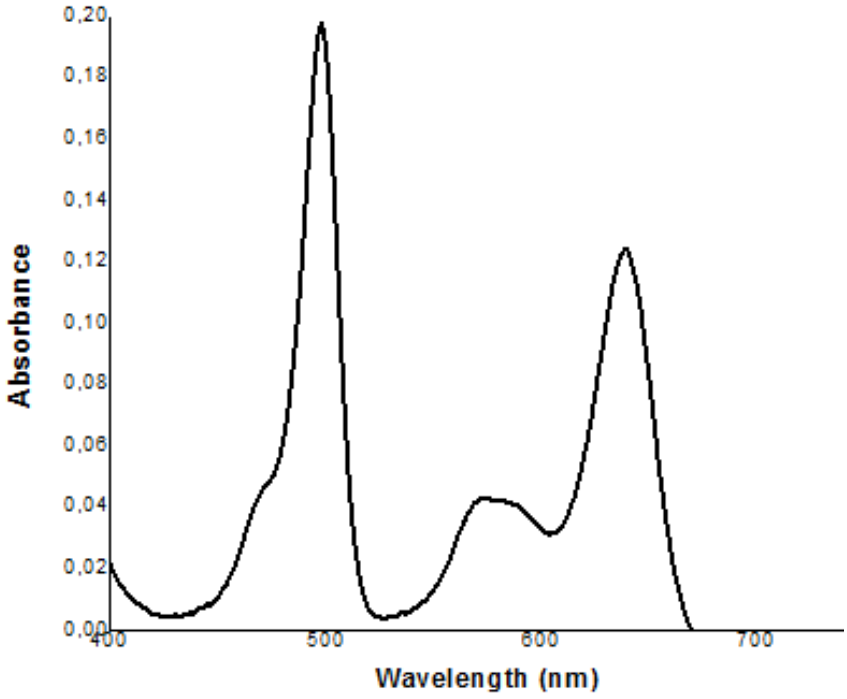

Figure 49: Absorbance spectrum of Compound 35.

4. CONCLUSION

In this study, BODIPY based Förster type energy transfer cascade was designed and synthesized. Characterization and photophysical properties of energy transfer units were shown and quantum yields and extinction coefficients were calculated.

The absorbance and emission spectra of energy transfer units has the spectral overlaps needed for efficient energy transfer between them. Passerini reaction was performed to synthesize Compound 35 in one step but it has very low yield and its characterization is in progress. Although its characterization is not complete, absorbance spectrum of Compound 35 is promising since it includes three different peaks belongs to three units and has different R_f than starting materials in TLC.

In conclusion, three different energy transfer unit was combined in one step by using Passerini reaction in order to obtain BODIPY based Förster type energy transfer cascade. The analysis results showed that designed energy transfer cascade is promising to work efficiently. Its characterization will be completed and FRET efficiency will be calculated as future work.

BIBLIOGRAPHY

1. Willenbacher, J. *et al.* Reversible single-chain selective point folding via cyclodextrin driven host-guest chemistry in water. *Chem. Commun. (Camb).* 7056–7059 (2014).

2. Alberti, S., Soler-Illia, G. J. a. a. & Azzaroni, O. Gated supramolecular chemistry in hybrid mesoporous silica nanoarchitectures: controlled delivery and molecular transport in response to chemical, physical and biological stimuli. *Chem. Commun.* 6050–6075 (2015).

3. Zhang, Yagang; Wang, Z. Research Progress in Nanocrystalline Solar Power System. *J. Comput. Theor. Nanosci.* **10,** 2912–2915 (2013).

4. Wu, C. What Are Core Polymer Chemistry and Physics . p. 132–134 (2013).

5. Steed, J., Turner, D. & Wallace, K. *Core Concepts in Supramolecular Chemistry and Nanochemistry*. (2008).

6. Lehn, J.-M. Supramolecular Chemistry—Scope and Perspectives Molecules, Supermolecules, and Molecular Devices (Nobel Lecture). *Angew. Chemie Int. Ed. English* **27,** 89–112 (1988).

7. Swiegers, G. F. Self-assembly: Terminology. *Encycl. Supramol. Chem.* **1,** 1263–1269 (2004).

8. Sessler, J. L. & Miller, R. a. Texaphyrins: New drugs with diverse clinical applications in radiation and photodynamic therapy. *Biochem. Pharmacol.* **59,** 733–739 (2000).

9. Online, V. A. Guanosine and isoguanosine derivatives for supramolecular devices. 5122–5128 (2014).

10. Singh, A. K., Pandey, D. S., Xu, Q. & Braunstein, P. Recent advances in supramolecular and biological aspects of arene ruthenium(II) complexes. *Coord. Chem. Rev.* **270-271,** 31–56 (2014).

11. Maksimov, A. L., Sakharov, D. a., Filippova, T. Y., Zhuchkova, A. Y. & Karakhanov, E. a. Supramolecular catalysts on the basis of molecules-receptors. *Ind. Eng. Chem. Res.* **44,** 8644–8653 (2005).

12. Delgado, Juan L.; Filippone, Salvatore; Giacalone, Francesco; Herranz, Ma Ángeles; Illescas, Beatriz; Pérez, Emilio M.; Martín, N. Buckyballs. *Top. Curr. Chem.* **350,** 1–64 (2014).

13. Schmidt, A., Casini, A. & Kühn, F. E. Self-assembled M2L4 coordination cages: Synthesis and potential applications. *Coord. Chem. Rev.* **275,** 19–36 (2014).

14. Raveendran, P., Fu, J. & Wallen, S. L. Completely 'Green' Synthesis and Stabilization of Metal Nanoparticles. *J. Am. Chem. Soc.* **125,** 13940–13941 (2003).

15. Kumar, A. & Gupta, S. K. Supramolecular-directed novel superparamagnetic 5′-adenosine monophosphate templated β-FeOOH hydrogel with enhanced multi-functional properties. *Green Chem.* **17,** 2524–2537 (2015).

16. Adhikari, B., Biswas, A. & Banerjee, A. Graphene oxide-based supramolecular hydrogels for making nanohybrid systems with Au nanoparticles. *Langmuir* **28,** 1460–1469 (2012).

17. Erbas-Cakmak, S., Bozdemir, O. A., Cakmak, Y. & Akkaya, E. U. Proof of principle for a molecular 1 : 2 demultiplexer to function as an autonomously switching theranostic device. *Chem. Sci.* 858–862 (2013).

18. Li, J. *et al.* Three-dimensional bicomponent supramolecular nanoporous self-assembly on a hybrid all-carbon atomically flat and transparent platform. *Nano Lett.* **14,** 4486–4492 (2014).

19. Ceroni, P., Credi, A. & Venturi, M. Light to investigate (read) and operate (write) molecular devices and machines. *Chem. Soc. Rev.* 4068–4083 (2014).

20. Guliyev, R., Ozturk, S., Sahin, E. & Akkaya, E. U. Expanded bodipy dyes: Anion sensing using a bodipy analog with an additional difluoroboron bridge. *Org. Lett.* **14,** 1528–1531 (2012).

21. Sun, X. & James, T. D. Glucose Sensing in Supramolecular Chemistry. *Chem. Rev.*, **115**, 8001–8037 (2015).

22. Dennison, G. H. & Johnston, M. R. Mechanistic Insights into the Luminescent Sensing of Organophosphorus Chemical Warfare Agents and Simulants Using Trivalent Lanthanide Complexes. *Chem. - A Eur. J.* **21,** 6328–6338 (2015).

23. Avvaru, B. S. *et al.* A short, strong hydrogen bond in the active site of human carbonic anhydrase II. *Biochemistry* **49,** 249–251 (2010).

24. Dong, Z., Yongguo Wang, Yin, Y. & Liu, J. Supramolecular enzyme mimics by self-assembly. *Curr. Opin. Colloid Interface Sci.* **16,** 451–458 (2011).

25. Calladine, C. R., Drew, H. R., Luisi, B. F. & Travers, A. a. *Understanding DNA. The Molecule and how it works.* (Academic Press, 2004).

26. Li, C. *et al.* Rapid Formation of a Supramolecular Polypeptide-DNA Hydrogel for In Situ Three-Dimensional Multilayer Bioprinting. *Angew. Chemie Int. Ed.* n/a–n/a (2015).

27. Greschner, A. a., Bujold, K. E. & Sleiman, H. F. Controlled Growth of DNA Structures from Repeating Units Using the Vernier Mechanism. *Biomacromolecules* **15,** 3002–3008 (2014).

28. Adronov, a. *et al.* Light Harvesting and Energy Transfer in Laser-Dye-Labeled Poly (aryl ether) Dendrimers. *J. Am. Chem. Soc.* **122,** 1175–1185 (2000).

29. Ward, M. D. & Raithby, P. R. Functional behaviour from controlled self-assembly: challenges and prospects. *Chem. Soc. Rev.* 1619–1636 (2013).

30. Aida, T. Tailoring assembled systems for light harvesting and energy conversion. *AIP Conf. Proc.* **76,** 1519 (2013).

31. Kolemen, S. *et al.* Intracellular Modulation of Excited-State Dynamics in a Chromophore Dyad: Differential Enhancement of Photocytotoxicity Targeting Cancer Cells. *Angew. Chemie Int. Ed.* **066004,** n/a–n/a (2015).

32. Wang, D. *et al.* Correction: Supramolecularly engineered phospholipids constructed by nucleobase molecular recognition: upgraded generation of phospholipids for drug delivery. *Chem. Sci.* **6,** 5090–5092 (2015).

33. Isaacs, L. Approaches to drug delivery based on the principles of supramolecular chemistry. *Adv. Drug Deliv. Rev.* **64,** 763 (2012).

34. Senesi, N. Molecular and quantitative aspects of the chemistry of fulvic acid and its interactions with metal ions and organic chemicals : Part II. The fluorescence spectroscopy approach. *Anal. Chim. Acta* **232,** 77–106 (1990).

35. Jameson, David M.; Croney, John C.; Moens, P. D. J. Fluorescence: Basic Caoncepts, Practical, Aspects and Some Anecdotes. *Methods Enzymol.* **360,** 1–43

36. Valeur, B. *Molecular Fluorescence: Principles and Applications*. (Wiley, 2001).

37. Bagchi, Biman; Oxtoby, David W.; Fleming, G. R. Theory of the time development of the stokes shift in polar media. *Chmical Phys.* **86,** 257–267 (1984).

38. Chan, J., Dodani, S. C. & Chang, C. J. Reaction-based small-molecule fluorescent probes for chemoselective bioimaging. *Nat. Chem.* **4,** 973–84 (2012).

39. Guo, T. *et al.* Molecularly imprinted upconversion nanoparticles for highly selective and sensitive sensing of Cytochrome c. *Biosens. Bioelectron.* **74,** 498–503 (2015).

40. Xue, W. *et al.* A Highly Sensitive Fluorescent Sensor Based on Small Molecule Doped in Electrospun Nanofibers: Detection of Explosives as well as Color Modulation. *J. Mater. Chem. C* 16–19 (2015).

41. Mathew, S. *et al.* Dye-sensitized solar cells with 13% efficiency achieved through the molecular engineering of porphyrin sensitizers. *Nat. Chem.* **6,** 242–7 (2014).

42. Higuchi, T., Nakanotani, H. & Adachi, C. High-Efficiency White Organic Light-Emitting Diodes Based on a Blue Thermally Activated Delayed Fluorescent Emitter Combined with Green and Red Fluorescent Emitters. *Adv. Mater.* n/a–n/a (2015).

43. Gall, A. *et al.* Conformational Switching in a Light-Harvesting Protein as Followed by Single-Molecule Spectroscopy. *Biophys. J.* **108,** 2713–2720 (2015).

44. Cakmak, Y. *et al.* Designing excited states: Theory-guided access to efficient photosensitizers for photodynamic action. *Angew. Chemie - Int. Ed.* **50,** 11937–11941 (2011).

45. Ji, S. *et al.* Molecular Structure–Intersystem Crossing Relationship of Heavy-Atom-Free BODIPY Triplet Photosensitizers. *J. Org. Chem.* **80,** 5958–5963 (2015).

46. Haedicke, K. *et al.* Multifunctional calcium phosphate nanoparticles for combining near-infrared fluorescence imaging and photodynamic therapy. *Acta Biomater.* **14,** 197–207 (2015).

47. Treibs, Alfred; Kreuzer, F.-H. Difluorboryl-Komplexe von Di- und Tripyrrylmethenen. *Eur. J. Org. Chem.* **718,** 208–223 (2006).

48. Spicka, J. K. *Design and Synthesis of Fluorescent Dyes for Use in Proteomic Research*. (UMI, 2008).

49. Zhu, S. *et al.* Controlled Knoevenagel reactions of methyl groups of 1,3,5,7-tetramethyl BODIPY dyes for unique BODIPY dyes. *RSC Adv.* **2,** 404 (2012).

50. Buyukcakir, O., Bozdemir, O. A., Kolemen, S., Erbas, S. & Akkaya, E. U. Tetrastyryl-bodipy dyes: Convenient synthesis and characterization of elusive near IR fluorophores. *Org. Lett.* **11,** 4644–4647 (2009).

51. Yogo, T., Urano, Y., Ishitsuka, Y., Maniwa, F. & Nagano, T. Highly efficient and photostable photosensitizer based on BODIPY chromophore. *J. Am. Chem. Soc.* **127,** 12162–12163 (2005).

52. Boyer, Joseph H.; Haag, Anthony M.; Sathyamoorthi, Govindarao; Soong, Mou-LingKannappan Thangaraj; Pavlopoulos, T. G. Pyrromethene–BF2 complexes as laser dyes: 2. *Heteroat. Chem.* **4,** 49 (1993).

53. Application, F. & Data, P. (12) United States Patent. **1,** 1–8 (2001).

54. Gorman, A. *et al.* In vitro demonstration of the heavy-atom effect for photodynamic therapy. *J. Am. Chem. Soc.* **126,** 10619–10631 (2004).

55. Ortiz, M. J. *et al.* Synthesis and functionalization of new polyhalogenated BODIPY dyes. Study of their photophysical properties and singlet oxygen generation. *Tetrahedron* **68,** 1153–1162 (2012).

56. Ulrich, G., Ziessel, R. & Harriman, A. The chemistry of fluorescent bodipy dyes: Versatility unsurpassed. *Angew. Chemie - Int. Ed.* **47,** 1184–1201 (2008).

57. Dziuba, D., Pohl, R. & Hocek, M. Bodipy-Labeled Nucleoside Triphosphates for Polymerase Synthesis of Fluorescent DNA. (2014).

58. Ehrenschwender, T. & Wagenknecht, H. A. 4,4-difluoro-4-bora-3a,4a-diaza-s-indacene as a bright fluorescent label for DNA. *J. Org. Chem.* **76,** 2301–2304 (2011).

59. Choi, H., Lee, J. H. & Jung, J. H. Fluorometric/colorimetric logic gates based on BODIPY-functionalized mesoporous silica. *Analyst* **139,** 3866 (2014).

60. Liu, J. *et al.* A BODIPY derivative for colorimetric and fluorometric sensing of fluoride ion and its logic gates behavior. *Sensors Actuators B Chem.* **208,** 538–545 (2015).

61. Yuan, M. *et al.* A multianalyte chemosensor on a single molecule: Promising structure for an integrated logic gate. *J. Org. Chem.* **73,** 5008–5014 (2008).

62. Niu, L. Y. *et al.* BODIPY-based fluorometric sensor array for the highly sensitive identification of heavy-metal ions. *Anal. Chim. Acta* **775,** 93–99 (2013).

63. Fu, L. *et al.* Highly efficient fluorescent BODIPY dyes for reaction-based sensing of fluoride ions. *Sensors Actuators B Chem.* **216,** 558–562 (2015).

64. Lakshmi, V. & Ravikanth, M. Boron-dipyrromethene based multi-anionic sensor and a specific cationic sensor for Fe3+. *J. Mater. Chem. C* **2,** 5576 (2014).

65. Kostereli, Z., Ozdemir, T., Buyukcakir, O. & Akkaya, E. U. Tetrastyryl-BODIPY-based dendritic light harvester and estimation of energy transfer efficiency. *Org. Lett.* **14,** 3636–3639 (2012).

66. Wu, W., Liu, L., Cui, X., Zhang, C. & Zhao, J. Red-light-absorbing diimine Pt(II) bisacetylide complexes showing near-IR phosphorescence and long-lived 3IL excited state of Bodipy for application in triplet-triplet annihilation upconversion. *Dalton Trans.* **42,** 14374–9 (2013).

67. Huang, L., Yang, W. & Zhao, J. Switching of the Triplet Excited State of Styryl 2 , 6-Diiodo-Bodipy and Its Application in Acid-Activatable Singlet Oxygen Photosensitizing. (2014).

68. Erbas, S., Gorgulu, A., Kocakusakogullari, M. & Akkaya, E. U. Non-covalent functionalized SWNTs as delivery agents for novel Bodipy-based potential PDT sensitizers. *Chem. Commun. (Camb).* 4956–4958 (2009).

69. Gibbs, J. H. *et al.* Synthesis, spectroscopic, and in vitro investigations of 2,6-diiodo-BODIPYs with PDT and bioimaging applications. *J. Photochem. Photobiol. B Biol.* **145,** 35–47 (2015).

70. Verwilst, P. *et al.* Synthesis and in vitro evaluation of a PDT active BODIPY-NLS conjugate. *Bioorganic Med. Chem. Lett.* **23,** 3204–3207 (2013).

71. Loudet, A. & Burgess, K. BODIPY Dyes and Their Derivatives: Syntheses and Spectroscopic Properties. *Chem. Rev.* **107,** 4891–4932 (2007).

72. Yuan, M. *et al.* A colorimetric and fluorometric dual-modal assay for mercury ion by a molecule. *Org. Lett.* **9,** 2313–2316 (2007).

73. Coskun, A., Yilmaz, M. D. & Akkaya, E. U. Bis(2-pyridyl)-Substituted Boratriazaindacene as an NIR-Emitting Chemosensor for Hg(II). *Org. Lett.* **9,** 607–609 (2007).

74. Bozdemir, O. A. *et al.* Selective manipulation of ICT and PET processes in styryl-bodipy derivatives: Applications in molecular logic and fluorescence sensing of metal ions. *J. Am. Chem. Soc.* **132,** 8029–8036 (2010).

75. Guliyev, R., Ozturk, S., Kostereli, Z. & Akkaya, E. U. From virtual to physical: Integration of chemical logic gates. *Angew. Chemie - Int. Ed.* **50,** 9826–9831 (2011).

76. Pascal, A. a *et al.* Molecular basis of photoprotection and control of photosynthetic light-harvesting. *Nature* **436,** 134–137 (2005).

77. Adronov, A. & Fréchet, J. M. J. Light-harvesting dendrimers. *Chem. Commun.* 1701–1710 (2000).

78. Pawlowski et al. United States Patent, no: 5,340,682, (1994).

79. Dexter, D. L. A Theory of Sensitized Luminescence in Solids. *J. Chem. Phys.* **21,** 836 (1953).

80. Sessler, J. L., Wang, B. & Harriman, A. Photoinduced energy transfer in associated, but noncovalently-linked photosynthetic model systems. *J. Am. Chem. Soc.* **117,** 704–714 (1995).

81. Murphy, C. B. *et al.* Probing Fo 1 rster and Dexter Energy-Transfer Mechanisms in Fluorescent Conjugated Polymer Chemosensors. *J. Chem. B* **17,** 1537–1543 (2004).

82. Lazarides, T., Sykes, D., Faulkner, S., Barbieri, A. & Ward, M. D. On the mechanism of d-f energy transfer in RuII/LnIII and OsII/LnIII Dyads: Dexter-type energy transfer over a distance of 20 Å. *Chem. - A Eur. J.* **14,** 9389–9399 (2008).

83. Cheriya, R. T., Joy, J., Alex, A. P., Shaji, A. & Hariharan, M. Energy transfer in near-orthogonally arranged chromophores separated through a single bond. *J. Phys. Chem. C* **116,** 12489–12498 (2012).

84. Yousaf, M., Lough, a. J., Schott, E. & Koivisto, B. D. BODIPY-phenylacetylene macrocycle motifs for enhanced light-harvesting and energy transfer applications. *RSC Adv.* **5,** 57490–57492 (2015).

85. Hussain, S. A. An Introduction to Fluorescence Resonance Energy Transfer (FRET). *Energy* **132,** 4 (2009).

86. Diring, S., Ziessel, R., Barigelletti, F., Barbieri, A. & Ventura, B. A pre-organised truxene platform for phosphorescent [Ru(bpy)2] and [Os(bpy)2] metal centres: A clear-cut switch from förster-to Dexter-type energy-transfer mechanism. *Chem. - A Eur. J.* **16,** 9226–9236 (2010).

87. Nakamura, Y., Aratani, N. & Osuka, A. Cyclic porphyrin arrays as artificial photosynthetic antenna: synthesis and excitation energy transfer. *Chem. Soc. Rev.* **36,** 831–845 (2007).

88. Fluor, A., Wojcik, K., Solarczyk, K. & Kulakowski, P. Measurements on MIMO-FRET Nano-Networks. **14,** 531–539 (2015).

89. Best, R. B., Hofmann, H., Nettels, D. & Schuler, B. Quantitative Interpretation of FRET Experiments via Molecular Simulation: Force Field and Validation. *Biophys. J.* **108,** 2721–2731 (2015).

90. Valeur, B. *Related Titles from WILEY-VCH Analytical Atomic Spectrometry with Flames and Plasmas Handbook of Analytical Techniques Single-Molecule Detection in Solution . Methods and Applications*. *Methods* **8,** (2001).

91. Cheng, H. & Qian, Y. Intramolecular fluorescence resonance energy transfer in a novel PDI–BODIPY dendritic structure: Synthesis, Hg2+ sensor and living cell imaging. *Sensors Actuators B Chem.* **219,** 57–64 (2015).

92. Xu, K., Xie, Y., Cui, X., Zhao, J. & Glusac, K. D. DiiodoBodipy-Rhodamine Dyads: Preparation and Study of the Acid-Activatable Competing Intersystem Crossing and Energy Transfer Processes. *J. Phys. Chem. B* **119,** 4175–4187 (2015).

93. Yang, L. *et al.* Two tandem multicomponent reactions for the synthesis of sequence-defined polymers. *Sci. China Chem.* (2015). doi:10.1007/s11426-015-5448-0

94. Koopmanschap, G., Ruijter, E. & Orru, R. V. a. Isocyanide-based multicomponent reactions towards cyclic constrained peptidomimetics. *Beilstein J. Org. Chem.* **10,** 544–598 (2014).

95. Liu, Z.-Q. Ugi and Passerini Reactions as Successful Models for Investigating Multicomponent Reactions. *Curr. Org. Chem.* **18,** 719–739 (2014)

96. Song, S. & Rudick, J. G. Efficient Syntheses of Star-Branched, Multifunctional Mesogens. *Org. Lett.*, 17, 3244–3247 (2015).

97. Ramozzi, R. & Morokuma, K. Revisiting the Passerini Reaction Mechanism: Existence of the Nitrilium, Organocatalysis of Its Formation, and Solvent Effect. *J. Org. Chem.* 80, 5652-5657 (2015).

98. Adib, M., Sheikhi, E. & Azimzadeh, M. A new modification of the Passerini reaction: a one-pot synthesis of α-acyloxyamides via sequential Kornblum oxidation/Passerini reaction. *Tetrahedron Lett.* **56,** 1933–1936 (2015).

99. Vázquez-Romero, A. *et al.* Multicomponent reactions for de novo synthesis of bodipy probes: In vivo imaging of phagocytic macrophages. *J. Am. Chem. Soc.* **135,** 16018–16021 (2013).

100. Lin, W. *et al.* Reduction-sensitive amphiphilic copolymers made via multi-component Passerini reaction for drug delivery. *Colloids Surfaces B Biointerfaces* **126,** 217–223 (2015).

101. Olmsted, J. Calorimetric determinations of absolute fluorescence quantum yields. *J. Phys. Chem.* **83,** 2581–2584 (1979).

APPENDIX

^{1}H and ^{13}C NMR Spectra

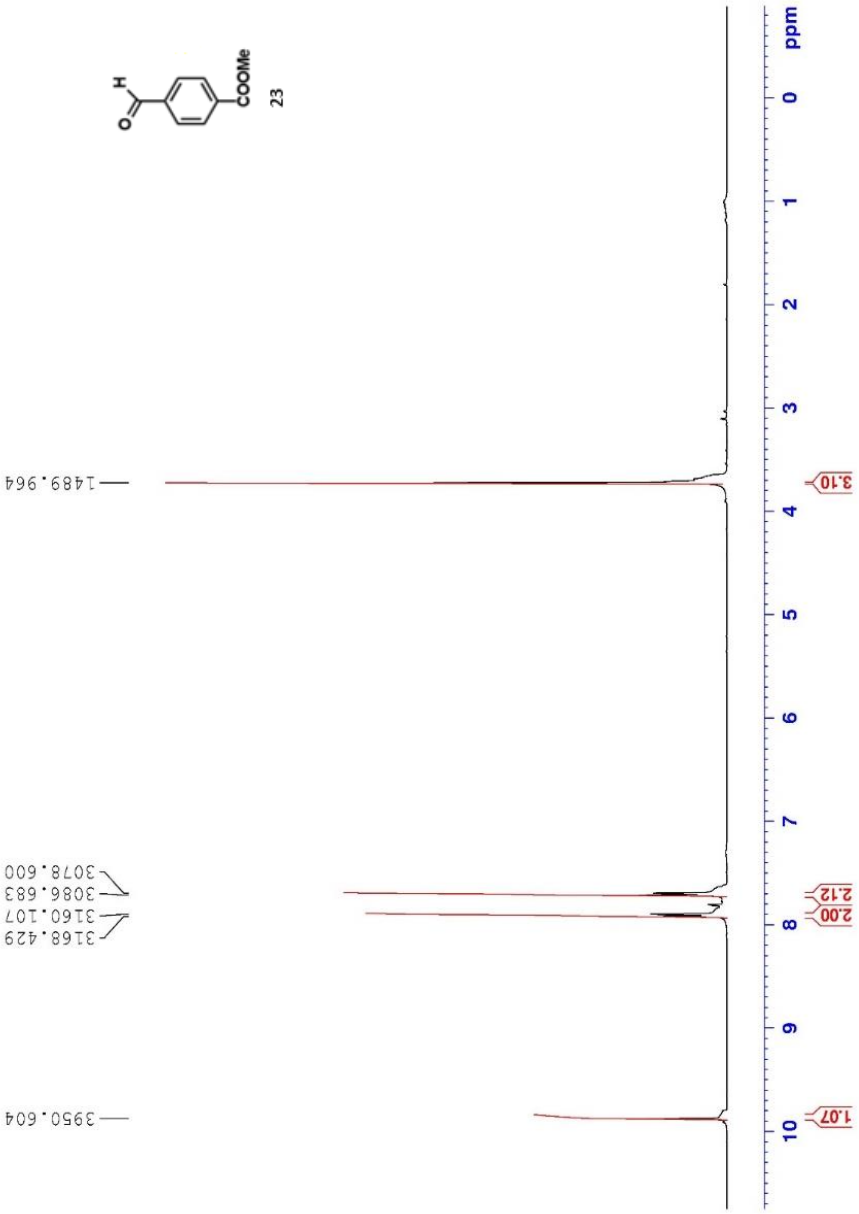

Figure 50: ^{1}H NMR spectrum of Compound 23.

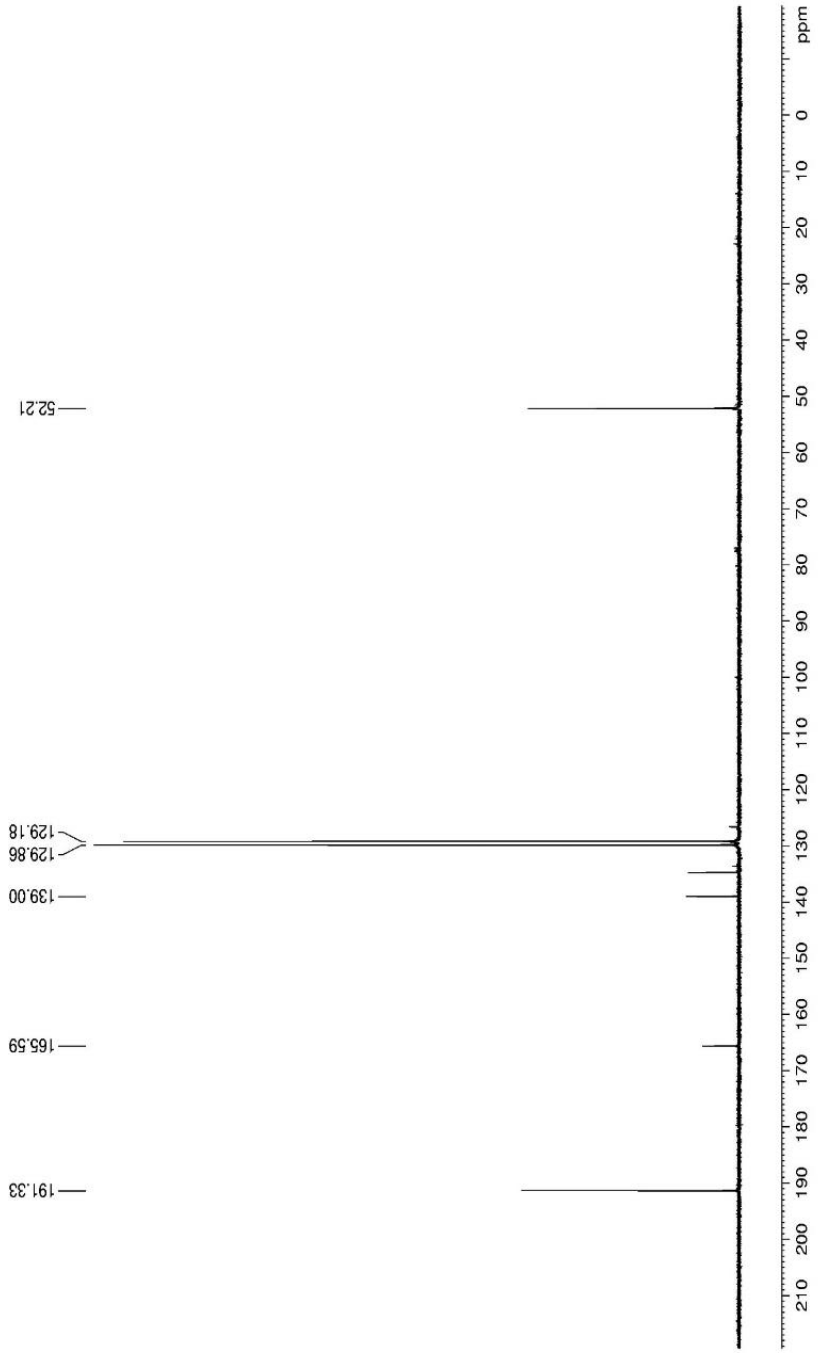

Figure 51: ^{13}C NMR spectrum of Compound 23.

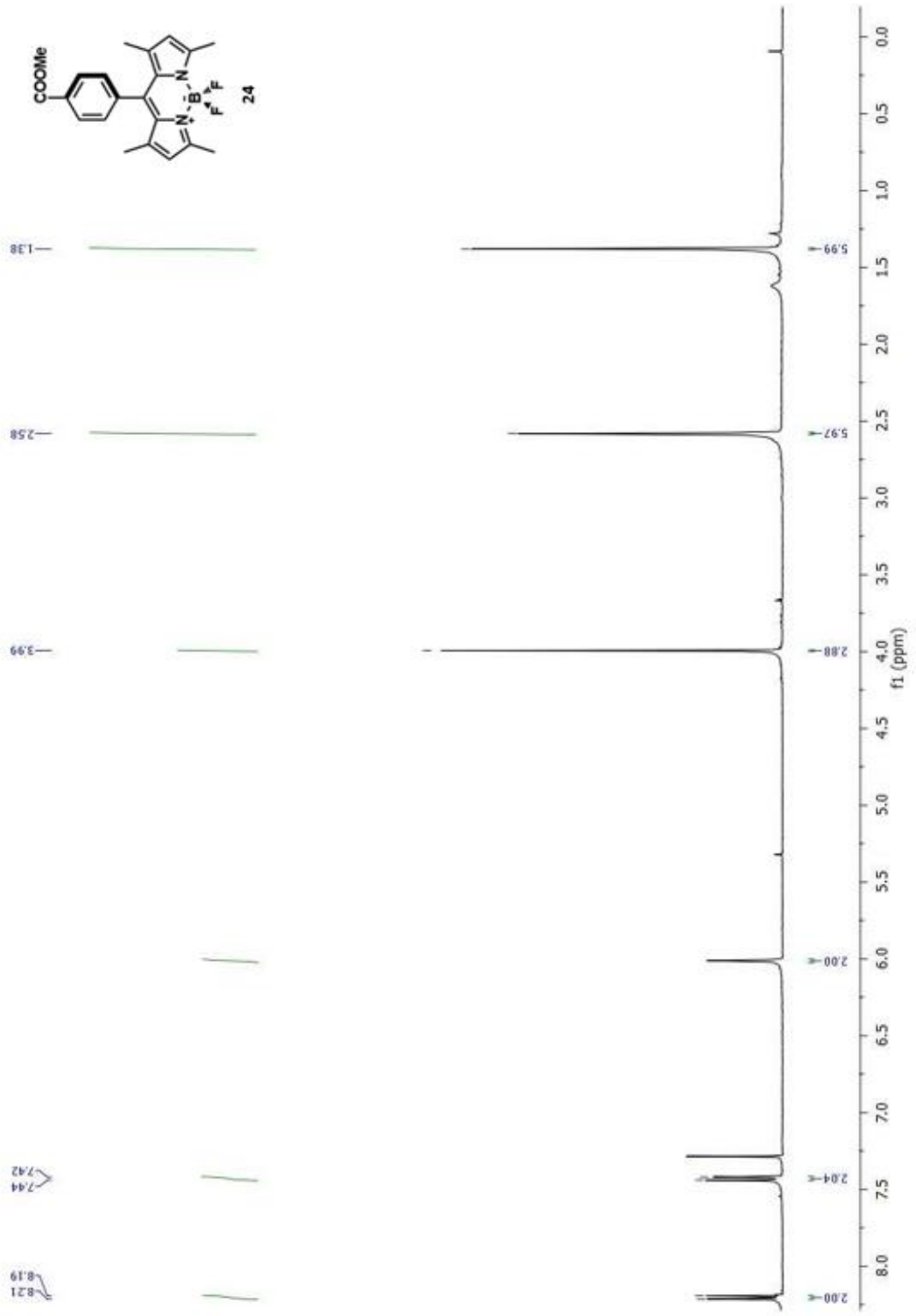

Figure 52: [1]H NMR spectrum of Compound 24.

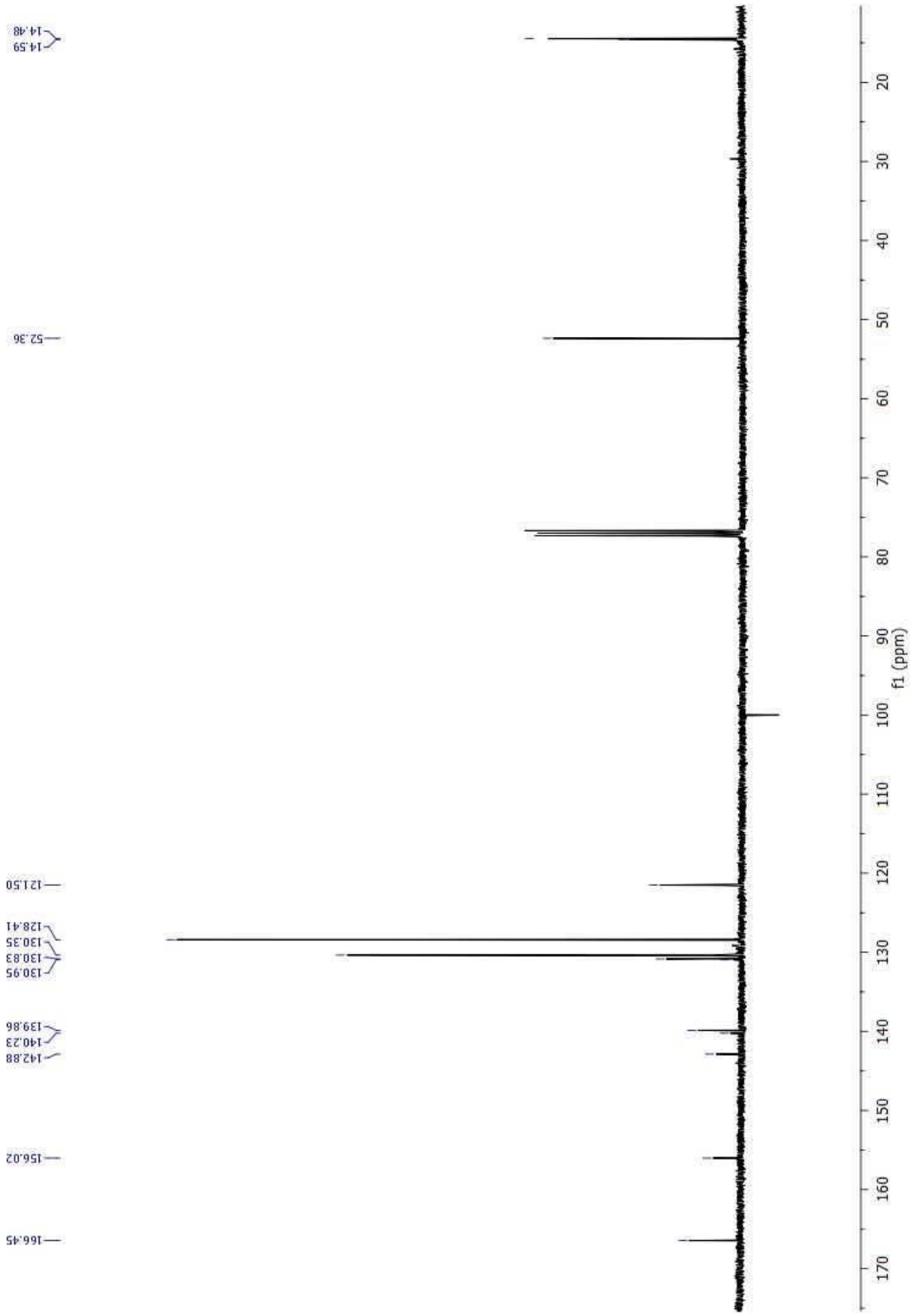

Figure 53: ^{13}C NMR spectrum of Compound 24.

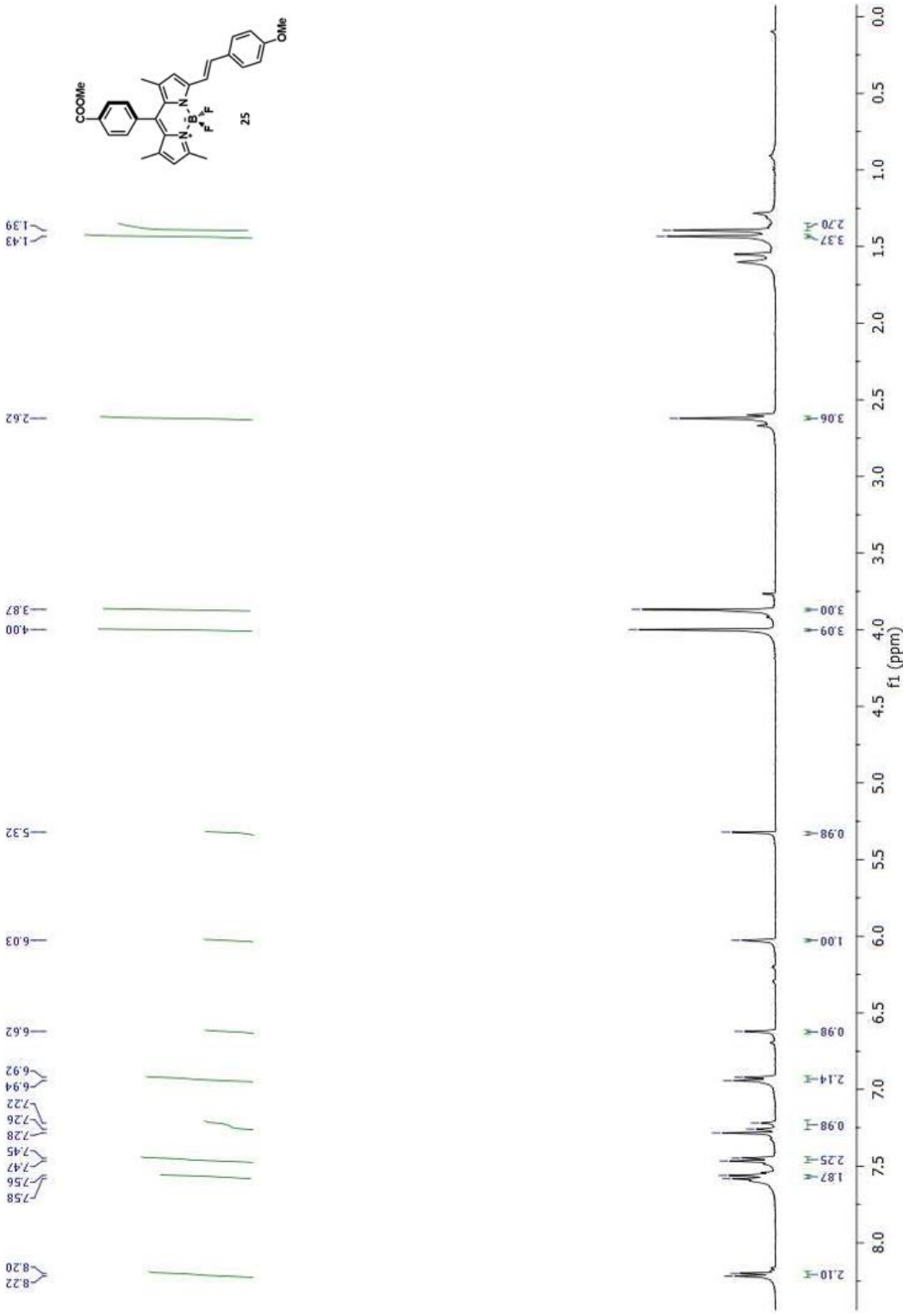

Figure 54: ^{1}H NMR spectrum of Compound 25.

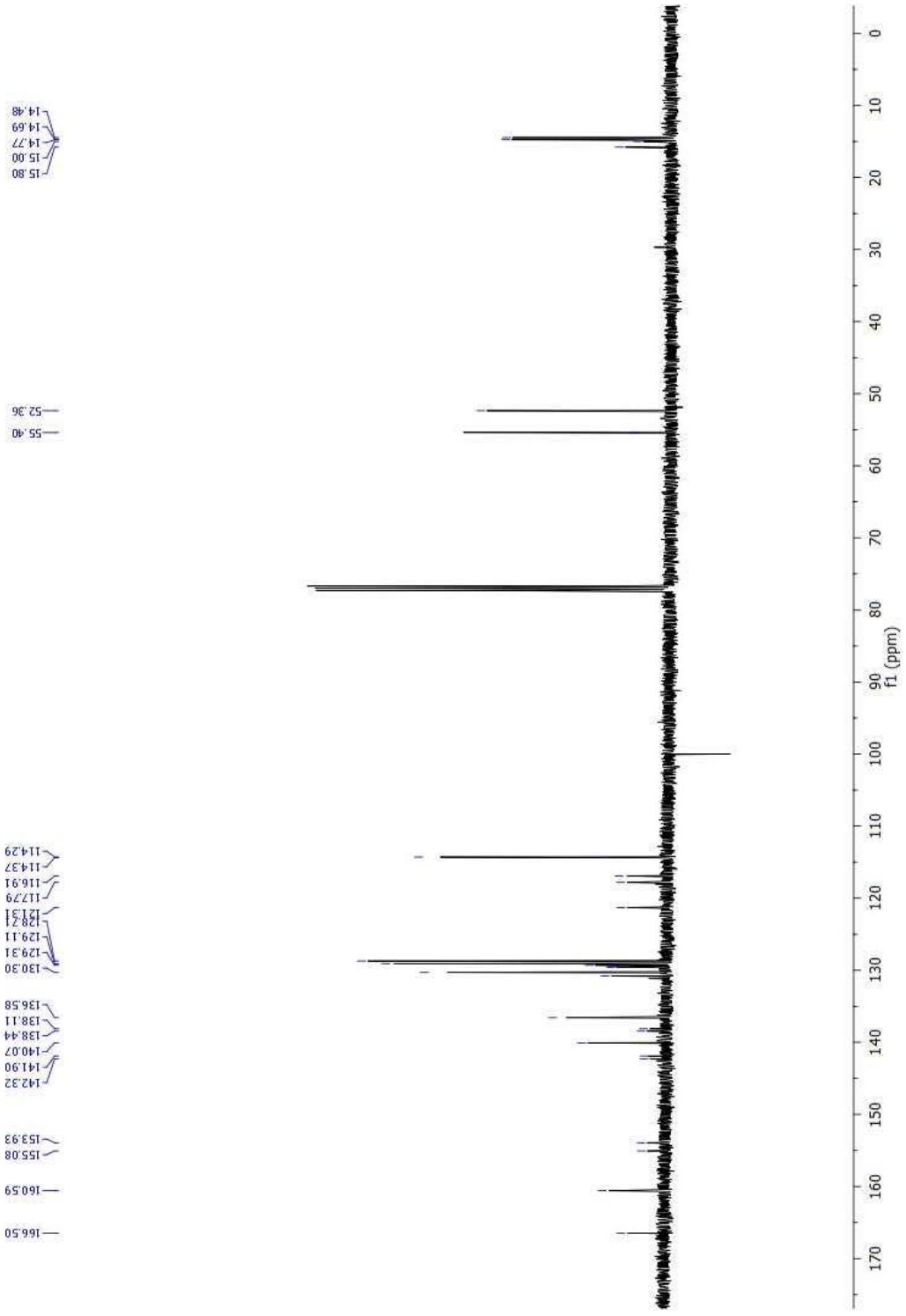

Figure 55:[13]C NMR spectrum of Compound 25.

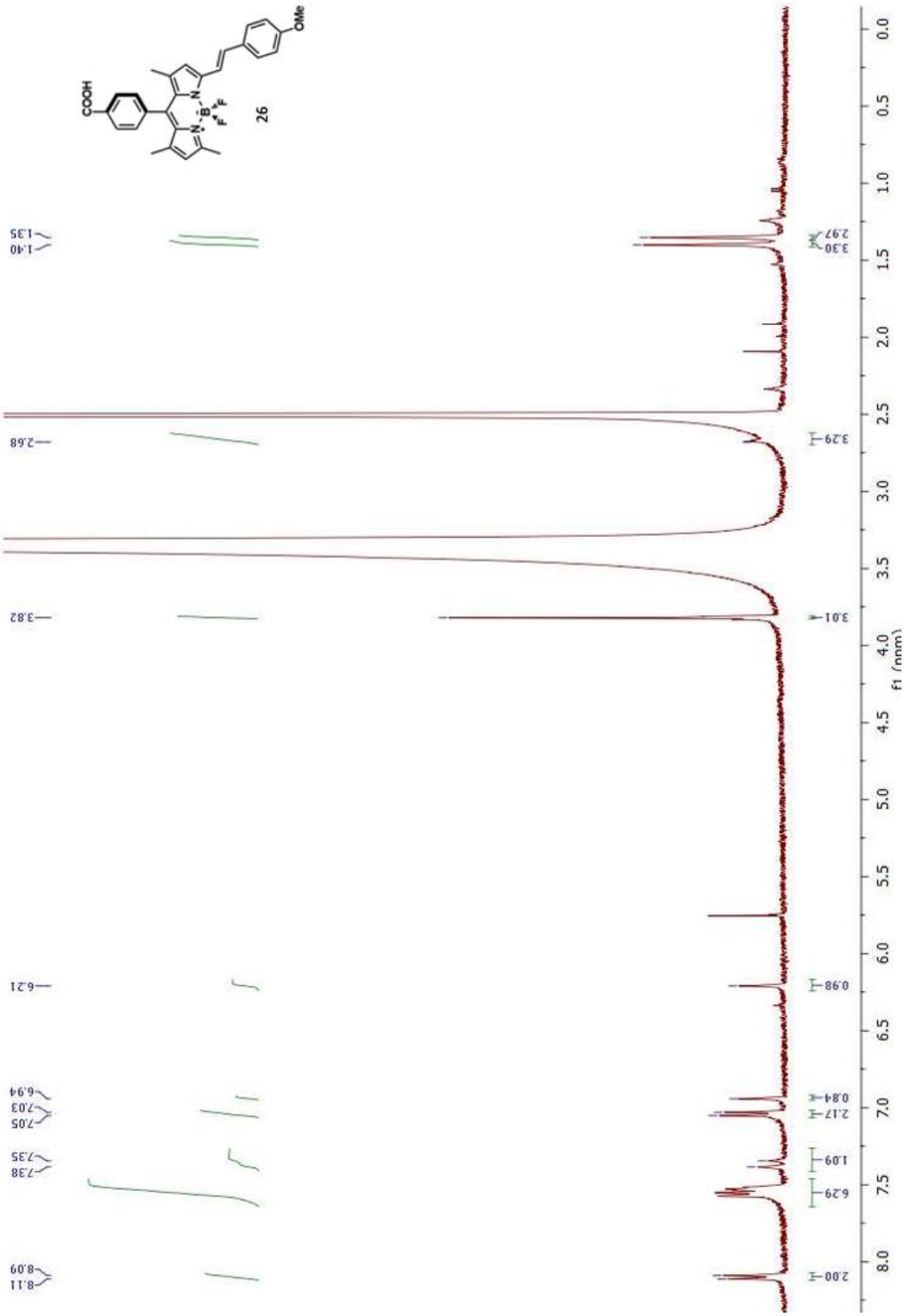

Figure 56: ^{1}H NMR spectrum of Compound 26.

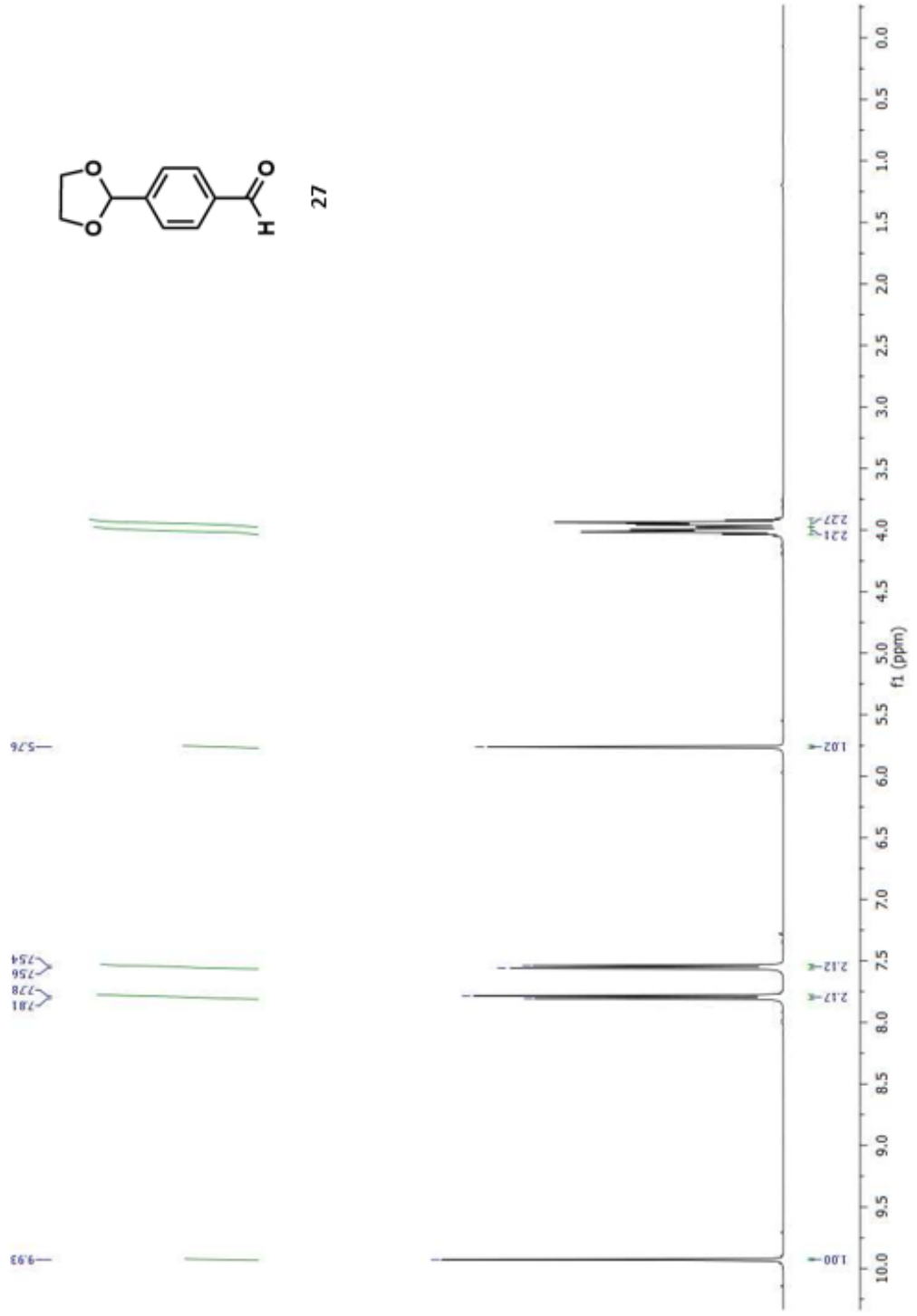

Figure 57:[1]H NMR spectrum of Compound 27.

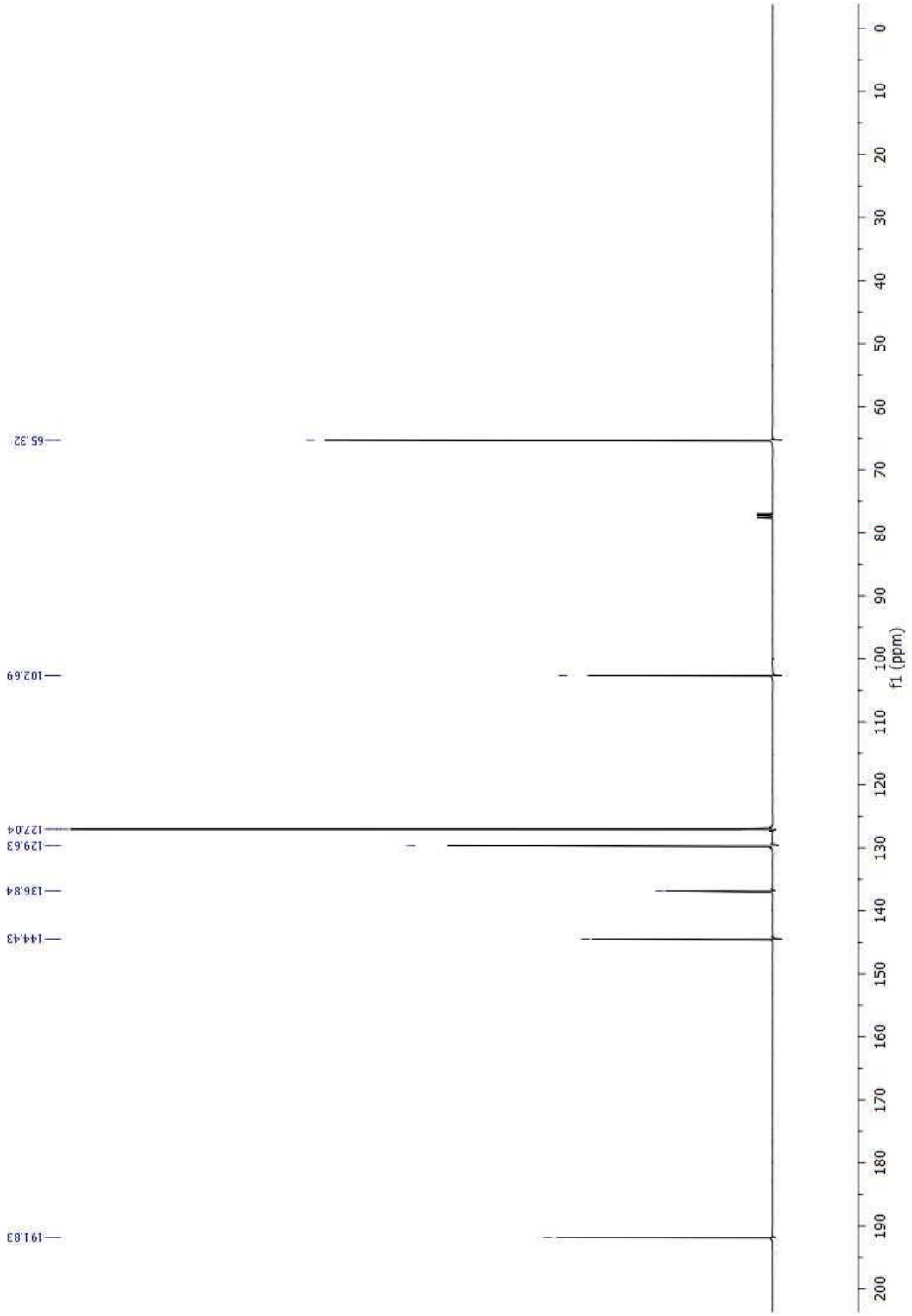

Figure 58: ^{13}C NMR spectrum of Compound 27.

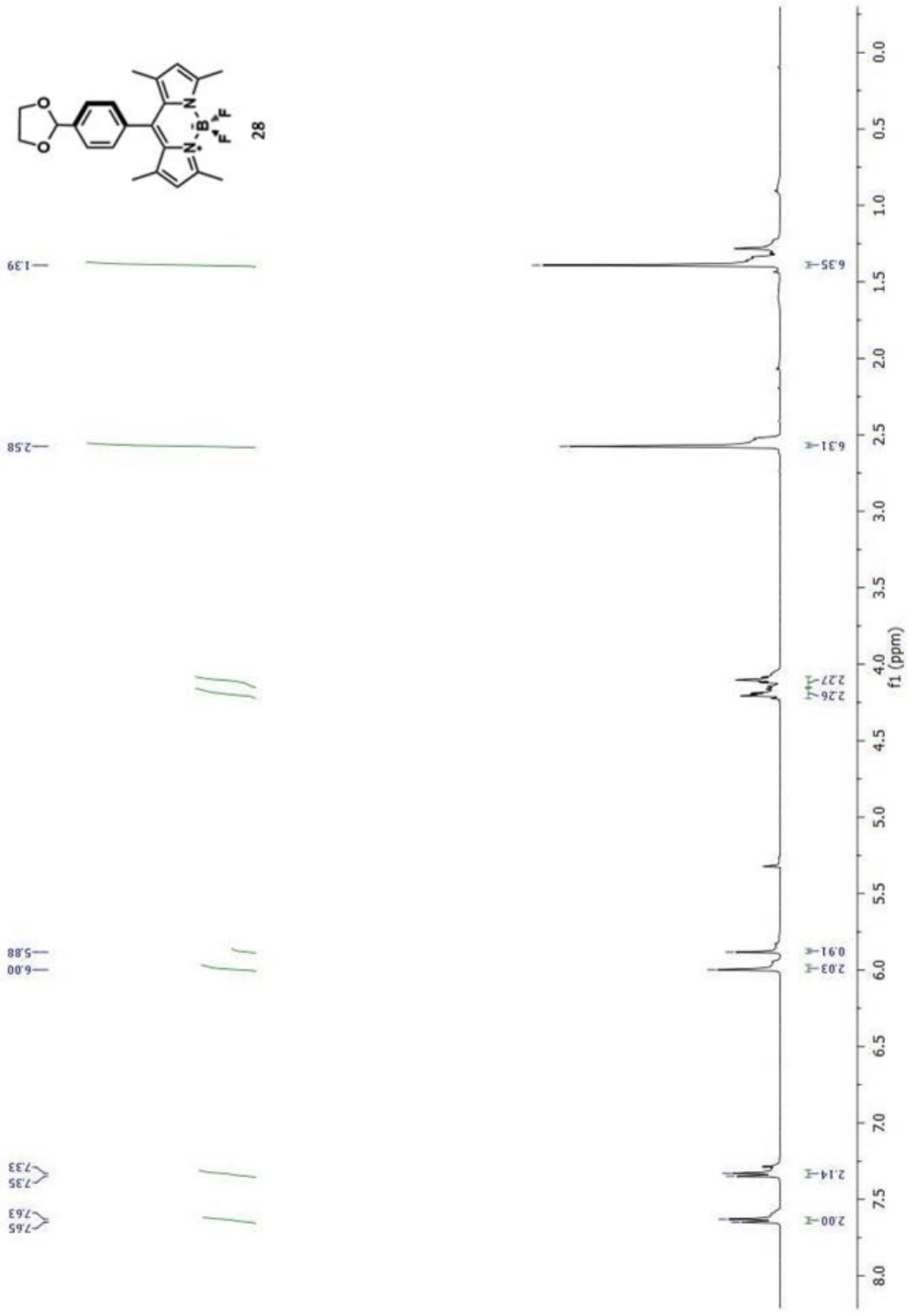

Figure 59: ^{1}H NMR spectrum of Compound 28.

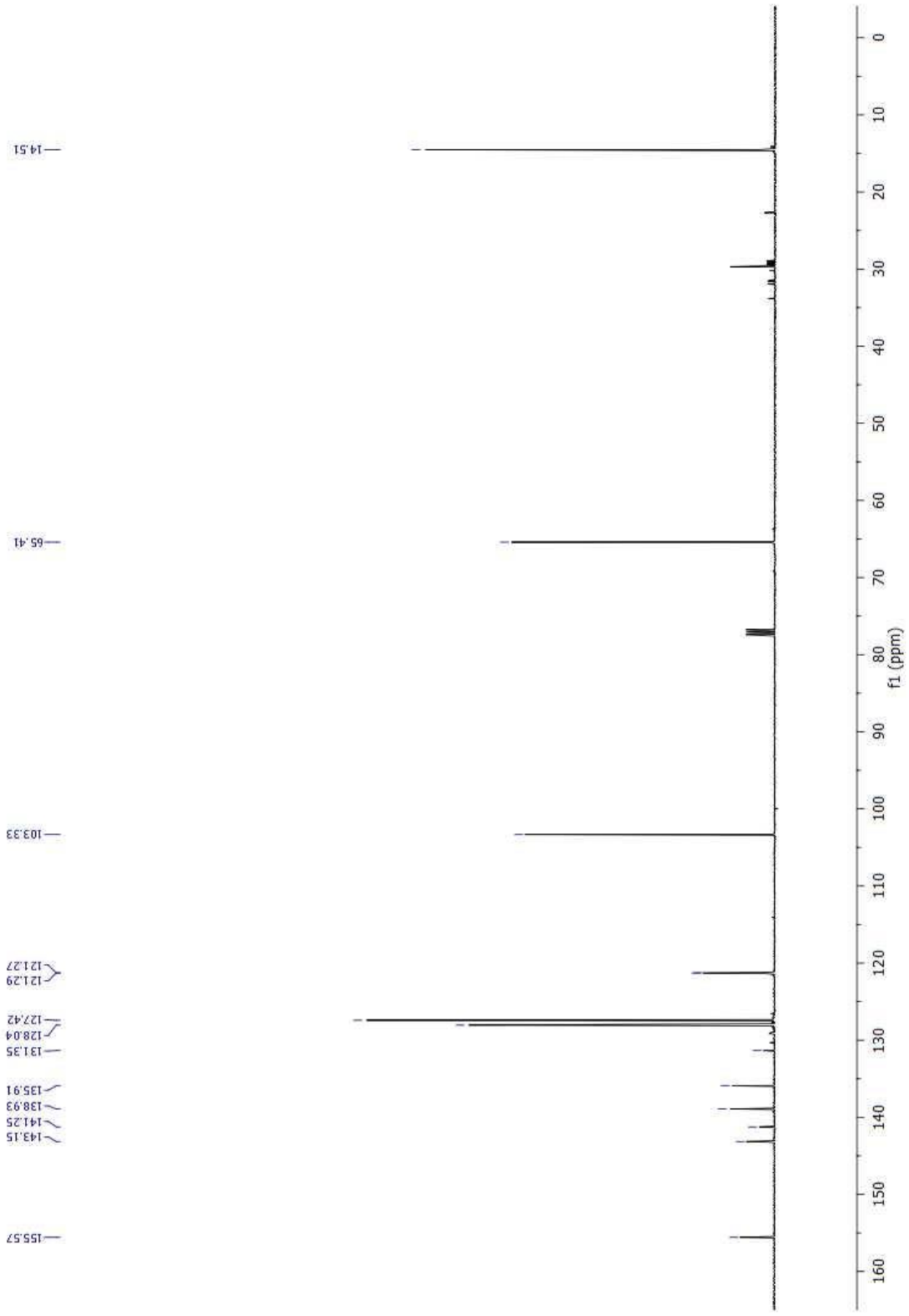

Figure 60: ^{13}C NMR spectrum of Compound 28.

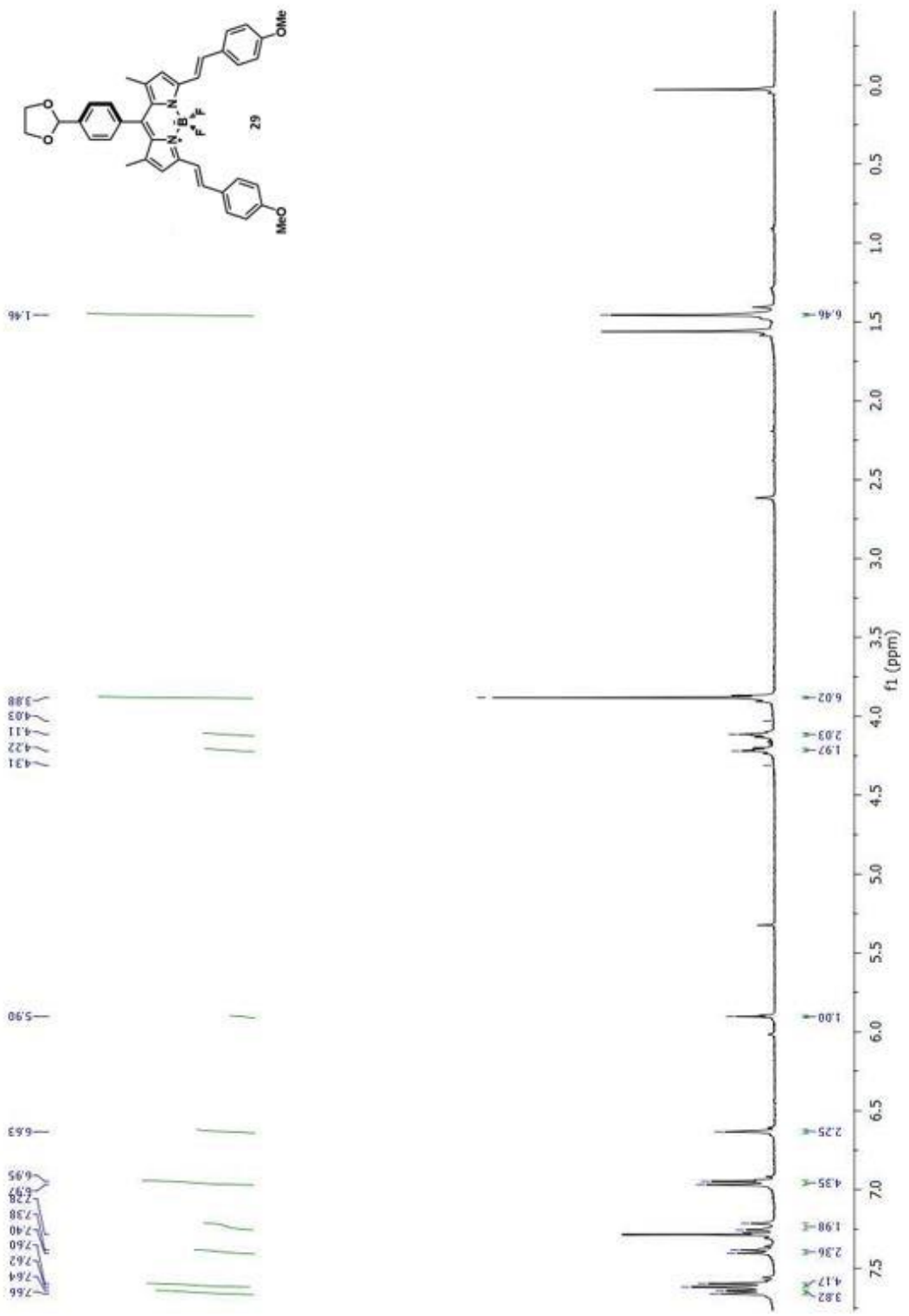

Figure 61: ^{1}H NMR spectrum of Compound 29.

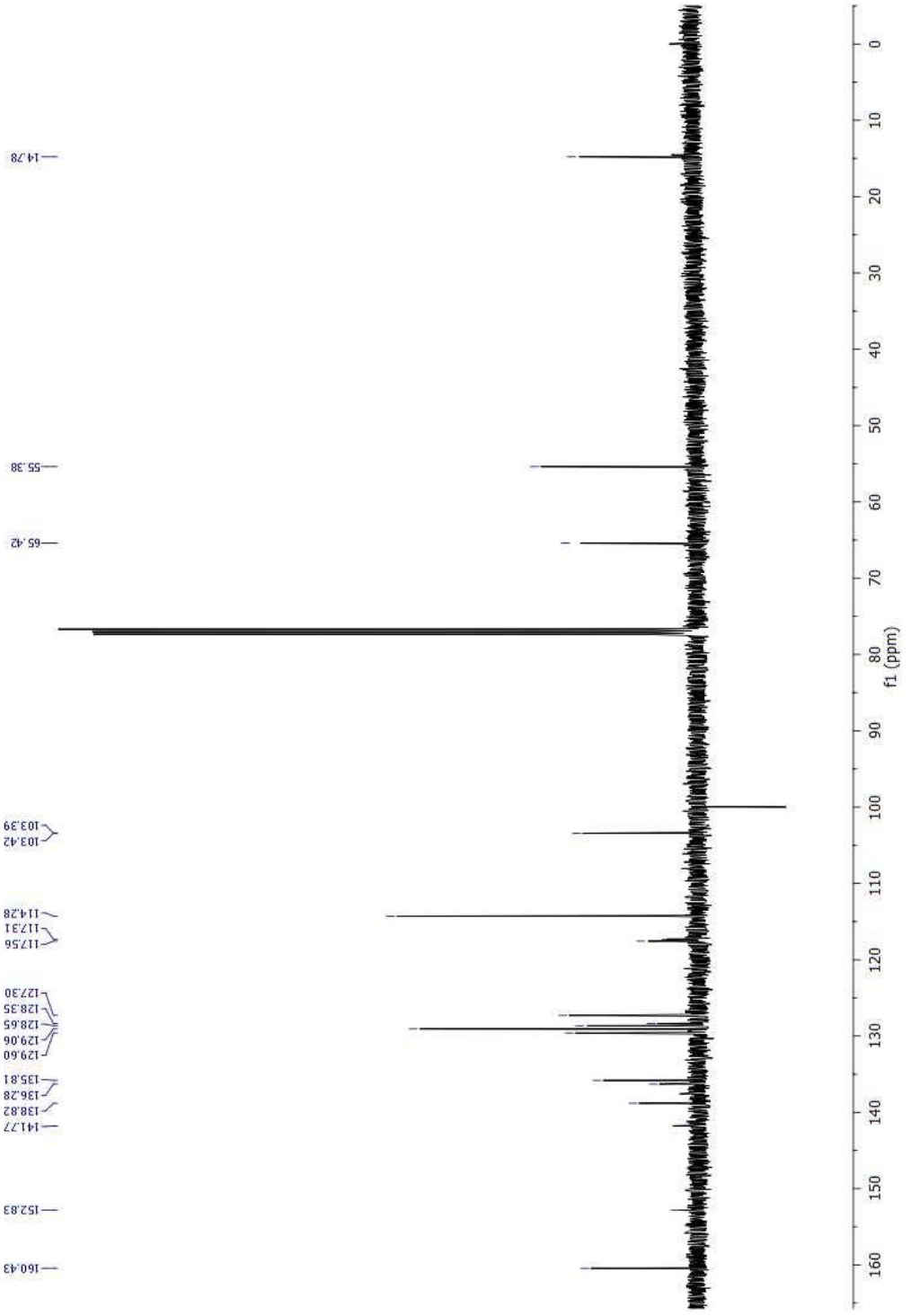

Figure 62: ^{13}C NMR spectrum of Compound 29.

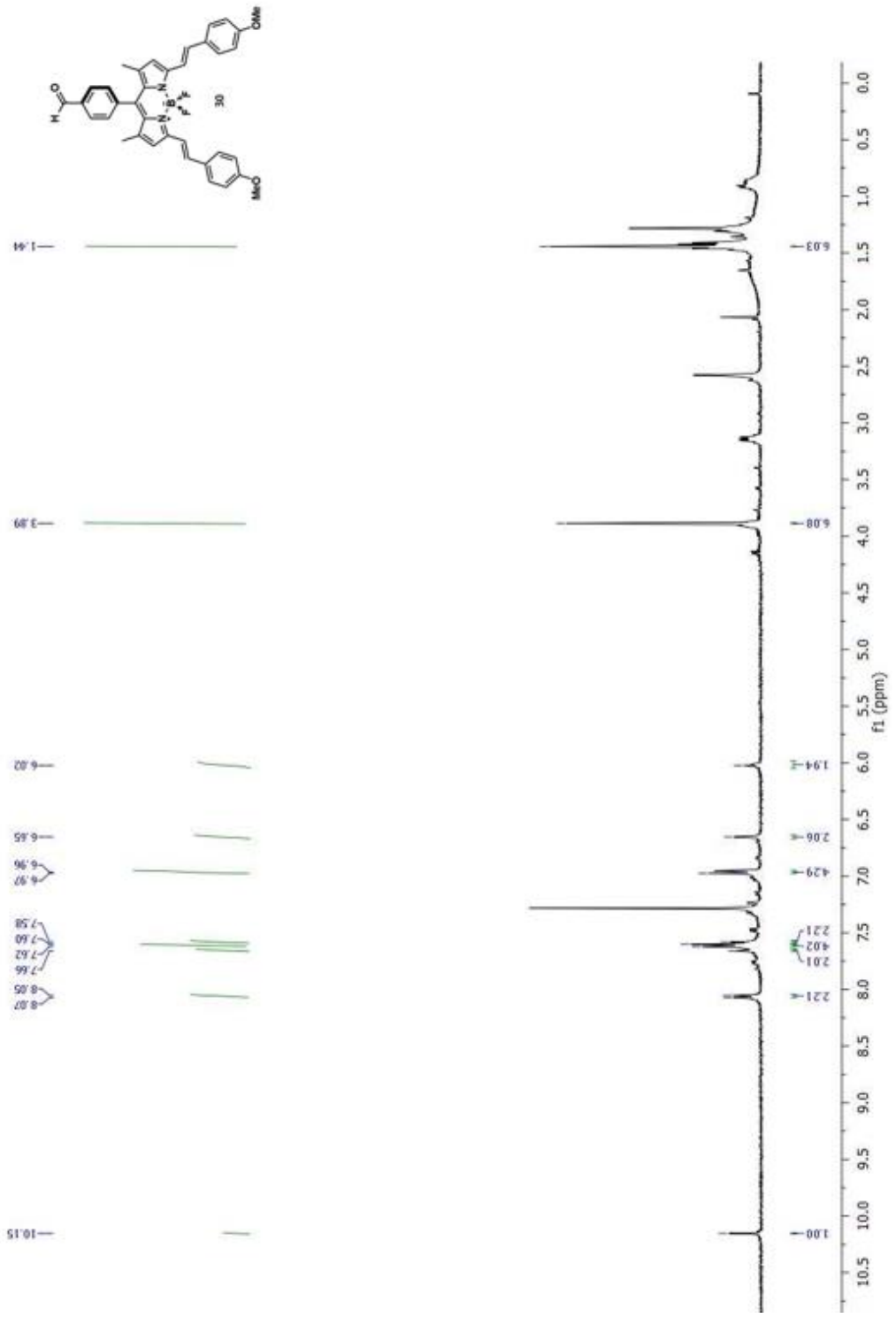

Figure 63: ^{1}H NMR spectrum of Compound 30.

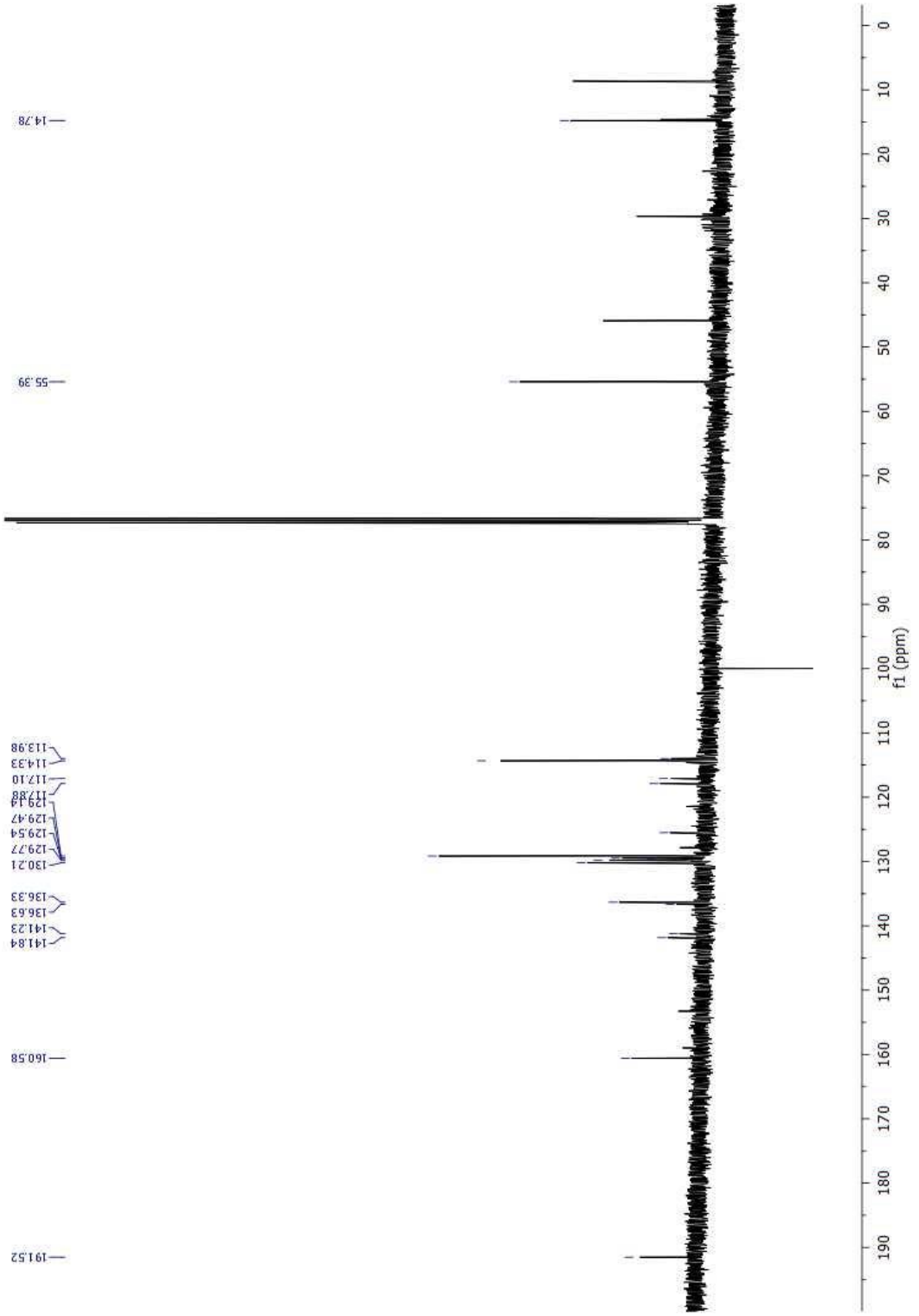

Figure 64: ^{13}C NMR spectrum of Compound 30.

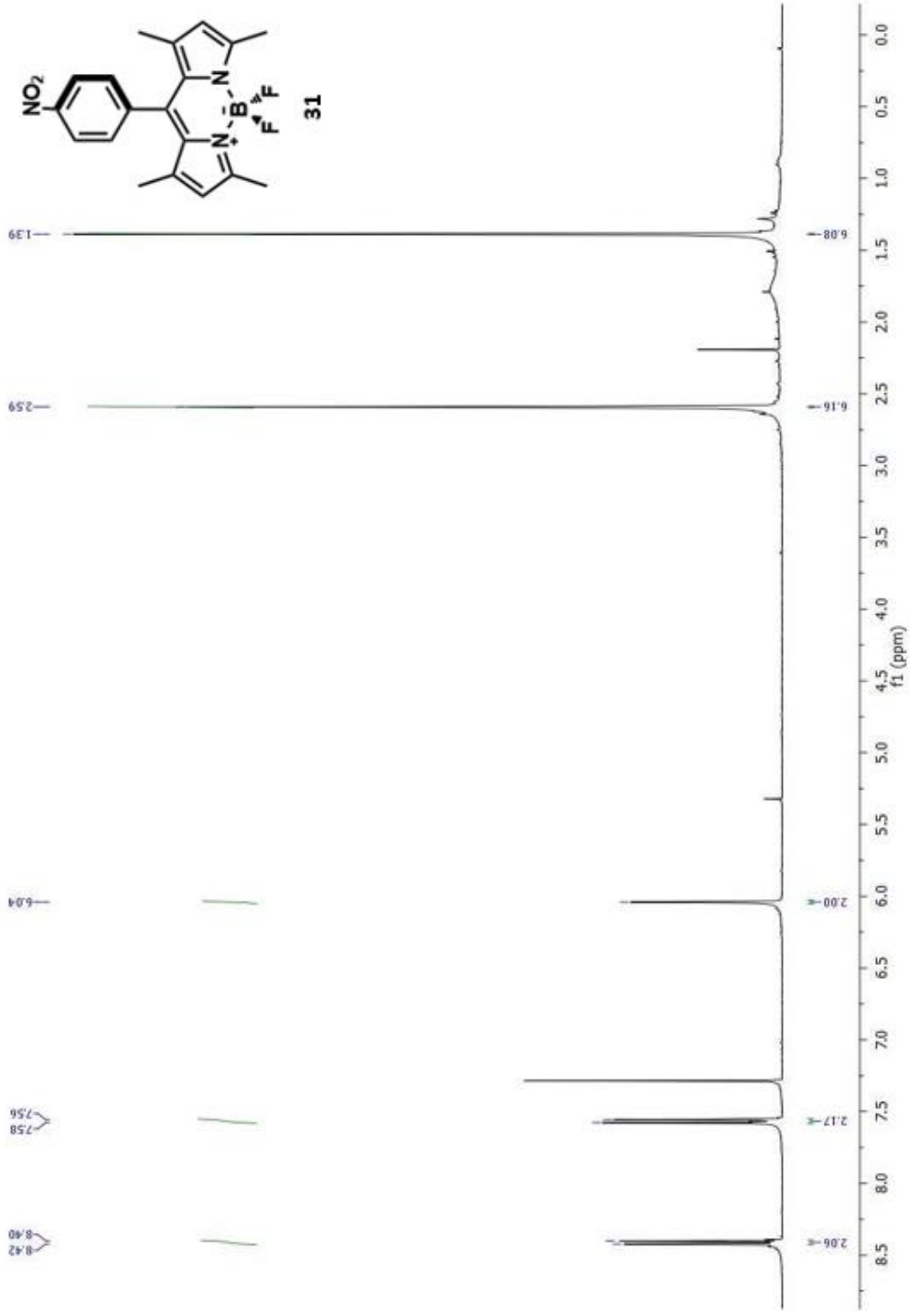

Figure 65: [1]H NMR spectrum of Compound 31.

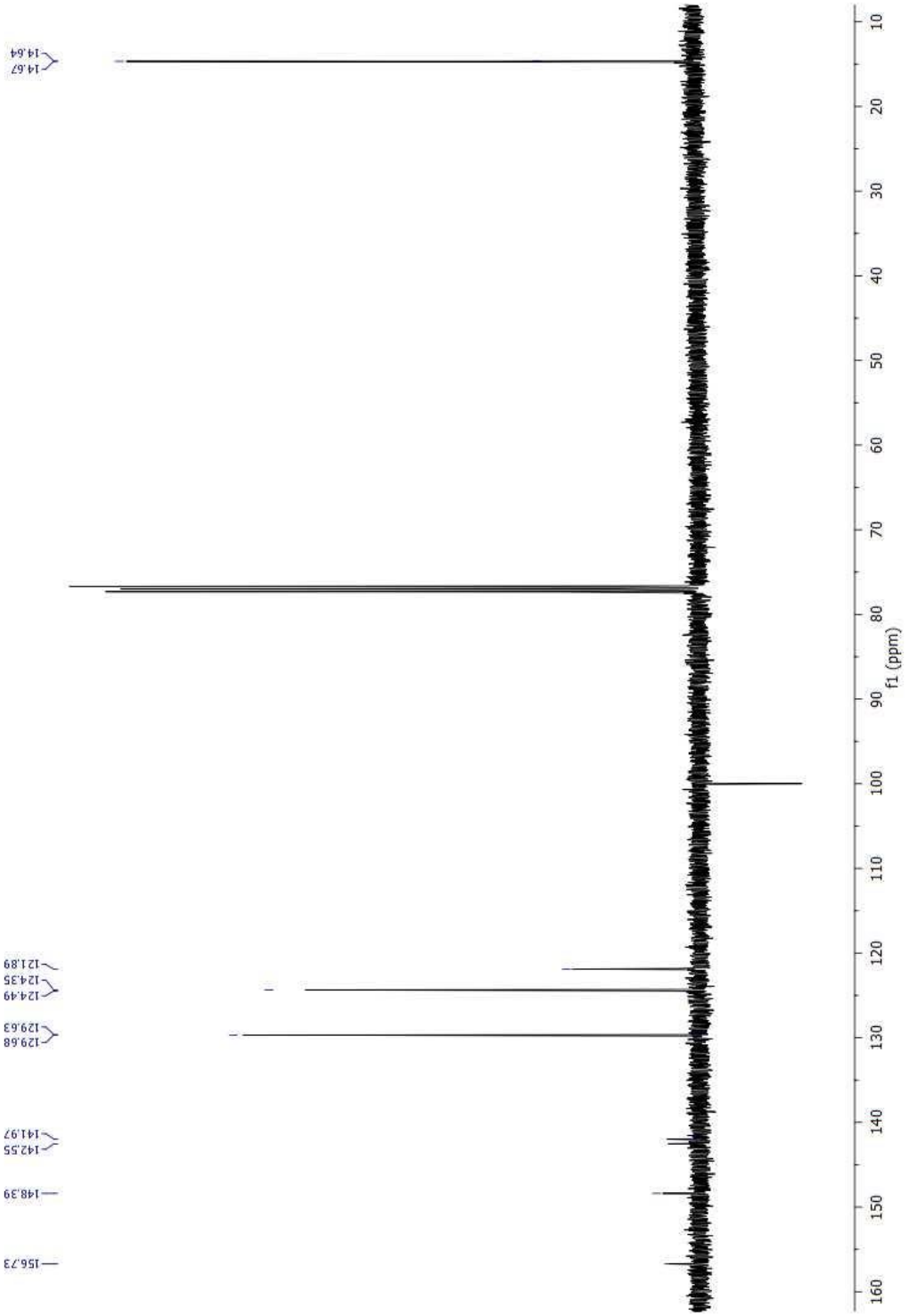

Figure 66: ^{13}C NMR spectrum of Compound 31.

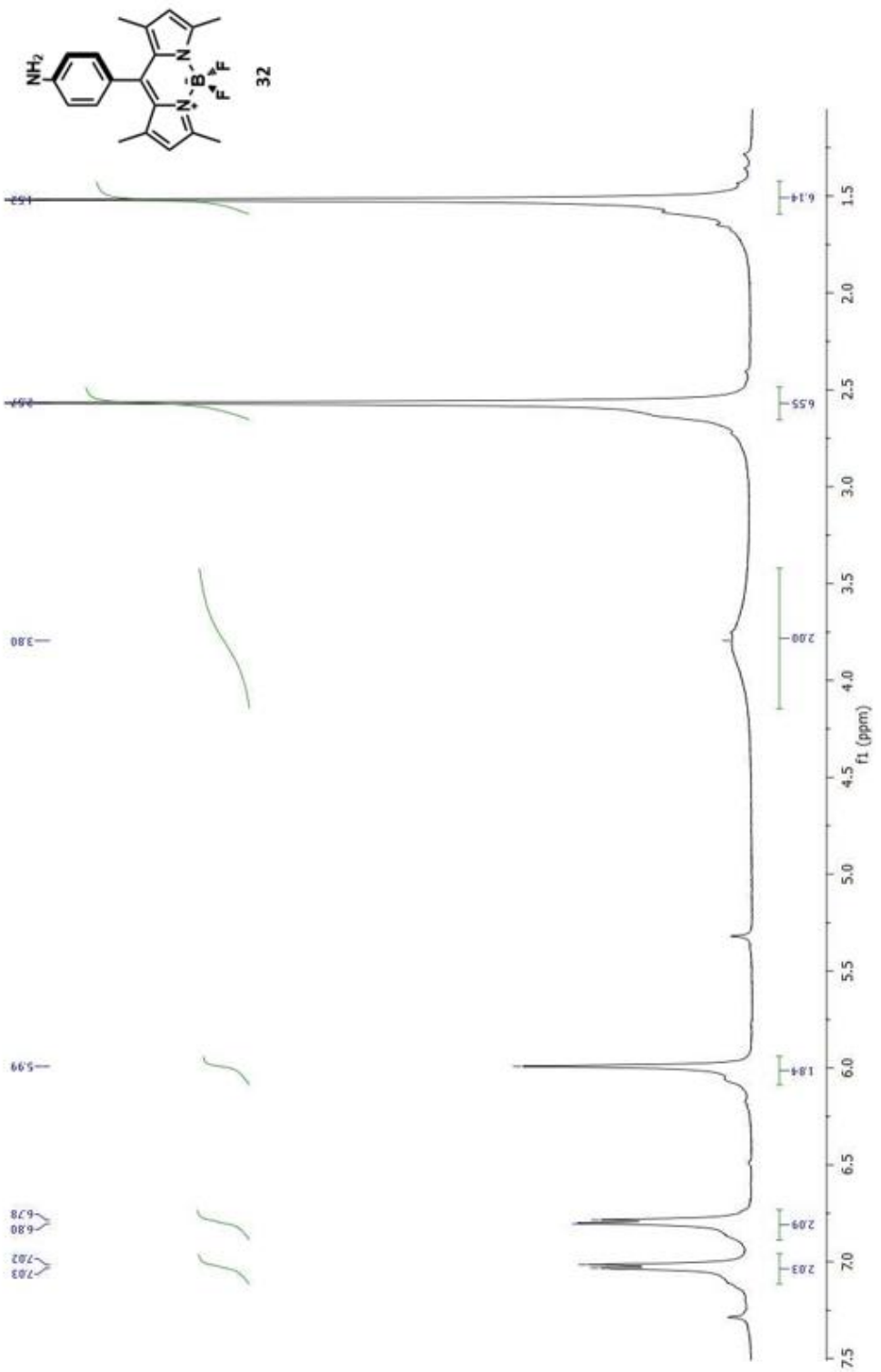

Figure 67: ^{1}H NMR spectrum of Compound 32.

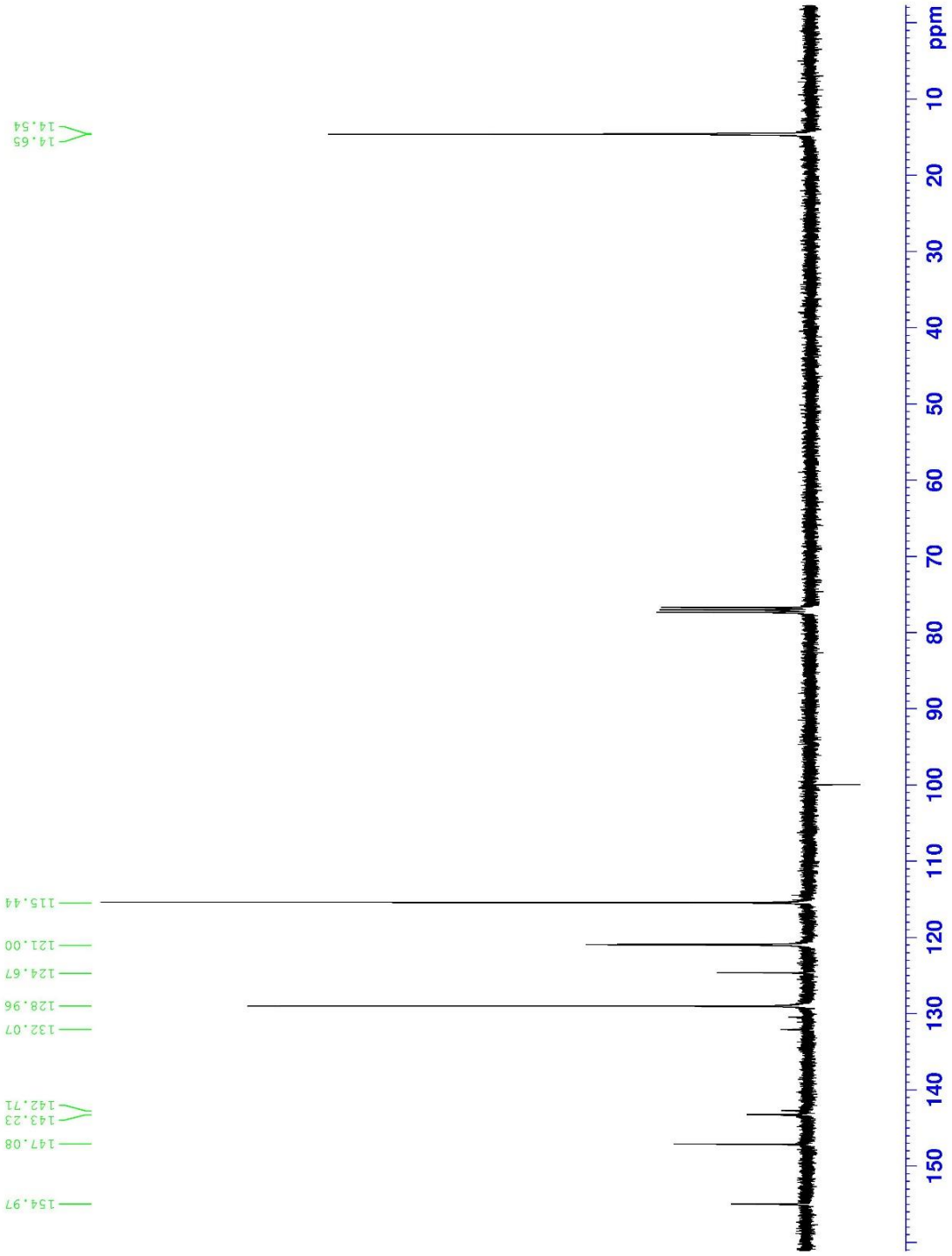

Figure 68:[13]C NMR spectrum of Compound 32.

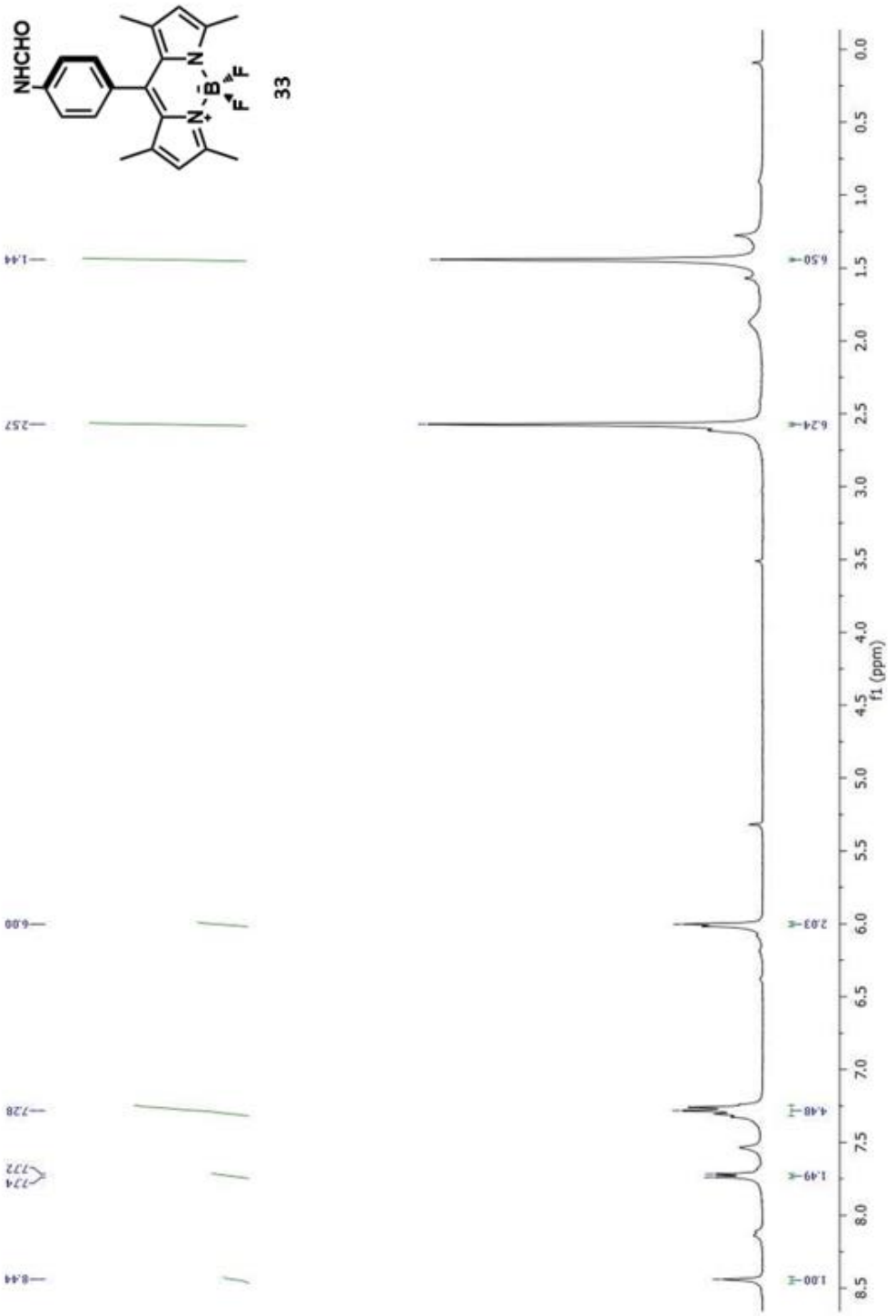

Figure 69: ^{1}H NMR spectrum of Compound 33.

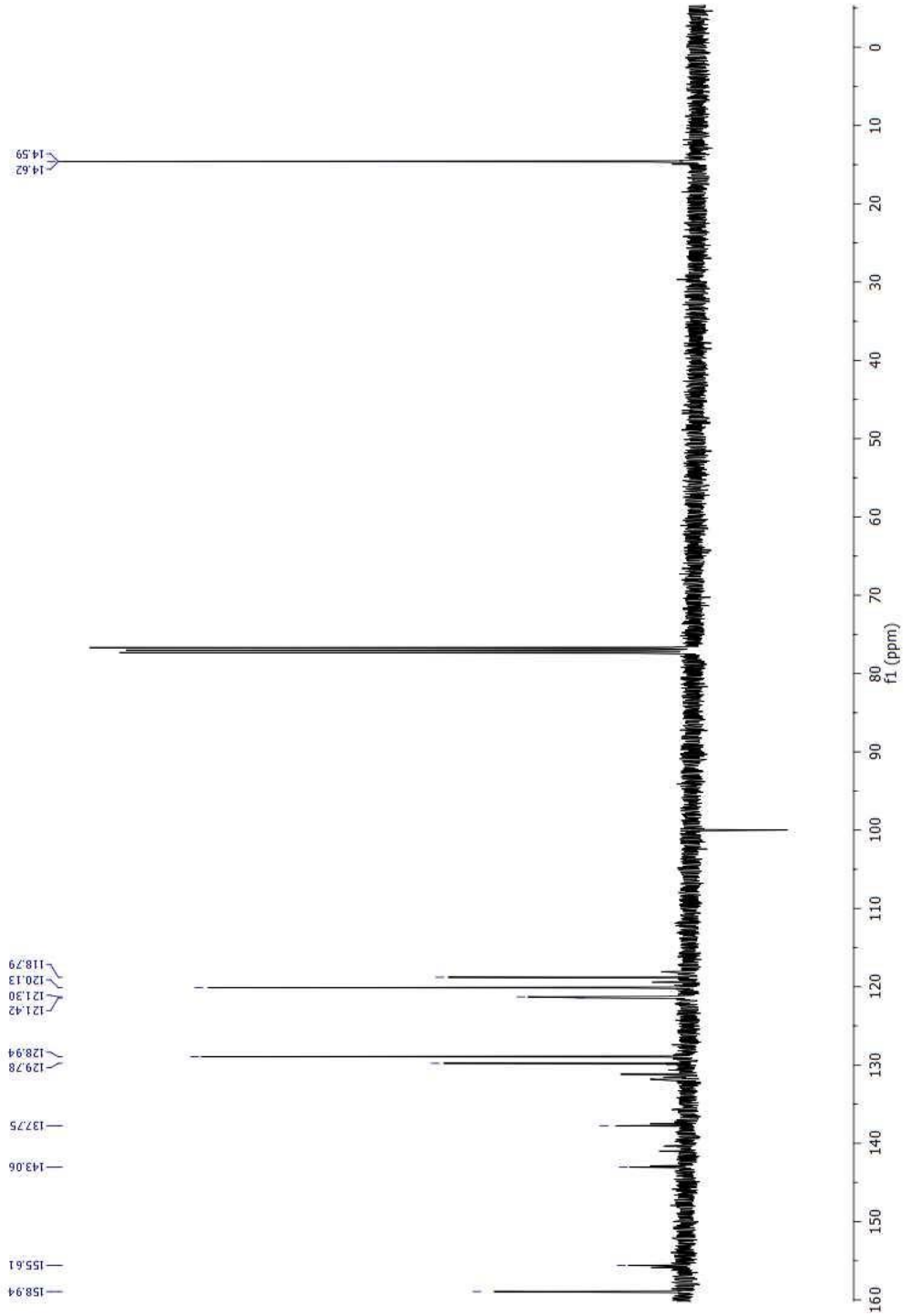

Figure 70:[13]C NMR spectrum of Compound 33.

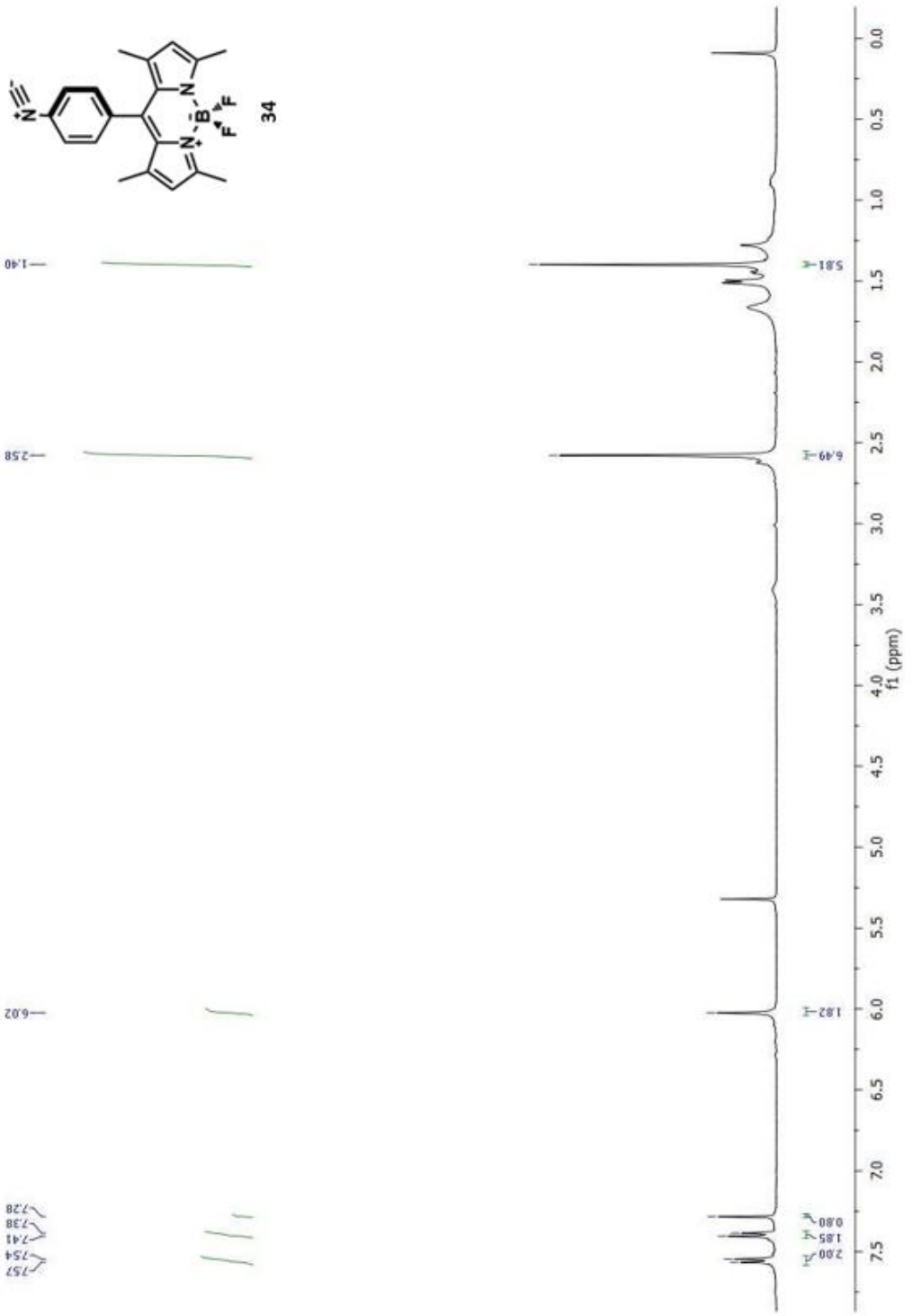

Figure 71:[1]H NMR spectrum of Compound 34.

Mass Spectra

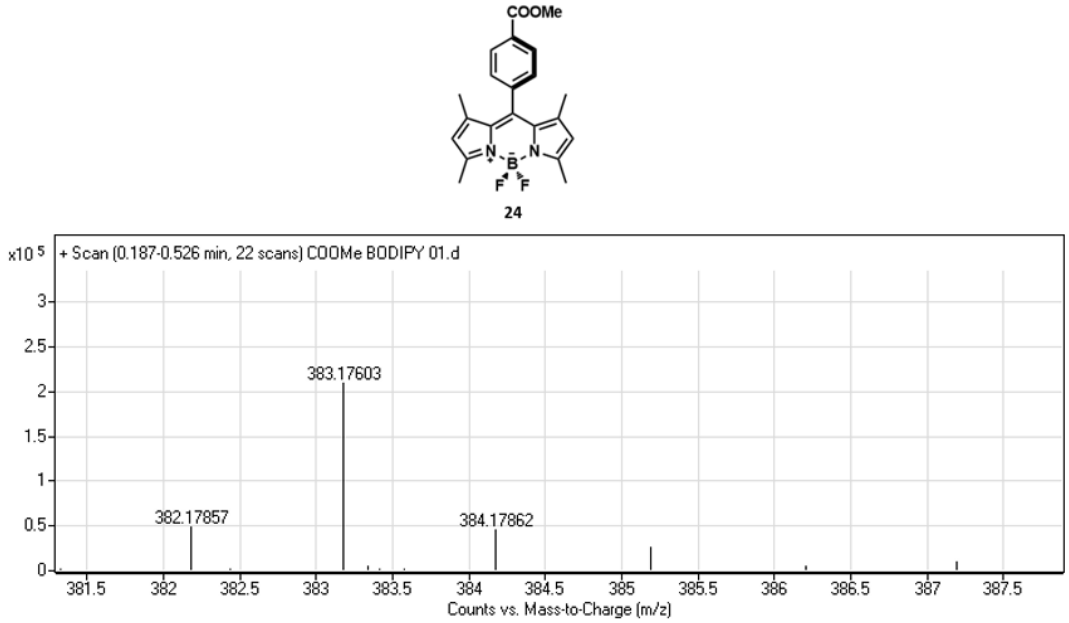

Figure 72: Mass spectrum of Compound 24.

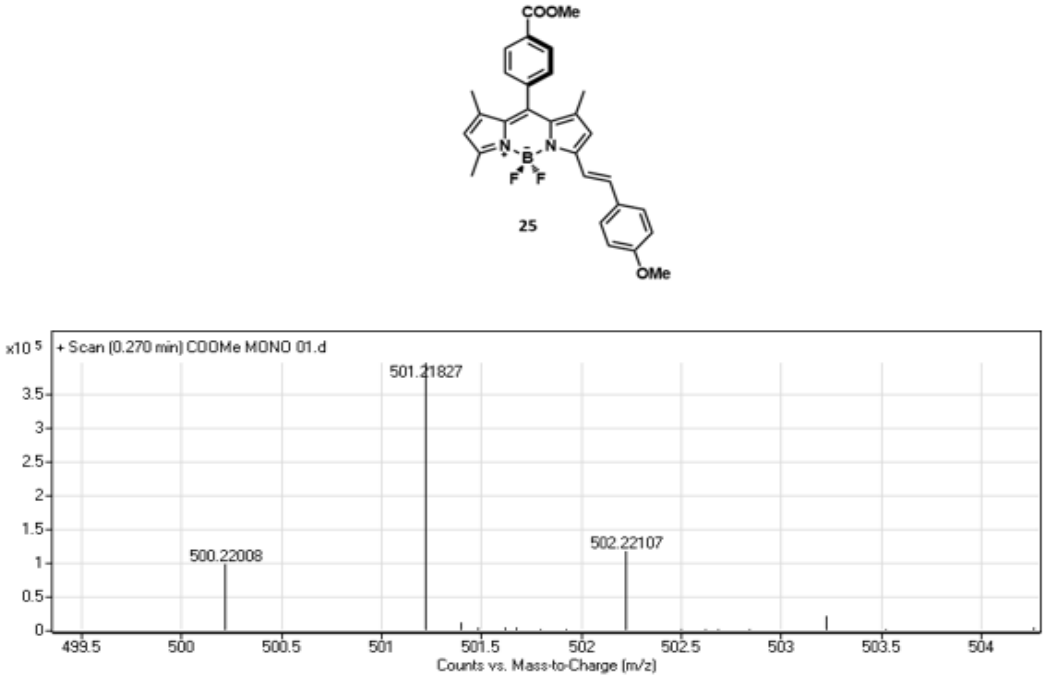

Figure 73: Mass spectrum of Compound 25.

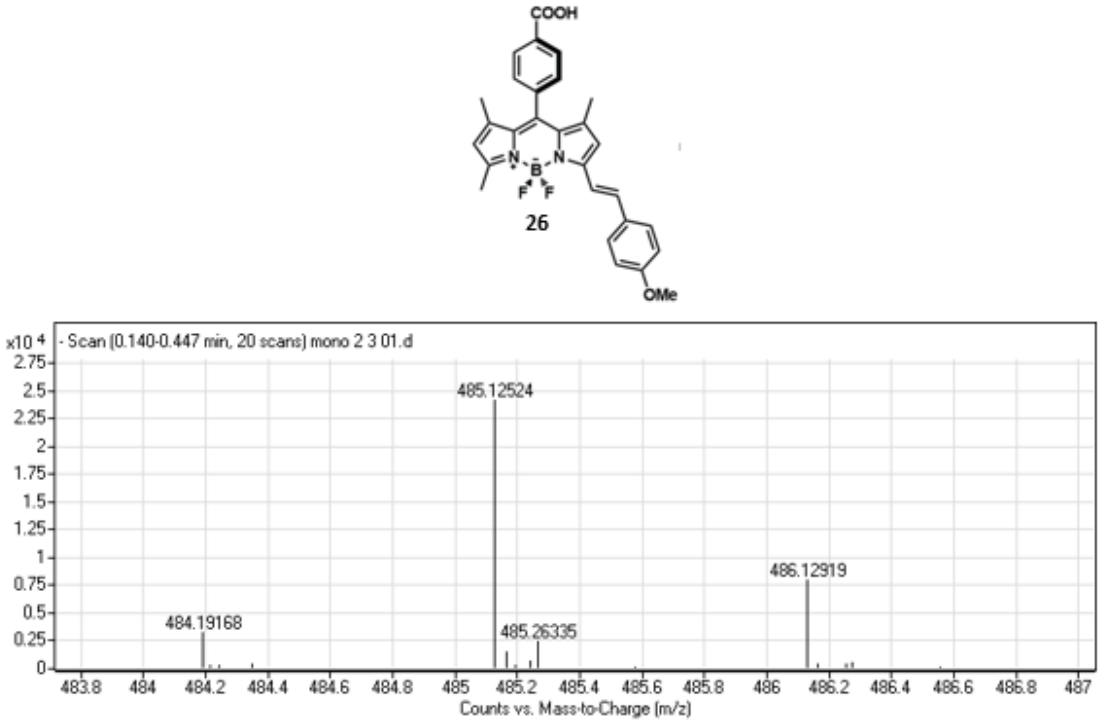

Figure 74: Mass spectrum of Compound 26.

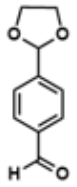

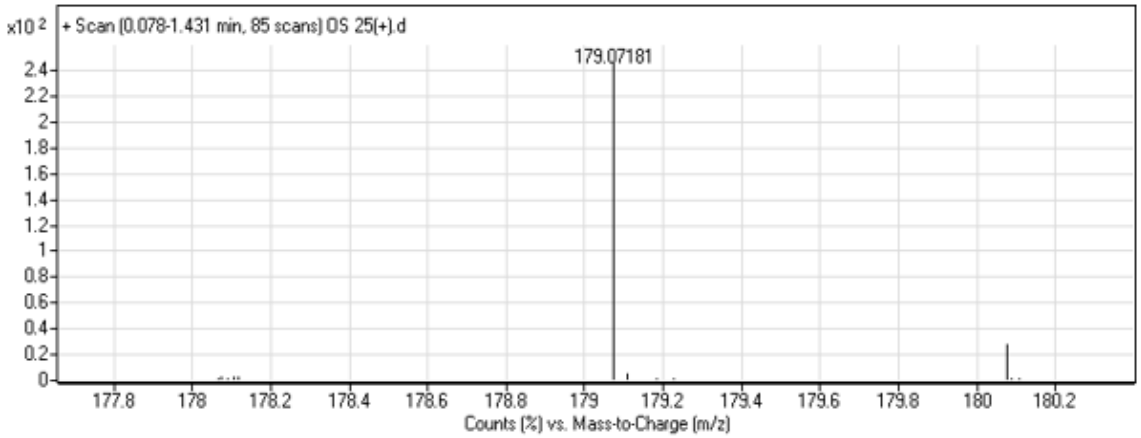

Figure 75: Mass spectrum of Compound 27.

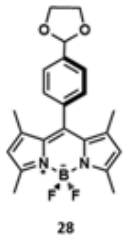

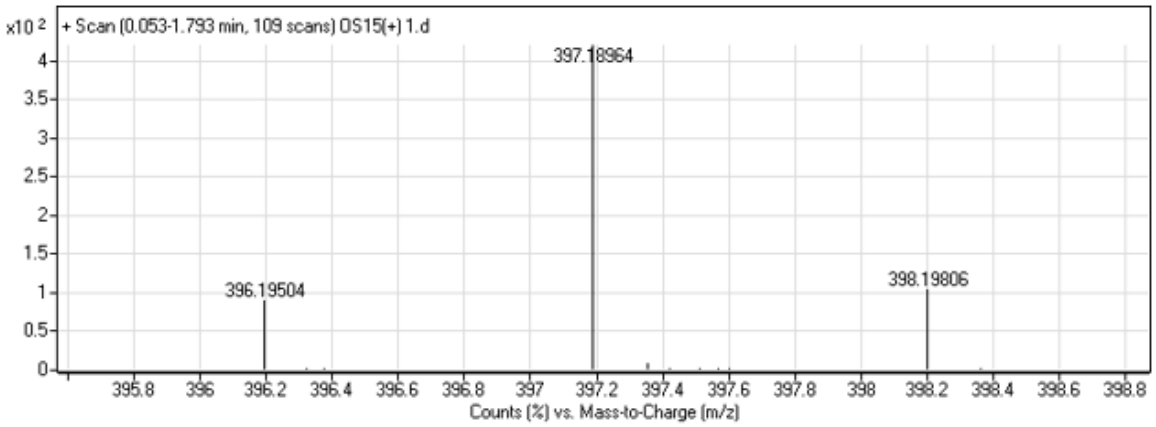

Figure 76: Mass spectrum of Compound 28.

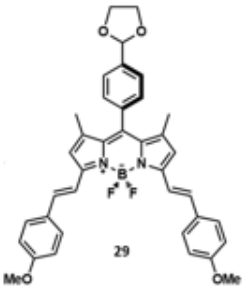

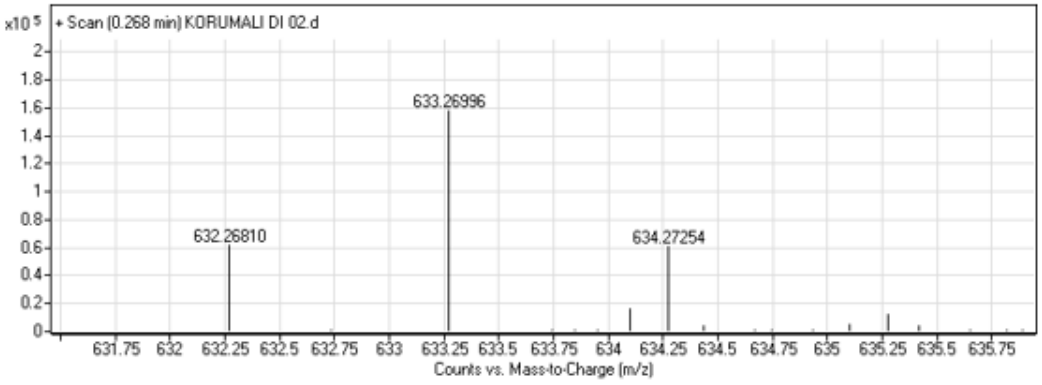

Figure 77: Mass spectrum of Compound 29.

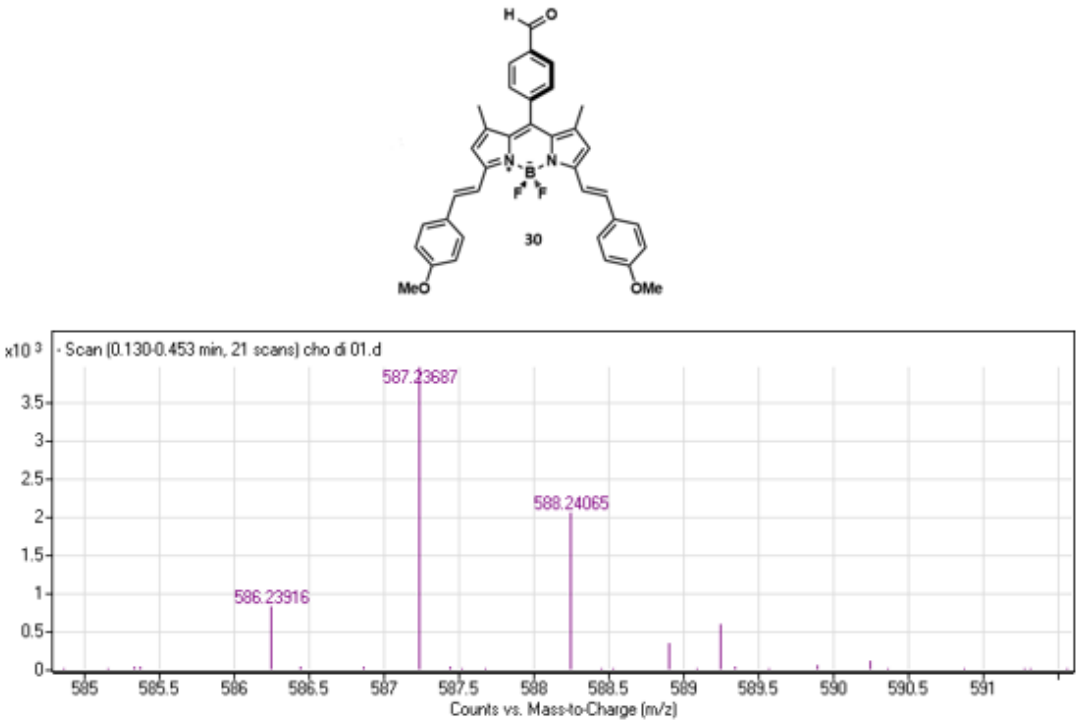

Figure 78: Mass spectrum of Compound 30.

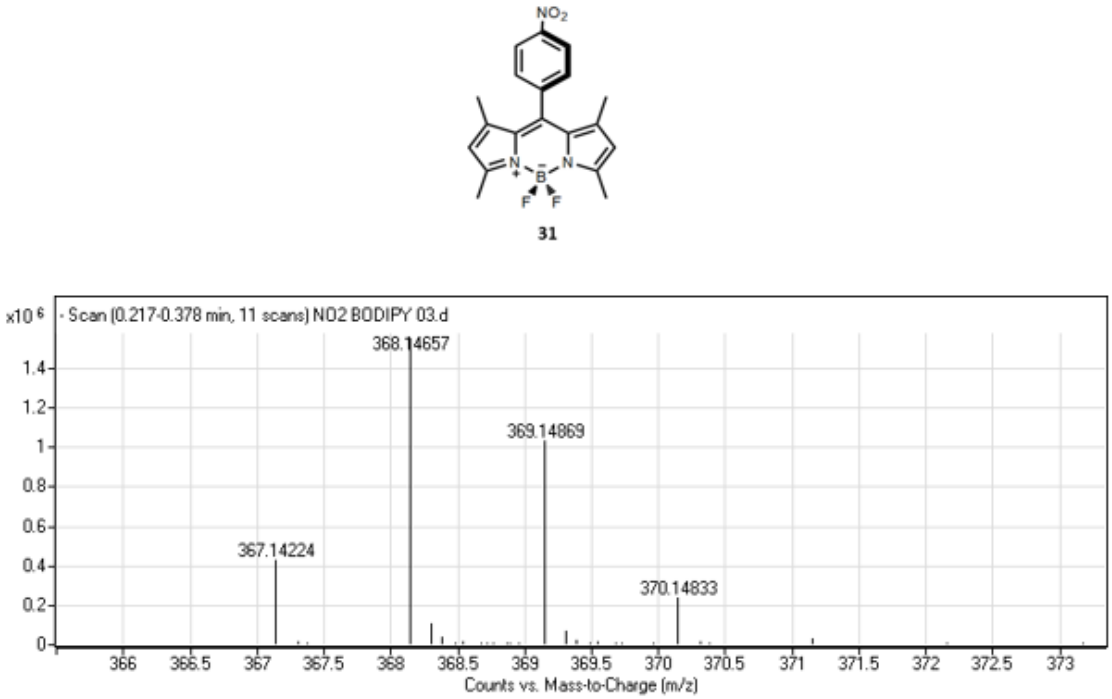

Figure 79: Mass spectrum of Compound 31.

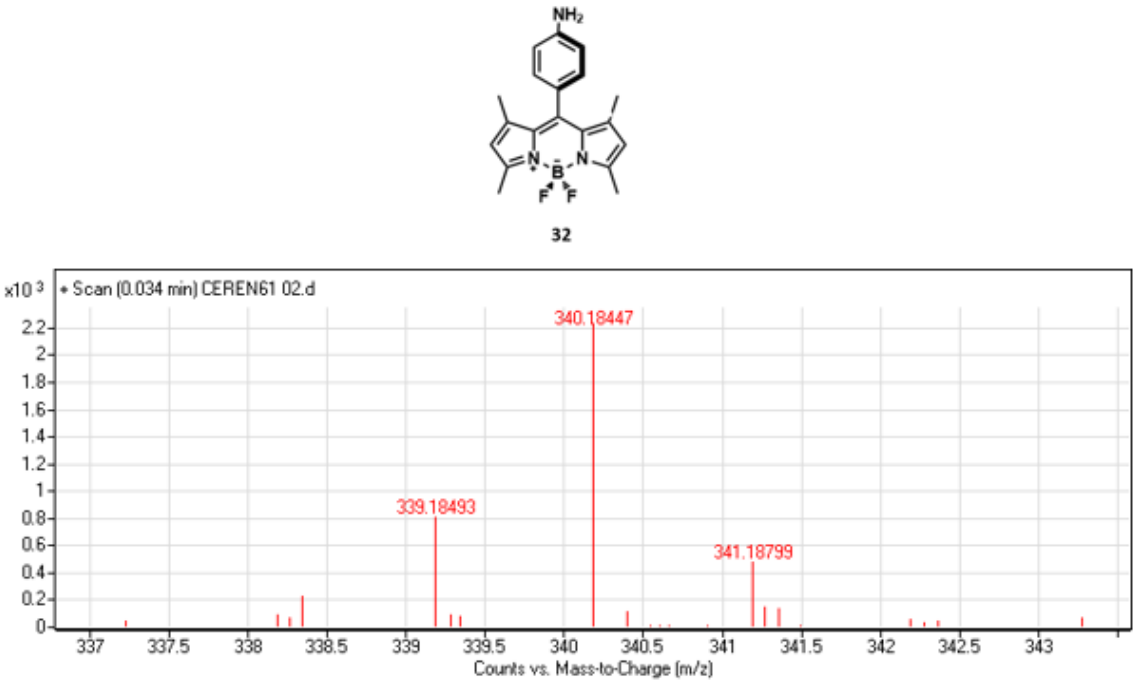

Figure 80: Mass spectrum of Compound 32.

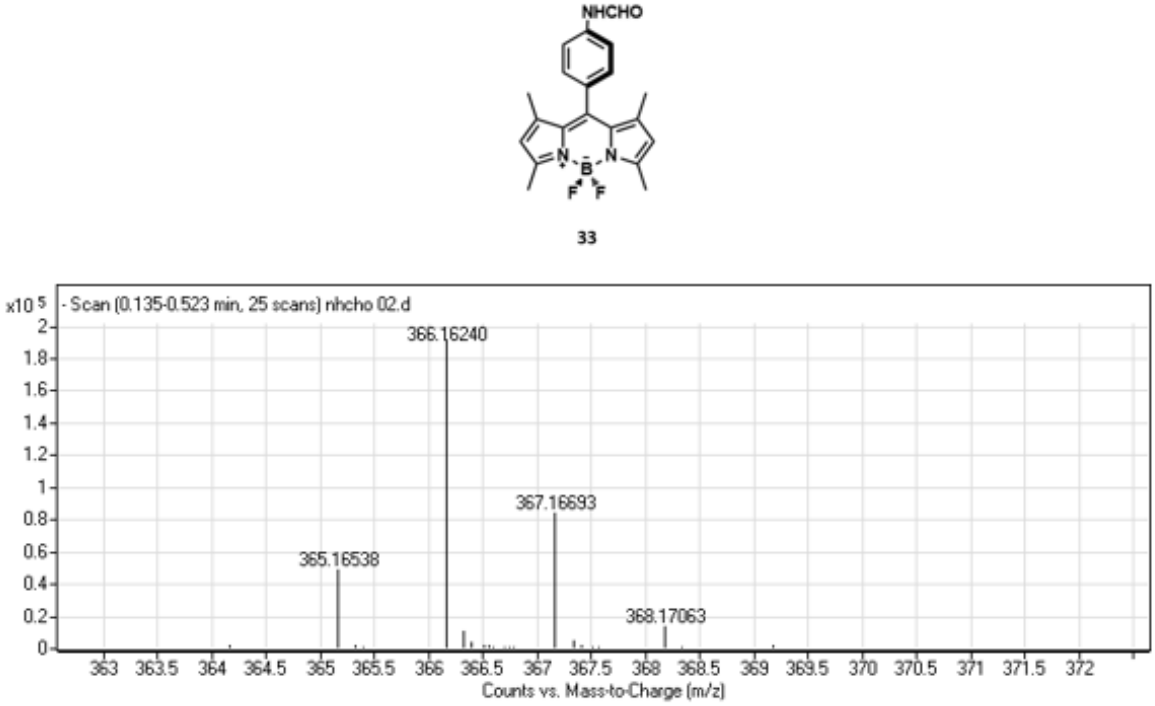

Figure 81: Mass specrum of Compound 33.

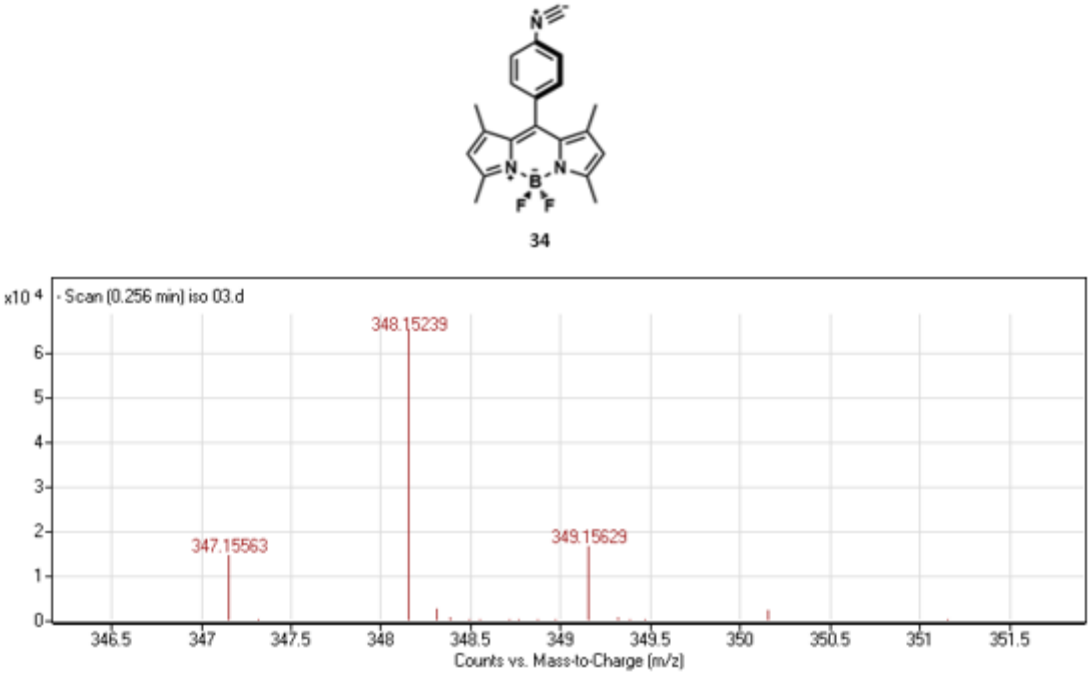

Figure 82: Mass spectrum of Compound 34.